

Kimberlites and related rocks
of the Nama Plateau of South
West Africa.

by *h*
A. J. A. Janse *h*

A thesis presented to the University
of Leeds, for the Degree of Doctor of
Philosophy

Research Institute of African Geology
The University of Leeds.

July 1964.

TABLE OF CONTENTS

	page
ACKNOWLEDGMENTS	17
ABSTRACT	19
I GENERAL INTRODUCTION	20
1. Aerial photographs and maps	22
2. Laboratory methods	22
3. Historical summary	23
(a) Previous work on the geology of the southern part of South West Africa	23
(b) Previous work on the kimberlites of the Gibeon province	25
(c) Previous work on the Gross Brukkaros	26
II GREAT NAMALAND	29
1. General geography and geomorphology	30
(a) Introduction	30
(b) Great Namaland	30
(i) Climate	31
(ii) Erosion scarps and plateaus	31
2. Regional geology	37
(a) Introduction	37
(b) Pre-Nama rocks	37
(i) Older gneisses and schists	37
(ii) Younger schists, marbles, lavas and pre-Nama sediments	39

II GREAT NAMALAND (continued)

(c) Nama system	42
(i) Kuibis series	44
(ii) Schwarzkalk series	45
(iii) Schwarzrand series	45
(iv) Fish River series	46
(d) Karroo system	48
(i) Dwyka series	48
(ii) Stormberg series	51
Cave Sandstone	51
Amygdaloidal basalt	51
(iii) Karroo dolerites	52
(e) Kalahari beds	52

III KIMBERLITES AND RELATED INTRUSIONS OF THE GIBEON PROVINCE

1. Kimberlites	55
(a) Description of kimberlite occurrences	55
(i) Introduction	55
(ii) Field occurrences in the Gibeon province	57
Location and distribution	57
Contact with host rock	66
Characteristics of the outcrop	66
Minerals and rock fragments in kimberlites	68
Size and shape	68
(iii) Conclusions	73

III KIMBERLITES AND RELATED INTRUSIONS OF THE GIBEON PROVINCE
(continued)

(b) Chemistry and mineralogy	75
(i) Introduction	75
(ii) Chemical features	76
(iii) Mineralogical features	82
Minerals	82
Groundmass	85
(iv) Conclusions	87
(c) Inclusions in kimberlite	88
(i) Introduction	88
(ii) Near-surface inclusions of host rock	88
Sedimentary fragments	88
Basalt and dolerite fragments	89
(iii) Deep-seated inclusions of monomineralic and composite nodules	94
Monomineralic nodules	94
Composite nodules	96
(iv) Deep-seated inclusions of polyminer- allic nodules	96
Group A: Pyroxene-bearing nodules	97
Group B: Olivine-bearing nodules	106
(v) Alteration of nodules	108
(vi) Discussion of results	109
(vii) Conclusions	112

III KIMBERLITES AND RELATED INTRUSIONS IN THE GIBEON PROVINCE (continued)

(d) Mineral chemistry	116
(i) Garnets	116
Chrome pyrope	117
Titanium-bearing chrome pyrope	123
Almandine-pyrope	123
Grossularite-pyrope	123
(ii) Clinopyroxene	126
Omphacitic chromediopside	126
Omphacitic diopside (chrome-poor)	127
Omphacite	127
(iii) Orthopyroxene	129
(iv) Olivine	129
(v) Ilmenite	129
(vi) Discussion of results	130
(vii) Conclusions	134
2. Calcium-rich rocks with kimberlitic affinities	137
(a) Introduction	137
(b) Hatzium vent	137
(c) Mukorob dyke	138
(d) Amalia dyke	139
(e) Other dykes	139
(f) Monticellite peridotite of the Blue Hills	141
(i) Description of the vent	141
(ii) Mineralogy	142

III KIMBERLITES AND RELATED INTRUSIONS OF THE GIBEON PROVINCE
(continued)

(iii) Calcite-phlogopite rock within the monticellite peridotite	145
(g) Discussion of results	146
3. Petrogenetic considerations	152
(a) The origin of the nodules in kimberlite .	152
(i) Monomineralic and composite nodules	152
(ii) Olivine-bearing nodules	153
(iii) Pyroxene-bearing nodules	158
(iv) Diamonds	165
(b) The origin of kimberlite	168
(i) Chemical nature	169
(ii) Physical state	171
(iii) Place of origin	173
(iv) Evidence of kimberlites on the Moho- rovicic discontinuity and on the nature of the upper mantle	175
(c) General conclusions	176
IV GROSS BRUKKAROS	179
1. Physiography of Gross Brukkaros and the surround- ing area	180
(a) Gross Brukkaros	180
(b) Linear structures	182
(c) Radial dykes	183
(d) Satellite vents	184
(e) Fracture zones	185
(f) Terrace deposits	186

IV GROSS BRUKKAROS (continued)

(g)	Ring structures on Gründorner Fläche and the Hatzium dome	186
2.	Structural relationships	188
(a)	Microbreccias	188
(i)	Bedding	188
(ii)	Subsidence of the central column	191
(iii)	Contact with host rock (Fish River series)	193
(b)	Host rock (Fish River series)	194
(c)	Satellite vents	195
(d)	Radial dykes	196
(e)	Faults	196
(f)	Age relationships	196
3.	Petrography	199
(a)	Fish River series (host Rock)	199
(i)	Sandstones	199
(ii)	Shales	201
(b)	Microbreccias of the central vent	201
(i)	Nomenclature	201
(ii)	Description	203
(iii)	Mineralogy	205
	Mineral content	205
	Rock fragments in the microbreccias	207
	Matrix of the microbreccias	208
	Heavy mineral concentrates from the microbreccias	212

IV GROSS BRUKKAROS (continued)

(iv) Discussion of formation	212
(c) Contact rocks	215
(d) Breccias of the satellite vents	215
(i) Description	215
(ii) Mineralogy	217
(iii) Discussion of formation	220
(e) Radial dykes	224
(f) Summary of results	225
4. Theories of formation of the Gross Brukkaros	226
(a) Previous theories	226
(b) Present hypothesis	228

V THE RELATIONSHIPS OF THE ERUPTIVE ROCKS IN THE GIBEON PROVINCE

1. Age relationships	231
2. Petrological and chemical relationships	232
3. Genetic relationships	233

VI APPENDICES

A. Description of the main satellite vents around Mt. Brukkaros	238
B. Drainage systems in Great Namaland	249
C. Derivation of Nama names	252
REFERENCES	254

Illustrations

- Plate 1. Current bedding in the Fish River sandstone
of the escarpment on the farm Hanaus near Gibeon 48a
2. Great Namaland Plain with eluvial pebble cover;
Mt. Brukkaros in the background, flat topped
hills to the left capped by Cave Sandstone . 53a
3. Mukorob rock. An erosion remnant of the
Kalahari Limestone Plain on the farm Bur-
gerville (part of Farm Mukorob) near Asab . . 53a
4. Contact of kimberlite Hanaus 1 (on the left),
with steeply upturned maroon shales (on
the right) 66a
5. Contact of fissure pipe Gibeon Reserve 1 with
steeply upturned maroon flagstones . . . 66a
6. Hardebank from Gibeon Reserve 1, light green
hardebank with partly serpentized olivine
phenocrysts and angular fragments of bleached
shale with baked boundaries (natural size) . 68a
7. Blue ground from Hanaus 1, note empty shell
of ilmenite nodule (left, natural size) . . 68a
8. Garnet nodule in kimberlite Hanaus 1 with
remnants of crystal faces (natural size) . . 93a
9. Photomicrograph of thin section F 10.018 (033)
Schiller structure in orthopyroxene (x 128) . 98a

Illustrations (continued)

page

- Plate 10. Photomicrograph of thin section F 9882 (DE13)
Clinopyroxene needles in zonal plagioclase (x13) 98a
11. Photomicrograph of thin section F 10.621 (Ha16)
Clinopyroxene with pyroxene lamellae and
rodlike inclusions (x32) 102a
12. Detail of plate 11 (x80) 102a
13. Photomicrograph of thin section F 9888 (Ha17)
Clinopyroxene with garnet lamellae 103a
14. Photomicrograph of thin section F 9884 (Do12)
Light brown garnet with kelyphitic rims embed-
ded in clinopyroxene; clear isotropic reaction
rims occur on the boundaries between the
pyroxene crystals (x13) 103a
15. Mukorob dyke with ilmenite-encased olivine
nodule (right bottom, natural size) 138a
16. Granular calcitic rock from Hatzium 1 with
empty cavities of previous ilmenite-olivine
nodules (natural size) 138a
17. Photomicrograph of thin section F 9890 (Ht13)
Concentric ilmenite shells around calcitized
olivine (x13) 139a
18. Kimberlitic-carbonatitic dyke on the farm
Amalia 140a

Illustrations (continued)

page

- Plate 19. Detail of plate 18. Light brown kimberlitic carbonatite with veins of calcite and inclusions of grey mudstone (host rock) 146a
20. Aerial view of Mt. Brukkaros 179a
21. Mt. Brukkaros from the south across the mud flat east of Berseba; the barranco breaks through the southern side of the ring . . . 181a
22. Mt. Brukkaros from the northwest with the "balcony" of fractured shale on the northwestern slope. Great Namaland Plain with maroon shales in the foreground; large terrace to the north of Mt, Brukkaros 181a
23. The first waterfall on the border of the central depression and the barranco 183a
24. Linear structure (narrow anticline) near Geinaggas 184a
25. Radial dyke of ankeritic carbonatite, 9" wide, near vent F west of Brukkaros 184a
26. Discordant contact between very fine grained buff coloured microbreccia and succeeding coarser layer 189a
27. Slump structures in the microbreccias . . . 189a
28. Spheroidal weathering in the hard microbreccia layer which causes the first waterfall . . . 190a

Illustrations (continued)

page

Plate 29. Cross bedding in microbreccia with relatively large inclusion of very fine grained microbreccia190a
30. Cross bedding in microbreccia	191a
31. Graded bedding in microbreccia	191a
32. Cross bedding in microbreccia with vug coated with opaline silica	192a
33. Graded bedding and cross bedding in microbreccia	192a
34. East wall of the barranco, showing the circular anticline and the inward dipping host rocks	194a
35. Central depression inside Mt. Brukkaros	194a
36. Contact of satellite vent breccia T with host rock, showing border zone free of inclusions	195a
37. Radial dyke with muscovite granite fragment, near vent F (x 1½)	195a
38. Yellow ankeritic carbonatite dyke cutting maroon shales, near vent T	196a
39. Detail of dyke in plate 38, showing intrusive character of apophyse in host rock	196a
40. Microbreccia of the central vent (natural size)	201a
41. Photomicrograph of thin section F 9755 (B60) Contact between shale fragment (right) and microbreccia (left) (x13)	207a

Illustrations (continued)

page

- Plate 42. Photomicrograph of thin section F 9544 (B61)
 Contact between chert fragment with clear contact
 zone and microbreccia, note plagioclase crystal
 pressed into chert (x13) 207a
43. Photomicrograph of thin section F 9543 (B58)
 Fragments of clouded feldspar contained in
 microbreccia (x32) 208a
44. Photomicrograph of thin section F 9545 (B65)
 Rounded fragments of plagioclase rock embedded
 in brownstained matrix of microbreccia (x80) 208a
45. Tuffisite. Intrusive microbreccia=invaded into
 maroon shale at the contact of the central vent
 (natural size) 215a
46. Fractured shale with small veinlets of potash
 feldspar and calcite (natural size) 215a
47. Coarse vent breccia, vent G1 (x $\frac{1}{2}$) 216a
48. Vent breccia, K 1 (natural size) 216a
49. Vent breccia, D . Note sandstone fragment with
 bleached and baked boundaries (natural size) 218a
50. Photomicrograph of thin section F 9737 (B12)
 Outline of olivine phenocryst in matrix of
 satellite vent breccia (x32) 218a

Maps (in back pocket)

1. Geological map of the area around Gross Brukkaros, Berseba Reserve, South West Africa; scale 1:50,000.
2. Cross section through the Gross Brukkaros; horizontal scale 1:25,000, vertical scale 1:12,000.
3. Geological sketch map of the Blue Hills vent; scale 1:7,200.

Tables

page

Table 1. Kimberlites of the Gibeon province, South West Africa	61
2. Relative abundances of minerals in kimberlite concentrates	74
3. Analyses of kimberlites	79
4. Trace element composition of some kimberlites and basalts from the Gibeon province	80
5. Analyses of basalt and dolerite fragments from kimberlites	93
6. Modal analyses of granulites, amphibolites and dolerites	100
7. Analyses of granulitic (noritic) inclusions	101
8. Modal analyses of garnet pyroxenite inclusions	104
9. Analyses of pyroxenitic and peridotitic inclusions	105
10. Analyses of chrome pyropes	121
11. Physical properties of garnets from kimberlites	122
12. Analyses of pyropes and almandine-pyropes	125
13. Analyses of omphacitic diopsides and omphacitic chromediopsides	128
14. Mode of occurrence of the heavy minerals in kimberlite concentrates	136

Tables (continued)

page

Table 15. Analyses of calcium-rich kimberlites and related rocks	140
16. Analyses of monticellite-bearing picrites and peridotites	150
17. Analyses of micaceous kimberlites and related rocks	151
18. Average composition of peridotites	157
19. Analyses of Fish River sandstone and Brukkaros microbreccia	210
20. Trace element composition of Fish River sandstone and Brukkaros microbreccia	211
21. Analyses of vent breccia and radial dykes from Mt. Brukkaros	223

Text-figures

page

Figure 1. Outline map of South West Africa	28
2. Outline map of the southern part South West Africa, showing topographical features	33
3. Schematic profile through the Nama sediments in Great Namaland	43
4. Gibeon kimberlite province	59
5. Kimberlites of South West Africa	70
6. Kimberlites of the Republic of South Africa	71
7. Kimberlites of the U.S.S.R. and of Basutoland	72
8. Von Wolff diagram. The average composition of some ultrabasic rocks	81
9. Von Wolff diagram. Composition of the Gibeon kimberlites and related rocks	114
10. Diagram after Nixon (et al, 1963). Weight percentage of Cr ₂ O ₃ in pyrope garnets	119
11. Diagram after Frietsch (1957) for garnets, relating unit cell size and refractive index	120
12. Von Wolff diagram. Composition of kimberlitic eclogites from various localities	164
13. Diagrams illustrating the petrogenetic relationships of the kimberlite-carbonatite series	236

ACKNOWLEDGMENTS

The writer wishes to thank Professor W. Q. Kennedy, director of the Research Institute of African Geology, for his advice and helpful discussion throughout this research.

The work was carried out with the aid of an Oppenheimer Scholarship awarded by the University of Leeds. A special debt of gratitude is due to the Anglo-American Corporation of South Africa, whose generosity has made these scholarships available and who granted permission to the writer to use the information on the research topic, acquired by him during his tenure of employment with the company.

Grateful acknowledgment is also made to Dr. T. N. Clifford and Dr. P. G. Harris for their critical reading of the manuscript and for many useful suggestions and comments and to Dr. O. von Knorring for helpful discussion and advice, in particular with reference to the mineralogy and mineral chemistry.

Sincere thanks are due to many colleagues in the Department of Geology and the Research Institute of African Geology for valuable discussions and encouragement.

For technical assistance received in the Department of Geology, the writer wishes to thank the following:

Mrs. M. H. Kerr, Miss J. R. Baldwin and Dr. O. von Knorring for chemical analyses; Dr. G. Hornung and Mr. R. M. Stewart for X-ray fluorescence analyses; Miss J. M. Rooke and Miss J. Brown for spectrochemical analyses; Mr. W. L. Wilson for X-ray photographs; and Mr. P. E. Fisher and his assistants for the preparation of thin sections.

In regard to fieldwork, the writer is much indebted to Messrs. R. Baxter-Brown, J. Boshof and J. A. Mills, who did the initial mapping of Mt. Brukkaros and surrounding area; in particular map 1 and map 3 are based on their work.

A special mention must be made of Mr. and Mrs. Peters-Hollenberg of Farm Lichtenfels, near Asab, South West Africa. Without their generous hospitality and encouragement this work would never have been undertaken.

ABSTRACT

The eruptive rocks of the Nama Plateau are divided into : (i) kimberlites, (ii) carbonatitic dykes, (iii) monticellite peridotite and (iv) rocks belonging to the Brukkaros complex. The Gibeon kimberlite province contains at least 46 pipes and 16 major dykes of mainly basaltic kimberlite.

The inclusions in kimberlite are divided into : (i) cognate monomineralic nodules consisting of kelyphitized titanium-bearing pyrope, coated diopside, serpentinized olivine, coated ilmenite, and composite ilmenite-encased olivines; and (ii) accidental polymineralic nodules consisting of garnet peridotite, garnet pyroxenite, retrograde eclogite and granulite.

The large phreatic volcano - Gross Brukkaros- is formed by a dome of Nama sediments. The centre of the dome contains a depression, $1\frac{1}{2}$ miles in diameter, underlain by fine grained clastic rocks (microbreccias) derived from brecciation of the Nama sediments. It is surrounded by 45 satellite vents and numerous radial dykes, both filled with coarse breccias in a carbonate-rich matrix. An outcrop of a monticellite peridotite occurs in a vent $\frac{3}{4}$ miles south of Mt. Brukkaros.

It is concluded that : (i) kimberlites are formed by zone refining of a magma, derived from a very deep source

in the mantle in places beneath very stable areas of the crust (cratons and platforms), and (ii) kimberlite may develop a volatile-rich carbonatitic top fraction, which under certain circumstances causes phreatic explosions (as happened in the case of Mt. Brukkaros). The top fraction, depleted of volatiles, is represented by a monticellite peridotite.

I. GENERAL INTRODUCTION

During 1958, 1959, 1960 and part of 1961 the writer was employed as a geologist by the Anglo-American Corporation of South Africa Ltd. to prospect for diamondiferous deposits, at first along the coast of Namaqualand and, later (from 1959 to 1961), in the southern part of South West Africa. The later project was carried out by a team consisting at various times of the following personnel : A. J. A. Janse, J. A. Mills, G. N. W. P. Mundell and D. B. Orr; during the course of this work a number of known occurrences of kimberlite along the middle course of the Fish River were examined and several were found which showed no signs of previous investigation.

In the same region, in 1958, a team of geologists of the Anglo-American Corporation consisting of Messrs. R. Baxter-Brown, J. Boshof and J. A. Mills mapped a large solitary mountain known as Geitsi/Gubib or Gross Brukkaros. This mountain was re-investigated in 1961 by the writer, who recognized the carbonatitic and kimberlitic affinities of this pseudovolcanic feature.

The aim of this thesis is : firstly to give a comprehensive description of the Gibeon Kimberlite Province as a whole (see figure 1) and to draw some conclusions with regard to the origin and nature of the kimberlite and its associated inclusions; and secondly to give a detailed

description of the Gross Brukkaros and its surrounding area and to draw some conclusions about the relation between this complex structure and the kimberlites.

1. Aerial photographs and maps

The initial prospecting was carried out by alluvial sampling, following the traces of characteristic kimberlite minerals found in dry rivers and creeks, and mapping and field traversing with the aid of aerial photographs.

The aerial photographs were taken by :

1. Area Berseba Native Reserve : Aero Service (Rhodesia) (Pvt) Ltd.,
P.O. Box 10535 Johannesburg
Job nr : A10658, date :
20th January 1958.
2. Area north of Berseba Native Reserve: Aircraft Operating Cy (Aerial Surveys) Ltd.,
P.O. Box 2830 Johannesburg.
Job nr : R.C.8, date :
October 1959.

The maps used were the official "Map of South West Africa 1955 scale 1:800,000" which shows the farm boundaries, and maps from aerial photographs, constructed in the field or in the cartographic department of the Consolidated Diamond Mines of South West Africa, Ltd. at Oranjemund.

2. Laboratory methods

The rock analyses by Miss J. R. Baldwin and Mrs. M. H. Kerr and the mineral analyses by Dr. O. von Knorring were made by the classical wet method. The rock analyses by Dr. G. Hornung were done by X-ray fluorescence, using a

Siemens and Halske "Kristalloflex 4" power unit, coupled to a 2 kw. chromium X-ray tube. The alkalies were determined by a flame photometer and the H₂O by the Penfield tube method, while the CO₂ was calculated as the difference between H₂O and the total loss on ignition. Rocks containing a large amount of volatiles usually give a total of over 100%, because not all the H₂O driven off by ignition is recovered in the Penfield tube and consequently the CO₂ factor is too high.

Mineral separations were done by carefully crushing the rocks in a hardened steel mortar and repeated separations with the aid of Clerici Solution and a Franz isodynamic separator. Several attempts were made to remove alteration rims from minerals by chemical methods but without much result. Good purification could only be obtained by repeated crushings and separations, followed by hand-picking under a strong binocular microscope.

Optical determinations of minerals were, where necessary, confirmed by X-ray diffraction methods.

3. Historical summary

(a) Previous work in the geology of the southern part of South West Africa

The first scientific explorer was Captain Sir James Edward Alexander, who in 1835 travelled from Goodhouse on the Orange River, via Warmbad, Keetmanshoop, Bethanien, the

Upper Konkiep River, Nomtsas, the Naukluft, Ababis, the Lower Kuiseb to Walvis Bay (Alexander, 1838). He passed quite near Mt. Brukkaros, but just too far away to have seen it and there is no mention of it on his map. On information received from Hottentots, Alexander did mark "iron" somewhere east of what is now Gibeon; this probably refers to the many fragments of a nickel-iron meteorite found in that area.

In 1884 Alfred Luderitz acquired the mineral rights over a large area of western Namaland and initiated a programme of scientific exploration and surveying.

A complete bibliography of the early work and a good account of the geology of Great Namaland is given in Dr. Paul Range's book "Geologie des deutschen Namalandes" (Range 1912). After the discovery of diamonds in the coastal deposits south of Luderitz, emphasis shifted to this area and the geology of the diamond deposits and the Diamond Area No. 1 (Sperrgebiet) has been described in a monumental work by Kaiser and Beetz (Kaiser 1926). Further work on the pre-Nama and lower Nama rocks has been done by Rogers (1910; 1912; 1915), Beetz (1922; 1924; 1926; 1929), Knetsch (1937), de Villiers (1945), and Söhnge & de Villiers (1959). The Dwyka series and overlying Kalahari beds have been described by Range (1912b), du Toit (1916), Wagner (1915), and Martin

(1953). Descriptions of several tillites, older than the Dwyka tillite, in Nama and pre-Nama rocks have been published by Gevers (1931), de Kock & Gevers (1932), le Roex (1941) Schwellnus (1941), de Villiers (1945) and Schönge & de Villiers (1959).

(b) Previous work on kimberlites in the Gibeon province

Kimberlites were first discovered in Gibeon village itself and soon afterwards occurrences on the farms Rietkuhl, Hanaus, Deutsche Erde, Freistadt (now part of the Gibeon Native Reserve) and Mukorob were discovered (see Figure 3). Samples of blueground from Gibeon and Mukorob were sent to Cape Town and Berlin and promising reports on the nature of the samples were received (unpublished reports of the Koeniglichen geologischen Landesanstalt und Bergakademie, dated 27th March, 1901 and 8th March, 1902). In 1902 the Gibeon Syndicate was founded to investigate the possible exploitation of the kimberlite occurrences in the Gibeon district.* The Mukorob kimberlites were to be exploited by the Mukorob Minen Gesellschaft. However, because of the Hottentot war work was delayed for three years. In 1906 the Gibeon Syndicate was changed into the Gibeon Schuerf-und Handelsgesellschaft (Gibeon Mining and Trading Cy) and started mining operations under the supervision at first of Dr. Hartmann and later of Professor

* The first prospectus, dated September 1902, was kindly presented to the writer by Mr. J. D. Peters-Hollenberg.

Scheibe. In 1908, diamonds were discovered in the coastal deposits near Lüderitz and all inland mining operations stopped at once while most employees hurried to the coast. Since that time, small-scale mining and testing of various pipes has been undertaken intermittently by small syndicates of local farmers. In 1948 a systematic investigation of several pipes in the southern part of the area was carried out by West-Rand Extensions Ltd. This was followed by a more detailed exploration by a team from the Anglo-American Corporation from 1958 onwards. Meanwhile, the large pipe on Hanaus has been worked by a syndicate of local inhabitants, headed by J. Steenkamp from Mariental.

The Gibeon kimberlites are casually referred to in many publications, but descriptions of individual pipes are rare. Short descriptions of the blueground and a kimberlitic dyke from Mukorob have been published by Scheibe (1906) and Frankel (1956). In addition descriptions of various occurrences are found in Range (1912) and Wagner (1914).

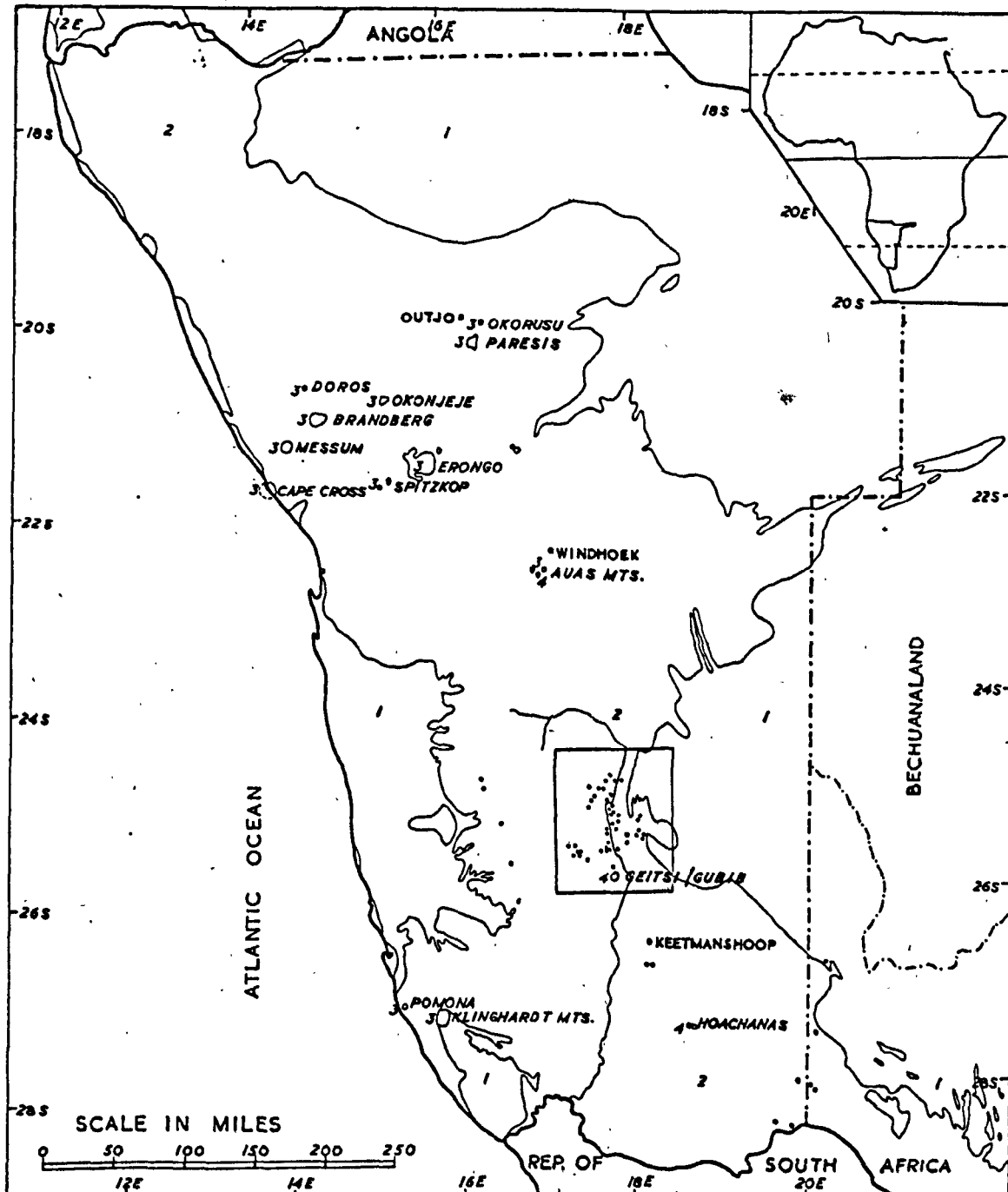
(c) Previous work on Gross Brukkaros mountain

Although much has been written on Gross Brukkaros, only two writers, Schenk and Rogers, give any details and most of the other references are derived from the descriptions of those two authors. The first report of an actual

visit to Mt. Brukkaros is by Schenk (1886), but Chapman mentions this imposing feature in his "Travels in the interior of South Africa", (1868) and shows its position on a map accompanying the book. Schenk wrote four more descriptions of the mountain (Schenk 1893; 1901a; 1901b; 1910) in which he refers to the mountain as a "Porphyrkegel" (porphyritic cone) and later as a "porphyrischer Strato-vulkan" built up by porphyry-tuffs. Other older publications all follow Schenk in using the terms strato-volcano, porphyry-tuffs and quartz porphyry, (Schinz 1891; Rehbock 1898a; Watermeyer 1899; Range 1909), or they quote Schenk's descriptions (Stromer von Reichenback 1896; Schultze 1907; Range 1912).

A paper with more extensive descriptions of the mountain and petrography of the clastic rocks was published by Rogers in 1915. He refers to the mountain as an explosion-pipe or explosion-crater built up by breccias and fine-grained clastic rocks of non-volcanic material. Subsequent descriptions by du Toit (1954) and Truter (1949) are based on this early account. Since then many geologists and other scientists have visited Mt. Brukkaros. From 1926 to 1930 a party of astronomers from the Smithsonian Institute stayed there and built a small observatory, the remains of which can still be seen on the southern rim of the mountain. Hans Cloos gives a report of a visit made in 1936 in company with Korn and Martin (Cloos 1937).

FIG. 1



Outline Map of SOUTH WEST AFRICA

1: area covered by desert sand & surface limestone 2: area with predominantly rock outcrops
 3: intrusions of alkaline rocks 4: agglomerate & breccia complexes • kimberlites

II GREAT NAMALAND

1. General geography and geomorphology

(a) Introduction

For descriptive purposes South West Africa can be divided into three parts, i.e. a northern part, stretching from the Angola border to about 21° S. Lat. and consisting of vast sandy steppe-plains, salt pans and bush-veldt at a general altitude of about 4000 feet; a central mountainous part, formed by a dissected plateau at an altitude of over 6000 feet (Khomas Highland) and several high narrow ranges with a S.W.-N.E. direction; and a southern part (Great Namaland), stretching from the tropic of Capricorn to the Orange River, and consisting of extensive plains and plateaus with very sparse vegetation.

(b) Great Namaland

The southern part of South West Africa can be divided into three regions:

(1) The coastal plain, or Namib desert, which rises from the Atlantic seaboard to an altitude of about 2000 feet at the foot of the Great Escarpment, 50 to 80 miles inland. The surface is made up of bare rock outcrops, stony plains and white sand dunes with solitary mountains (Inselbergs) rising out of the sand at many places.

(2) The central plateau, Great Namaland proper, bounded by the Great Escarpment in the west and by the

Kalahari Basin in the East, formed mainly of unfolded, nearly horizontal arenaceous sediments of the Nama System.

(3) The Kalahari region, an extremely flat surface of calcrete, covered by longitudinal dunes of red sand.

(i) Climate

The climate of South West Africa is influenced by the cold Benguela current which causes the general aridness of the country and in particular of the coastal desert. The mean annual rainfall decreases from the north east to south west; in Andara on the Okavango (N.W. Bechuanaland) it is 565 mm. while in Lüderitz (see figure 2) it averages 20 mm. per annum. Because of the extremely low rainfall, continuously flowing rivers are unknown within the boundaries of South West Africa; most of the rivers flow only for 2 or 3 weeks in a year and contain shallow pools for some time afterwards. The largest river, the Fish River, contains pools throughout the year.

(ii) Erosion scarps and plateaus

Owing to the general arid and semi-arid climate, erosion proceeds mainly by pediplanation and scarp retreat (Dixey 1955). Accordingly most of Great Namaland is broken up into high plateaus and table mountains, bounded by erosion scarps. The most striking feature is the Great African Escarpment, which here separates the coastal plain

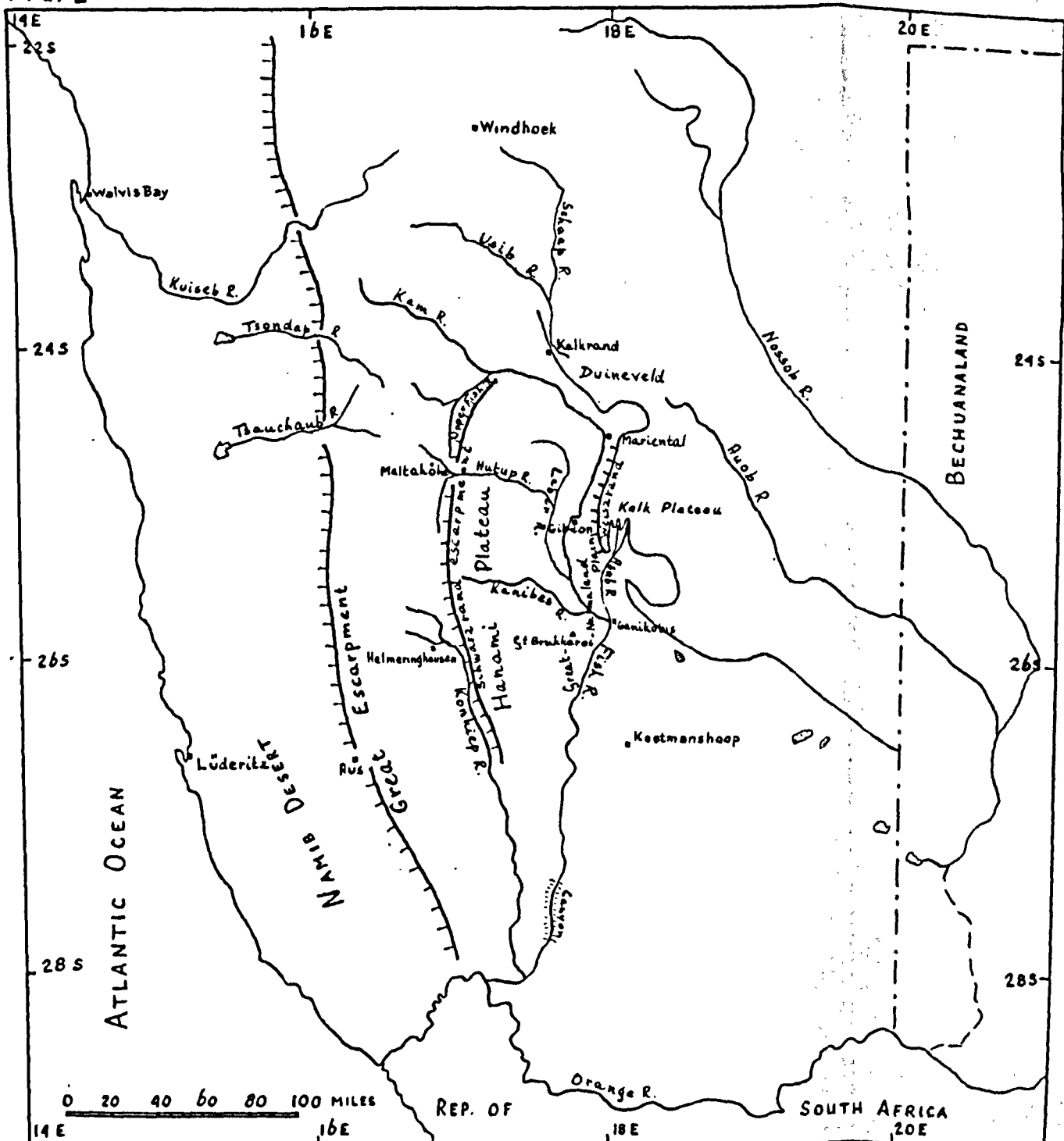
from the central plateau. The Great Escarpment is mainly formed of gneisses and granites and rises abruptly from 2000 feet to an altitude of 5000 feet in southern and over 6000 feet in northern Namaland.

Thirty to forty miles to the east of the Great Escarpment and trending roughly parallel to it, there is a second escarpment, which can be traced from the upper reaches of the Fish River southwards to the Luederitz-Keetmanshoop railway (figure 2). It forms the western edge of the Schwarzrand plateau, which reaches altitudes of over 6000 feet along its western border.

The surface of the Schwarzrand plateau is formed of red sandstones with intercalated resistant quartzites, which give rise to a landscape with flat rocky plateaus, cut by narrow, flat-bottomed, sandy, dry valleys with steep sides and "free faces" on top.

One can distinguish between a higher western Schwarzrand plateau (the Hanami plateau) sloping from west to east from about 6000 feet to 5000 feet and a lower, more undulating, dissected plateau, the lower Schwarzrand, at an altitude of about 4200 feet to 4000 feet. Both the higher and the lower Schwarzrand plateaus have an east-flowing drainage, which on the lower Schwarzrand forms a rectangular-dendritic pattern, governed by a rectangular joint-system in the sandstones at N 120° - 125°E and N 30° - 35° E.

FIG. 2



Outline Map of the Southern Part of South West Africa
topographical features

Between the Schwarzrand plateau in the west and the Kalahari margin in the east stretches a large plain, the Great Nama(qua)land Plain, drained by the south-going Fish River and its tributaries and rising with a regional slope of 4 feet per mile from 3100 feet in the south to 3600 feet altitude north of Mariental (Mabbutt, 1955). A low escarpment 150 to 200 feet high separates it in the east from a higher plain with an extremely flat calcrete surface, the Kalahari Limestone Plain, or Kalk plateau as it is locally named. The escarpment is most prominently developed in the area between Asab and Mariental and here it is called the Uri-nanib (white scarp or Weiszrand).

North of Mariental the Uri-nanib escarpment loses height rapidly and, north of Kalkrand, it becomes obscured by the Duineveld (the most westerly extension of the Kalahari sands) and finally loses its identity where the Great Nama-land Plain and the Kalahari Limestone Plain merge just north of Tsumis (see figure 2). Mabbutt (1955) considers that both these plains remnants represent one erosion surface of the African Cycle. The escarpment between the Great Nama-land Plain and the Kalahari Limestone Plain would then not be the expression of an erosional break separating two continental cycles, but a regional lowering of base level in the Great Namaland Plain, due to a reorientated drainage system, the Fish River system, superimposed upon an older

southeasterly Kalahari drainage. The names Atlantic- and Kalahari-phase, belonging to the same African cycle, were proposed (Mabbutt, 1955).

The lowering of base level in the Great Namaland Plain has rejuvenated the drainage in the Schwarzrand, now belonging to the western tributaries of the Fish River. The streams are incised in deep gorges which almost reach the western edge of the Schwarzrand plateau and in fact the most important stream, the Hutup, cuts back through the Schwarzrand escarpment at Maltahöhe and drains the Grootfontein Plain west of the escarpment.

The Great Namaland Plain has been cut into the argillaceous sandstones and arenaceous shales of the Nama formation and in tillites and mudstones of the Dwyka series. The area underlain by the arenaceous shales is very flat, the drainage proceeding by sheetwash or very shallow rivulets and gullies. The clayey parts of the shale accumulate in mud-flats or vleis. The sandy parts are blown out and form small dunes.

Out of the middle of the Great Namaland Plain, in the Berseba Native Reserve rises one large solitary mountain, the Gross Brukkaros or Geitsi/Gubib, the subject of discussion below (see plate 2).

In an area, stretching from Mount Brukkaros to points 70 miles to the north, roughly between 25° and 26° S. Lat. and 17° 30' and 18° 30' E. Long. 46 pipes and 16 fissures of kimberlite and associated rocks were mapped. This area is

named the Gibeon Kimberlite Province.

Eleven of the pipes lie in the lower Schwarzrand, and two very near the Uri-nanib escarpment, one of them actually in a small outlier of the Kalahari Limestone Plain; the rest of the pipes are in the Great Namaland Plain.

2. Regional geology

(a) Introduction

The earliest rocks in Great Namaland, which can be dated with reasonable certainty, are the sedimentary rocks of the Nama system. Primitive fossils, mainly sponges, have been found in the lower part of the Nama, the Kuibis quartzites (Gürich, 1930, 1933; Haughton, 1960; Richter, 1955). They suggest a late Pre-Cambrian or Eo-Cambrian age.

The basal beds of the Nama rest in many places on a surface of highly metamorphosed rocks, gneisses, migmatites and intrusives, but in some areas, for example along the Orange River (de Villiers 1945) and at Helmeringhausen (Range 1912; Beetz 1922) (see figure 2), less metamorphosed tuffs and sediments, slates, conglomerates and greywackes can be observed between the basement and the Nama rocks.

(b) Pre-Nama rocks

(i) Older gneisses and schists

Pre-Cambrian gneisses containing no recognizable sediments have a wide distribution in the neighbourhood of the coast near Lüderitz and along the Great Escarpment (Beetz 1922; Range 1912). They are mainly basic gneisses, much injected by plagioclase-rich granitic material (Beetz 1924); in the field these comprise gneissic granite and

granite-gneiss, grading into injection-gneisses, migmatites and amphibolites surrounded by biotite-schists. Range refers to these rocks as Gneis-granithorizont (the injection gneiss) and Gneisschieferhorizont (biotite-schists). They will be referred to simply as older gneiss and older schists. Most of the Basement of South West Africa probably consists of these older gneisses and schists, which apart from the coastal and escarpment exposures, reappear to the east from below the cover of Nama rocks as fault- and erosion- inliers.

The irregular surface of the older gneisses and schists is clearly demonstrated by 3 residual mountains (monadnocks), which protrude as inliers of older gneisses and schists through the Kuibis Quartzites and the Schwarzkalk of the Nama formation on the plain west of the Konkiep River between Konkiep and Helmeringhausen (figure 2). The southernmost one, the Schwarze Kuppe, is 6270 feet high and is situated just north of the road from Konkiep to Kuibis, 15 miles west of Konkiep. The surrounding plain is at about 3650 feet altitude and the surface is made up of Schwarzkalk limestone, overlying Kuibis quartzites. The dark coloured biotite schists of the Schwarze Kuppe are unconformably overlain by these sediments. The second mountain, 3 miles due west of Bethanien contains muscovite-schists and muscovite-biotite-schists with porphyroblastic feldspars

The basal conglomerate of the Nama formation is exposed at several places in gullies around the mountain.

The third mountain is situated on the farm Karadaus, 15 miles south of Helmeringhausen.

(ii) Younger schists, marbles, lavas and pre-Nama sediments

Remnants of a thick succession of sedimentary rocks can be observed between the older gneisses and schists and the Nama formation at various places along the Great Escarpment. The rocks generally form isolated outcrops and cannot clearly be correlated with one another. They have been subjected to different degrees of metamorphism and probably belong to quite different series or systems.

These rocks may be described in five groups as follows :-

1. A group of distinctly bedded, undoubted sediments is found in the neighbourhood of Aus (Beetz 1924). They consist of mica-schists, marbles and conglomerates and are intruded and injected by a gneiss-granite. The granite is contaminated and rich in garnet; it is characterized by schlieren and xenoliths, and surrounded by an aureole of migmatites and amphibolites (Beetz 1924);

2. Several different series of low-grade metamorphosed sediments, tuffs and lavas are exposed in the Helmeringhausen area (figure 2). They were previously grouped together under the name of Konkiep System (Range 1912, Beetz 1922)

and separated into three series as follows (Beetz 1922):

Nama formation

Unconformity

Auborus series - unmetamorphosed red sandstones
and conglomerates

Unconformity

Sinclair series - acid- and basic meta-lavas

Unconformity

Kunjas series - conglomerates, slates, tuffs

Unconformity

It is evident in the field that the Auborus rocks represent a quite distinct series, resting unconformably upon the low-grade sediments and lavas or directly upon the older gneisses and schists, but there is no reason why all three series should be grouped in one system. Furthermore, it seems likely that instead of three, only two different series exist, because it seems that the Kunjas sediments are intercalated with the Sinclair volcanics. On the basis of these data Martin has suggested that the names Konkiep System and Kunjas series should be abolished and only the names Sinclair and Auborus series retained (Martin 1950);

3. A group of conglomerates, tuffs, quartzites and marly sandstones is exposed on the farms Kunjas and Korais, 10 miles west of Helmeringhausen (see figure 2). They appear to occur below and intercalated with the Sinclair

volcanics - and are on the whole steeply folded in an E - W direction. The basal bed consists of a steeply dipping conglomerate, lying discordantly on a red granite. Younger leucocratic and aplitic granites have intruded and altered the sediments and lavas. On the farms Goais and Helmeringhausen the sediments are transformed into an aureole of hornblende gneisses, amphibolites and epidote-amphibolites, round a red granite, while the lavas have been partially melted and assimilated and form a striking sight of large black hornblende-rich patches in a leucocratic granite;

4. A group of low grade mica schists, slates and greywackes is exposed on the farms Mooifontein and Goais, 10 miles south of Helmeringhausen. They are folded along a NW-SE direction and intruded by an aplitic granite, not far from Mooifontein farmhouse. The relation to the nearby Sinclair meta-lavas is not yet clearly established. Another isolated outcrop of NW-SE folded mica schists occurs on the farm Wittmanshaar, 15 miles north west of Helmeringhausen;

5. The quite distinct series of the Auborus sandstones and conglomerates rests unconformably upon the volcanics and sediments of the Sinclair series or directly on the crystalline basement of older gneiss and schists or red granite. The colour, and granularity of the red granite and the red sandstone are so similar that from a short

distance it is difficult to distinguish between the two rocks.

The Auborus rocks do not show signs of metamorphism, but they are tilted and locally folded. Sloping table mountains are formed where the beds have only low dips, as on the farm Auborus, the type locality.

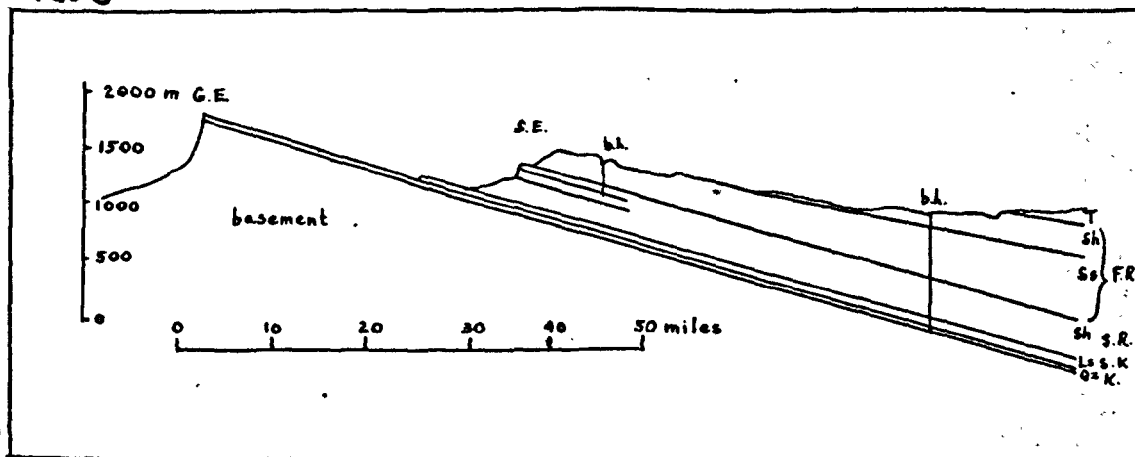
(c) Nama system

Range (1912) subdivided the Nama System as follows:-

Fish River series	}	Upper Nama
Schwarzrand series		
Schwarzkalk series	}	Lower Nama
Kuibis series (including		
Basal beds)		

This subdivision is based on the development of the system in the Bethanien district of South West Africa. There is no particular reason for the division into Upper and Lower Nama, as all series overlies each other conformably and there is no stratigraphical break. The whole succession consists of nearly horizontal beds, with the result that most of the higher inland plateaus are formed by the youngest series, the Fish River series, which underlies most of the Schwarzrand plateau and the Great Namaland Plain with a homoclinal dip of ca. 3° to the northeast (figure 3). The complete sequence is only occasionally present; the Basal beds and the Kuibis quartzites are very much reduced in thickness or are absent in areas north of Bethanien, while in other places the deposition of limestone continued

FIG. 3



Schematic profile through the Nama sediments in Great Namaland (after Haughton & Martin 1956).

G.E. - Great Escarpment; S.E. - Schwarzrand Escarpment;

b.h. - borehole; Qz. K - quartzite Kuibis series;

Ls.S.K. - limestone Schwarzkalk series;

Sh. S.R. - shales Schwarzrand series;

Ss. Sh. F.R. - sandstones & shales Fish River series;

T. - tillite Dwyka series.

throughout the succession up to the base of the Fish River series, and the Schwarzrand series cannot be separated from the Schwarzkalk (Martin 1956).

(i) Kuibis series (including Basal beds)

The stratigraphical succession in the Kuibis region is as follows :-

Pinkish soft shales	}	Kuibis series
White to pink quartzites		
Arkose	}	Basal beds
Conglomerate		

Over wide areas the basal beds of the Nama system rest unconformably on an irregular surface of older rocks. They consist of a basal conglomerate and arkose and are overlain by the pinkish quartzites of the Kuibis series, which can attain a thickness of several hundred feet. On the farm Helmeringhausen only a few feet of arkose and quartzite occur between the basement granite and the Schwarzkalk limestone, while the basal conglomerate is only found in small depressions in the granite. The Basal beds and Kuibis quartzite are similarly restricted at places north of Helmeringhausen, (e.g. Kleinfontein and Portjes), where the Schwarzkalk limestone rests directly on the basement (Beetz 1922).

Immediately below the boundary with the Schwarzkalk limestone, is a three to four feet thick layer of soft pinkish-white shale, which has a wide distribution and forms

a good marker-horizon between the Kuibis and Schwarzkalk series. It is quarried locally and used for road surfacing.

(ii) Schwarzkalk Series

The Schwarzkalk series consists of a group of calcareous sediments, with intercalated black shales. The thickness varies from about 150 feet to 1000 feet (Beetz 1922, Martin 1956). The magnesia content is generally less than 2% (Range 1912).

(iii) Schwartrand Series

The soft bluish-grey to grey-green shales of the Schwartrand series are particularly well exposed in the escarpment which forms the western edge of the Schwartrand plateau. The series is about 1150 feet thick (Martin 1956) and builds up the slope of the escarpment between Bethanien and Maltahöhe, gradually moving lower in the slope and then forming the land in front of it. Near Maltahöhe the Schwartrand shales no longer form the escarpment (which swings to the east, north of Maltahöhe) but underlie large parts of the country between the Schwartrand escarpment and the Zaris and Naukluft Mts. Numerous intercalations of sandstone and quartzite occur between the soft shales, especially in the area towards the Naukluft Mts., where quartzite ridges constitute the watershed between the Fish River drainage and the Tsondap and Tsauchaub rivers. The soft shales are easily eroded and

form large shallow depressions, filled with alluvium, e.g. the Grootfontein-, Urikos- and Bullsport-plains.

A conglomeratic quartzite with pebbles of milky quartz and jasper has been chosen as the boundary between the Schwarzrand and the Fish River series (Beetz 1922, Martin 1956). Pebble covered surfaces, derived from this bed are conspicuous at the top of the Schwarzrand escarpment on the farms Dreylinge, Stockdale and Chamchawib and on a low hill in the Grootfontein plain, on the farm Grootplaas Noord, 15 miles west of Maltahöhe (figure 2).

(iv) Fish River Series

This series consists of a thick succession of red and purple quartzites, sandstones and arenaceous shales. The base is formed by a conglomeratic quartzite, and the lower part of the series is arenaceous becoming more argillaceous towards the top. The maximum thickness is 2300 feet, but as the boundary with the overlying Dwyka tillite is an unconformity the original thickness must have exceeded this (Martin 1956).

The succession is as follows:

500 feet	{ shale sandstone (current-bedded) maroon shale
400 feet	argillaceous sandstone
1400 feet	{ sandstone quartzite

Hard sandstones and quartzites of the lower 1400 feet

of the succession from the 30 miles wide Hanami plateau or higher Schwarzrand. A topographically prominent quartzite forms a definite step separating the higher smooth plateau from the more dissected lower Schwarzrand, which is built up of softer sandstones with more and more intercalations of arenaceous shales. The sandstones have a well developed joint pattern at N 35° E and N 125° E and are traversed by many normal faults with a downthrow to the east. The faults are usually less than 10 miles long and start in a northerly direction (occasionally beginning in a monocline), which later changes to NNW to NW.

The fissured sandstones and quartzites are highly permeable, but intercalated shale beds form water reservoirs which are occasionally tapped by some of the larger faults, giving rise to natural springs, (e.g. on Alt. Rietkuil 10 miles west of Gibeon, figure 2).

The upper 500 feet of the Fish River series are formed by the arenaceous maroon coloured shales which underlie large parts of the Great Namaqualand Plain. The most argillaceous rocks occur in the middle of the stage and many thin layers of flagstones are intercalated between the shales towards the top.

The flagstones and sandy shale horizons have a definite joint pattern trending N 65° to 75° E and N 145° to 160°E; they are particularly well expressed where they

cross mud flats. The NW-SE direction is the most pronounced and is ca N 147° E in the Berseba Reserve and ca N 159° E on the farm Gelwater.

As a result of the homoclinal northeasterly dip of the Fish River series, younger horizons, mainly consisting of softer, more reddish shales appear in the areas further to the north.

Perfect examples of many shallow water features such as ripple marks, clay pellets and current bedding can be observed in these horizons (see plate 1). A persistent, hard, current bedded sandstone forms an escarpment of local importance near the boundary with the Dwyka series.

(d) Karroo system

The Karroo formation rests on the Nama formation with a slight angular unconformity, which represents a large stratigraphical hiatus. The whole sequence of the Cape System is missing in South West Africa.

(i) Dwyka Series

Rocks of the Dwyka series are exposed in large areas in Great Namaland between the Kalahari Limestone Plain and the Fish River from Mariental in the north to 40 miles south of Keetmanshoop (figure 2). The lower stages of the series consist of glacial beds alternating with marine beds. The higher stages of the sequence consist of a succession of blue-black shales with sandstone and coal lenses, which

Plate 1. Current bedding in the Fish River sandstone
of the escarpment on the farm Hanaus near
Gibeon.

Wright (1953) considers to be upper Devon shale - lower



Dark-gray calcareous shale with lime-
stone lenses containing graptolites and
plant stems.

Calcareous grit

Coarser-grained shale with *Surelyana*-shells in
lower part.

Dark-gray shale & mudstone with lime-
stone lenses and plant-in-plant stems
especially developed in a few
layers.

Dark-colored mudstone with limestone
lenses containing fish bones and
plant stems.

Mudstone and sandstone-shales

Dark-colored, silty mudstone to sandstone
with scattered, irregularly shaped
plant stems.

Dark-colored mudstone

Dark-colored mudstone

Wright (1953)

Martin (1953) considers to be upper Dwyka while other authors prefer to regard this as the lower part of the Eccca series (du Toit 1954).

The stratigraphical succession is as follows
(modified after Martin 1953):

Kalahari Beds
unconformity

600 to 700 ft.	blue shales with sandstones and coal-lenses	
	(grey boulder-shales with two persistent sandstones	} 3rd glacial beds
	(green boulder-mudstone with large yellow marl concretions	
	(boulder-shale (containing giant blocks)	
	(Dark-grey calcareous shale with limestone lenses containing crinoids and gastropods	} 2nd marine beds
800 to 1000 ft.	calcareous grit	} 2nd glacial beds
	(boulder-shale with Euredysma-shells in lower part	
	(blue-grey shale & mudstone with limestone lenses and cone-in-cone marl sandstone (locally developed in Gibeon Reserve)	} 1st marine beds
	(dark coloured mudstone with limestone lenses, containing fish fauna at Ganikobis	
	(tillites and boulder-shales	} basal beds max. 300 ft.
	(impersistent gritty sandstone (forms an irregular escarpment between Lichtenfels and Gibeon)	
	(green boulder-mudstone	
	(tillite	
	(green mudstone or sandy shale	
	unconformity	
	maroon shales	

The basal beds of tillites and boulder shales with impersistent gritty sandstones, underlie the area west of the railway from Tses to Mariental and form hummocky stony surfaces with pebbles and boulders of all sizes up to 2 yards diameter.

Dr. Martin has recognized three to four ground-morainic sheets (tillites) separated by boulder-mudstones or boulder-shale in the area west of Asab where the basal beds have their greatest development (Martin 1953). Near Gibeon one of the hard tillite bands forms a small scarp around a local pene plain on the farm Hobby Garden.

In many places a thin bed of light-green mudstone or soft sandy shale occurs between the tillite and the top of the Nama rocks; these may represent a periglacial deposit. Tillite resting on a striated glacial pavement of Nama rocks can be observed in little streams southwest of Gibeon.

The tillites and boulder-shales of the basal beds are followed by the soft dark coloured calcareous mudstones of the first marine beds. The soft mudstones are easily eroded and form large shallow depressions in front of the Urinanib escarpment, which are filled with hillwash and alluvium to a depth of 5 to 8 feet, e.g. Gründorner Plain on the farm Gründorner Fläche (figure 4).

Where parts of the Kalahari Limestone Plain have been removed by the Asab River drainage, between Asab and

Tses (figure 2), the higher stages of the Dwyka series are exposed.

(ii) Stormberg Series

Cave Sandstone. A light-grey compact aeolian sandstone rests with a slight unconformity on outliers of 6 to 8 feet of tillite and boulder-mudstone on several small table-mountains 5 miles east of Mt. Brukkaros, and transgresses across the tillite on to the Fish River series (see plate 2). It bears a strong lithological resemblance to the Cave Sandstone and it is tentatively correlated with it (Martin 1953).

The area, in which the table mountains are located, is traversed by several small normal faults of post-Stormberg age. The vertical displacement of the largest N-S fault, measured by the difference in altitude between levels of the Cave Sandstone on both sides of the fault, is 200 feet.

Amygdaloidal Basalt. Outcrops of amygdaloidal basalt occur in many places in the area between Mariental, Kub and Hoachanas. Fine-grained bluish-black basalt as well as coarser ophitic dolerite exist, both types are amygdaloidal. The amygdules are filled with chlorite, calcite and natrolite. Pipe-amygdules are frequent in the bottom part of the series. The basalt rests on the Upper Dwyka sandstones east of Mariental and transgresses over the lower Dwyka beds on to the Fish River series. At Kub they rest on a few feet of

tillite, but on the farm Gras, 15 miles southwest of Kalkrand, they rest on Nama shales (figure 2). Accidental inclusions of amygdaloidal basalt in the kimberlites around Gibeon show that the Kub-Hoachanas lavas covered a far more extensive area at the time of formation of the kimberlites.

(iii) Karroo dolerites

Sills and dykes of dolerite occur in a wide area around Keetmanshoop and Karasburg. The northern limit of the Karroo dolerites runs from about 5 miles west of Seeheim to Tses. The northernmost occurrence is at Okameamihi, 10 miles northeast of Tses, where a dyke, 30 feet wide and with northeasterly direction, forms a mile long ridge in front of the Urinanib escarpment before disappearing under the calcrete of the Kalahari Limestone Plain.

(e) Kalahari beds

In the Urinanib escarpment the Upper Dwyka sandstones are overlain by 50 feet of bedded gravels and sands of fluvial origin (Range 1912; Mabbutt 1955). The gravels rest on the deeply weathered "pre-Kalahari surface" of Cretaceous age (Mabbutt 1955). They consist mostly of opaque white quartzite pebbles, derived from the Nama quartzites and sandstones in the west and northwest (Range 1912), and deposited by the ancient east to southeast interior drainage (Kalahari drainage) in a wetter period

during the early-Middle Tertiary (Mabbutt 1955).

Subsequent calcification in a dry period during the early Pliocene (Mabbutt 1955) changed the top 10 to 20 feet of gravels and sands into a sandy limestone, Kalahari Limestone, with hard crust of calcrete.

The carving of the Great Namaqualand Plain out of the Kalahari Limestone Plain by the SSW Fish River drainage system in the Upper Tertiary (Mabbutt 1955) pushed the western edge of the Kalahari Beds far to the east (see plate 3). At the moment the greatest erosion takes place in the Asab River drainage system. Large areas in front of the Urinanib escarpment are covered by white quartz gravels which, according to Range (1912), represent eluvial pebble gravels left behind when the escarpment receded (see plate 2). From the extent of these pebbles Range deduced that the escarpment once lay at least 45 miles further west.

The calcrete crust extended probably far beyond the boundary of the Kalahari Limestone Plain. Only on the calcareous Dwyka rocks and the calcareous sands and gravels is surface limestone thickly developed, but thin calcrete surfaces occur on the Nama sandstone and shales near the down-throw side of small faults in the lower Schwarzrand.

Larger calcrete surfaces exist in the Bullsport plain at 4920 feet and at Helmeringhausen at 4450 feet (figure 2).

Plate 2. Great Namaland Plain with eluvial pebble cover. Mt. Brukkaros in the background; flat topped hills to the left capped by Cave Sandstone.

Plate 3. Mukorob Rock. An erosion remnant of the Kalahari Limestone Plain on the farm Burgerville (part of farm Mukorob) near Asab.



PROVINDE



III KIMBERLITES AND RELATED
INTRUSIONS OF THE GIBEON
PROVINCE

The intrusive rocks, which occur in the Nama plateau of South West Africa, can be divided into two groups :

1. Kimberlites.
2. Calcium-rich rocks with kimberlitic affinities.

The kimberlites are characterized by their typical occurrence in vents and fissures, their specific mineralogy and by containing nodular inclusions of deep-seated origin.

The rocks of group 2. combine some or all these characteristics with a high content of calcite or monticellite and show similarities to carbonatites.

1. Kimberlites

(a) Description of the kimberlite occurrences

(i) Introduction

The term "kimberlite" was first introduced by Lewis (1888) for the brecciated, serpentized, peridotitic rocks occurring in the Kimberley area of South Africa. Chemically kimberlites are ultrabasic rocks characterized by a very low silica content, combined with a comparatively high content of alkalis and volatiles.

Rocks of this group often contain a large number of inclusions, fragments of other rocks of mixed origin, sedimentary, metamorphic and plutonic. Previously it was thought that these inclusion-rich rocks were the expression of highly explosive volcanism (Wagner 1954). Kimberlites

typically occur in stable areas, the Precambrian shield areas or "high cratons"; their presence in the "low cratons" (ocean basins) is not yet known.

The form of kimberlite bodies, revealed by diamond mining (Wagner 1941; Williams 1952) is that of a vertically downward-tapering vent, which in cross section is irregularly rounded and lobed, probably resulting from the coalescence of two or more channels of intrusion (du Toit 1954; Dawson 1963; Nixon et al 1963).

The surface expression of many vents is a roughly circular outcrop hence the colloquial name "pipe". The vents occasionally retain their roughly circular cross section for short distances, but there is a strong suggestion that they change shape with depth (Williams 1952).

Most vents show elongated or irregular outcrops, generally connected with fissures and dykes; many outcrops are only a local widening of a fissure, a so called "blow" or "fissure-pipe" (Williams 1952).

Near the surface kimberlite typically occurs as a soft clayey rock, called blue ground, which results in a slight depression on the outcrop. Some kimberlite, however, occurs as hard brittle rock, called hardebank, which forms low humps. Blue ground is changed into yellow ground in the topmost layer on the outcrop of the vents.

(ii) Field occurrences in the Gibeon province

Location and distribution

The Gibeon province forms a part of the stable South African Shield which in the southern part of South West Africa is built up by Precambrian metamorphic rocks (base-ment) and late-Precambrian to early Palaeozoic sedimentary rocks (Nama formation), while late Palaeozoic sediments (Dwyka series) are less extensive.

The location and distribution of kimberlites is shown in table 1 and figure 4.

In total, 46 kimberlite-pipes or fissure-pipes and 16 fissures have been mapped. The intrusion in the western part of the area cut the Nama rocks, whereas those in the eastern part cut also the Dwyka rocks. Further to the east the Dwyka is overlain by the calcified sands and gravels of the Kalahari Beds which are younger than the kimberlites. In one case a kimberlite (Mukorob M2) has been found, which is actually covered by an outlier of the Kalahari Beds. The outlier has been reduced to a little hill and the kimberlite forms outcrops under the Kalahari beds on the side of the hill. It is probable that many more kimberlites are hidden under the Kalahari deposits.

The kimberlites were found by a method of alluvial prospecting combined with air photo interpretation. The air photo interpretation works very well in the western part of the area where the colour difference between the

blue ground and red Nama rocks is very obvious, but small mud pans or abandoned sheep- and cattle-kraals obscure the picture, as they produce the same grey tone colours on the air photographs as kimberlites.

It is much more difficult to delimit the kimberlite outcrops in the Dwyka rocks. The colour difference of blue ground and Dwyka rock is not very marked and upturned slabs of host rock are generally absent owing to the friable character of the host rock. Furthermore most of the surface indications are obliterated by the formation of rubble plains derived from the tillite or pebble covered surfaces from the Kalkplateau. The presence of a kimberlite is only indicated by a concentration of typical kimberlite minerals on the surface and has to be verified by test pits and trenches.

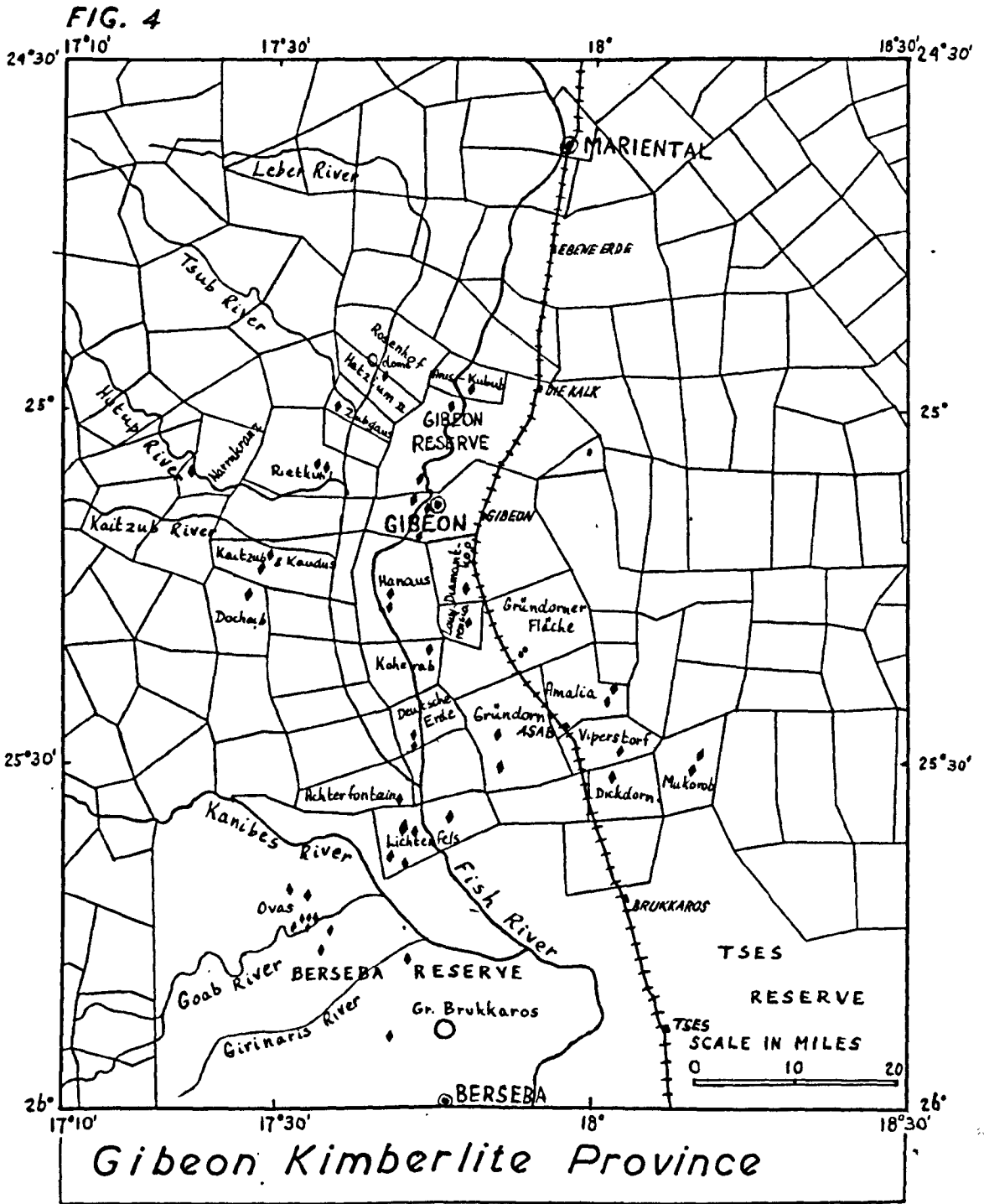


TABLE 1. Kimberlites of the Gibeon Province, South West Africa

Number and form of occurrences (diameter of pipes in yards, followed by elongation or strike direction, if any)	Nature of rock in/outcrop	Nature of inclusion
Keetmanshoop district : Berseba Native Reserve Ovas area		
01 oval pipe 145 x 65 52°	hardebank	dolerite encased in calcrete
02 fissure pipe 140 x 34 99°	dolerite + some hardebank	dolerite, amphibolite, gabbro (probable feeding duct)
03 fissure pipe 115 x 75 on a dyke, strike 83°	hardebank	dolerite, amphibolite, gabbro, hypersthene-granulite, norite
04a 12 x 6) -two fissure 04b 10 x 8) pipes on the same dyke as 03, strike 83°	hardebank, calcrete-rubble	dolerite encased in calcrete
05 size & shape uncertain, probably roughly circular 110 y.	partly covered by river alluvium hardebank	dolerite, amphibolite
06 oval pipe 250 x 110 92°	blue ground, calcrete rubble	dolerite
07 oval pipe 100 x 70 92°	dolerite + hardebank	(probable feeding duct)
08 size & shape uncertain, very small	blue ground, calcrete rubble covered by river alluvium	
09 size & shape uncertain plus 9 narrow fissures	- do - micaceous kimberlite, calcrete rubble + kimb. min.	

Table 1 continued :

Berseba Native Reserve : Brukkaros area

B10 oval pipe 155 x 90 75°	blue ground, calcrete rubble	dolerite, micro- breccia
B11 fissure pipe 280 x 40 150°	blue ground out- crop 140 x 40 rest covered by sheetwash	garnet pegmatite
Farm Lichtenfels		
L1 size & shape uncertain roughly circular 90 y.	blue ground, yellow- ground covered by terrace gravels	micaceous kimb- erlite, garnet peridotite olivine-dolerite
L 2 oval pipe 90° x 150	green hardebank- breccia sheetwash debris	olivine dolerite, many discrete garnet and diop- side nodules.
L3 20 ft. wide dyke 10°	slightly micaceous hardebank	large olivine phenocrysts
L 4 size & shape uncertain	covered by sheet- wash debris yellowground	
L5 roughly circular pipe 60 x 45	green bardebank- breccia	olivine-dolerite
L6 10 inch wide dyke	greenish grey harde- bank	garnet- peridotite
L7 fissure pipe 70 x 50 on a fissure 18°	green hardebank	olivine-dolerite baked shale
Farm Dickdorn (including Viperstorf)		
Di 1 oval pipe 120 x 80 35°	blue ground, yellow ground	large phlogopite flakes, corroded ilmenite
Di 2 circular pipe 150 x 140 Di 1 & Di 2 are on a line, striking 35°	blue ground, yellow ground	garnet-lherzolite altered shale

Table 1 continued :

Farm Mukorob

M1 size & shape uncertain ca. 200 y.	blue ground, yellow ground, surface covered by gravels windpump erected on outcrop	micaceous kimberlite, amphibolite.
M2 roughly circular pipe 130 y.	blue ground, yellow ground, covered by a little hill of calc. gravels, capped by calcrete	micaceous kimberlite, garnet-peridotite, amphibolite, norite, pyroxene gabbro.
M1 and M2 are on a line,	striking 34°	
M3 5 to 4 ft. wide dyke strike 34° not visibly connected with M2, running to one mile south of M2	limestone; calcitized olivine melilitite?	ilmenite-encased olivine nodules, norite, ilmenite garnet rocks.

Gibeon district : Farm Achterfontein I (part of Lichtenfels)

a

LAl fissure pipe 45 x 35	hardebank, blue ground	micaceous garnet-peridotite, garnet-lherzolite olivine-dolerite, large garnet-nodules
--------------------------	------------------------	---

Farm Gruendorn

G1 oval pipe 200 x 150 44°	blue ground, yellow ground, windpump & kraal on the outcrop	
G2 oval pipe 60 x 40 44°	blue ground covered by gravel from Dwyka tillite	leuco-norite, pyroxene nodules with exsolution lamellae
G1 & G2 are on a line strike 44°		

Table 1 continued :

Farm Deutsche Erde

DE1 oval pipe 160 x 100 161°	blue ground	gabbro, norite, anorthosite, garneteproxenite, serpentinite.
DE2 circular pipe 24 x 24	blue ground covered by shale debris	large corroded ilmenite.
DE1 & DE 2 are on a line strike 161°		

Farm Amalia

A1 oval pipe 120 x 65 34°	hardebank, yellow ground covered by terrace gravels	large garnet and olivine nodules
A2 oval pipe 250 x 150 34°	yellow ground, covered by terr- ace gravels	chromediopside- enstatite nodules.
A3 4 to 5 ft. wide dyke, strike 34° connecting A1 & A2	calcitized yellow ground	mudstone, large ilmenite.

Farm Koherab

K1 size & shape uncertain	blue ground covered by gravel from Dwyka tillite	
------------------------------	--	--

Farm Louwrensia

Lol roughly circular pipe 65 x 55	blue ground, yellow ground farmhouse, wind- pump & kraals on the outcrop	peridotite, garnet-peridotite, garnet-lherzolite, glimmerite
--------------------------------------	--	---

Farm Diamantkop

Dal oval pipe 300 x 160 160°	dolerite + basalt, some hardebank	(probably feeding duct for Kub- Hoachanas lava)
---------------------------------	--------------------------------------	---

Table 1 continued :

Farm Hanaus

Ha1 kidney shaped pipe 500 x 300 45° multiple intrusion vent	blue ground dolerite + basalt	amygdaloidal basalt, basalt, garnet- peridotite, pyroxenite, mica- ceous peridotite, very large garnet nodules. (probable feeding duct)
Ha2 oval pipe 135 x 120	amygdaloidal basalt + some blue ground	

Gibeon Townlands

GT1 circular pipe 60 x 60	blue ground, main road, church & post office are built on or along the outcrop.	garnet- peridotite
GT2 fissure pipe 350 x 75 26°	very hard green hardebank-breccia forms a hill south end; softer blue ground	garnet-lherzolite amygdaloidal basalt.
GT3 circular pipe 35 x 30	blue ground	

Gibeon (or Kranzplatz) Native Reserve

GR1 fissure pipe 300 x 50 26° on the same fissure as GT2	harde green harde- bank-breccia; black hardebank	serpentinized peridotite
GR2 size & shape uncer- tain ca. 350 x 100	blue ground-breccia	

Farm Anis-Kubub

AK1 oval pipe 120 x 80	hardebank-breccia	garnet-lherzolite
------------------------	-------------------	-------------------

Farm Kabiais

Kal 1 ft. wide fissure	blue ground, calcrete rubble	
------------------------	---------------------------------	--

Table 1 continued :

Farm Docheib

Do 1 fissure pipe 400 x 60 40°	blue ground, yellow ground	garnet-pyroxenite
-----------------------------------	-------------------------------	-------------------

Farm Kaudus & Kaitzub

KK1 fissure pipe 400 x 80 42°	yellow ground, calcrete	garnet-pyroxenite, dolerite encased in calcrete.
KK2 fissure pipe 60 x 40 42° on the same fissure as KK1	blue ground, cal- crete hardebank	garnet-pyroxenite, basalt.

Farm Rietkuhl

R1 S-shaped fissure 200 x 70	hardebank	basalt.
R2 circular pipe 100 x 90	basalt + amygdal- oidal basalt	some blue ground (probable feed- ing duct)
E-W trending fissure links R1 and R2		

Farm Zubgaus

Z1 fissure pipe 90 x 35	hardebank	basalt
-------------------------	-----------	--------

Farm Narrnkranz

N1 size & shape uncer- tain exposed in river cutting 250 y. long	greenish-grey hardebank	amphibolite
---	----------------------------	-------------

Farm Hatzium

Ht1 circular pipe 120 x 120 with dyke entering southeast part	green hardebank black calcitized hardebank yellow phosphatic rock	ilmenite-encased nodules
--	--	-----------------------------

Contact with host rock

The outcrops of the vents, which cut the Nama rocks are very distinct. The Nama sandstones or shales are steeply upturned at the contact, but dips flatten out in a distance of less than 15 yards (see plates 4 and 5). Contact metamorphism is absent or very slight; the red sandstones or shales have been changed into green ones for less than 10 yards in two or three cases, but this is probably due to a slight chemical reaction by circulating groundwater. The accidental inclusions of country rock (Nama sandstones and shales) in the kimberlite itself, however, are often bleached and surrounded by baked boundaries, which indicates that some thermal reaction has taken place.

Characteristics of the outcrop

The most prominent characteristic feature of the outcrops in the Gibeon province is that kimberlite blue ground is only present in minor quantities.

In several cases (Ovas, Diamantkop, Hanaus 2, Rietkuhl) most of the outcrop of the vent is occupied by a large continuous mass of dolerite and amygdaloidal basalt and it is thought that these vents represent the feeding ducts to the lava outpourings. In these cases blue ground only forms a very minor part of the outcrop at one side of the vent or in

Plate 4. Contact of kimberlite Hanaus 1 (on the left),
with steeply upturned maroon shales (on the right)

Plate 5. Contact of fissure pipe Gibeon Reserve 1
with steeply upturned maroon flagstones.



veins through the dolerite and it seems that the kimberlite used the dolerite feeding duct as a channel.

In general, however, most of the outcrop of the vents is formed by kimberlite itself, which in many of the Gibeon occurrences is present as hardebank. In one case (Gibeon Townlands 2) a large mass of hardebank forms a little neck about 60 feet high (see figure 5).

Hardebank from Amalia 1, Gibeon Reserve 1, Gruendorn 1 and Hatzium 1 is greyish black and rather homogeneous and could be described as a porphyritic peridotite. It contains small rounded olivine phenocrysts and many elongated and flattened nodules of garnet and ilmenite, embedded in a fine granular groundmass. Hardebank from Gibeon Townlands 2, Gibeon Reserve 1 and Lichtenfels 2 is light green and contains many angular fragments of friable bleached shale or sandstone (see plate 6), and few garnets or ilmenites. The two types of hardebank together with soft blue ground can occupy the same vent and have very intricate irregular boundaries on the outcrop.

Soil formation is negligible in the existing dry climate. Physical erosion predominates over chemical breakdown, and so the typical yellow ground is mostly absent from kimberlite outcrops in South West Africa, except where they occur under old river terraces or are cut by little gullies.

The kimberlite bodies act as water reservoirs, so that windpumps, drinking troughs and kraals have been erected on the actual outcrop at many places. At Louwrensia the house and farmyard, etc. have been built on and around the actual pipe.

Minerals and rock fragments in Kimberlites

Each kimberlite is in some way slightly different from the others; each has its own characteristic nodules, its characteristic relative abundances of heavy minerals, etc. (see table 2). Louwrensia 1 and Achterfontein 1 are noted for their beautiful garnet peridotites and garnet lherzolites; Deutsche Erde 1 for its norites and garnet pyroxenite. On the other hand, kimberlites tend to occur in small clusters with internal similarities, e.g. the garnet pyroxenites in Docheib and Kaitzub and Kaudus 1 and 2 are similar, likewise the gabbroic rocks in the Ovas pipes, etc.

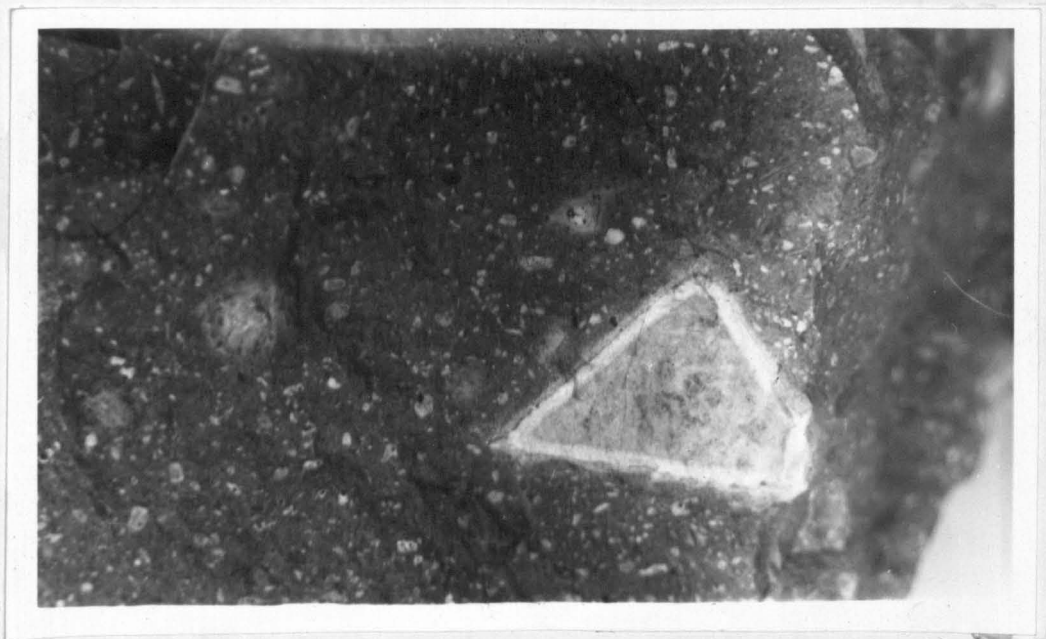
Table 2 sets out the relative abundances of the most important minerals in the kimberlite concentrates. It is noted that there seems to be a connection between the relative proportions of phlogopite and ilmenite.

Size and shape

The sizes and shapes of the outcrops vary greatly. They range in size from a mere ten yards up to 900 yards for the longest diameter. Figures 5, 6 and 7 show the size

Plate 6 Hardebank from Gibeon Reserve l. Light green hardebank with partly serpentinized olivine phenocrysts and angular fragment of bleached shale with baked boundaries (natural size).

Plate 7 Blue ground from Hanaus l. Note empty shell of ilmenite (left) (natural size).



and shape of the Gibeon kimberlites compared to certain well-known kimberlites from other areas. It is evident that the size of the Gibeon occurrences is rather small. The shape of many outcrops is roughly circular or oval in shape, but many others have irregular outlines (notably Hanaus 1) resulting from the coalescence of several intrusions (see figure 5).

Most of the occurrences are distinct fissure-pipes composed of two or three elongated pipes on the same fissure (Gibeon Townlands 2 - Gibeon Reserve 1) or, alternatively, three elongated pipes in a row not visibly connected by a dyke (Ovas).

The strike of the fissures and in many cases in particular the elongation of individual pipes follows the directions of the joint pattern of the Nama sandstones (N 35°E and N 125°E) or of the Nama shales (N 65° to 75°E and N 145° to 160°E).

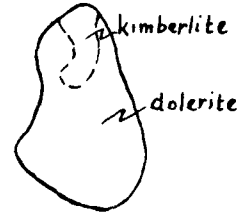
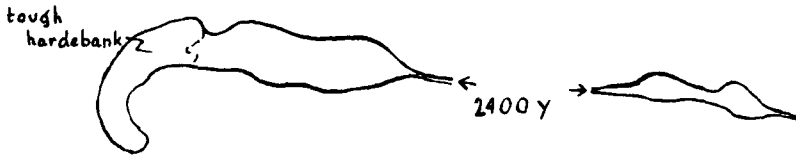
The distribution of the kimberlites, however, is not influenced by local structures, but seems to follow a north-south alignment from Berseba to Mariental (see figure 4). This is consistent with a north-south line of weakness postulated by Beetz (1933, 1938), running from Windhoek via the alkaline rocks in the Auas Mts., the Regenstein vent, the hot springs in Rehoboth, the kimberlites of the Gibeon

FIG.5 KIMBERLITES OF SOUTH WEST AFRICA

GIBEON TOWNLANDS 2

GIBEON RESERVE 1

DIAMANTKOP



DICKDORN 2

MUKOROB 2

HATZIUM

BRUKKAROS 10



KAUDUS & KAITZUB 1

DOCHEIB

DEUTSCHE ERDE 1

LOUWRENSIA



HANAUS 2

HANAUS 1



LICHTENFELS 2

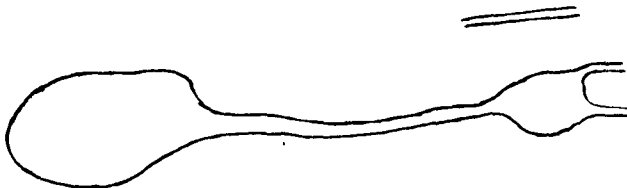
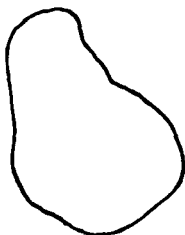
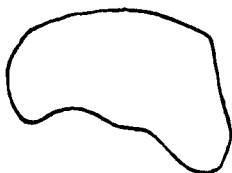


FIG.6 KIMBERLITES OF THE REP. OF SOUTH AFRICA

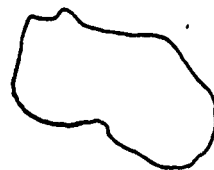
BULTFONTEIN 600' LEVEL



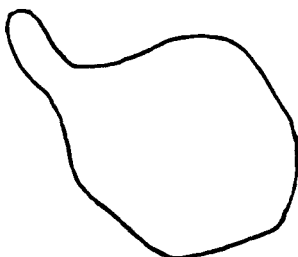
WESSELTON 500' LEVEL



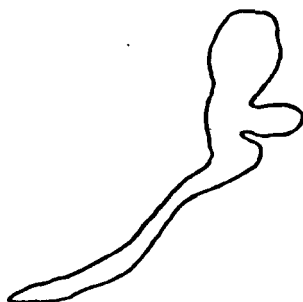
DE BEERS



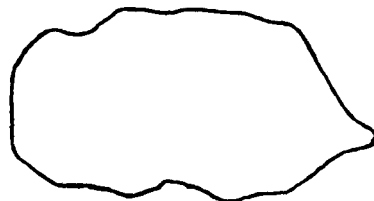
KOFFIEFONTEIN



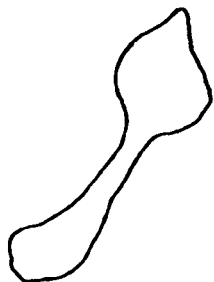
OTTO'S KOPJE



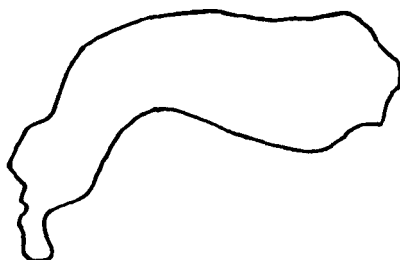
KIMBERLEY



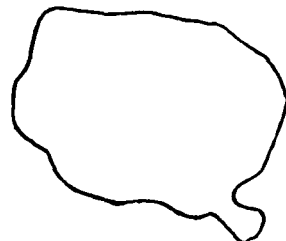
SMITH - WELTEVREDEN



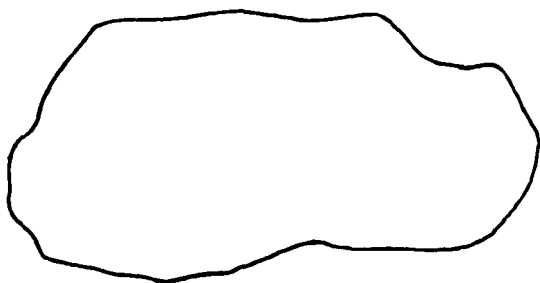
DU TOIT'S PAN



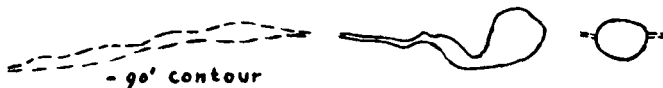
JAGERSFONTEIN



PREMIER



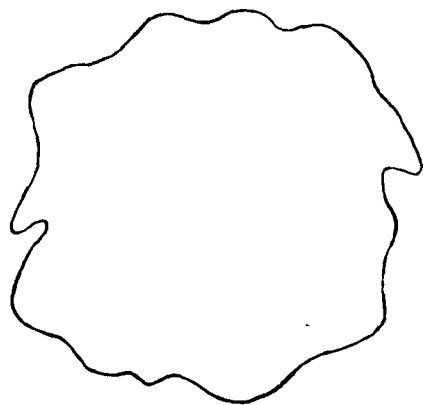
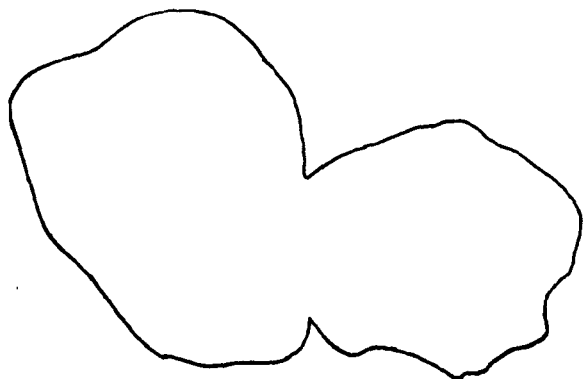
ROBERTS - VICTOR



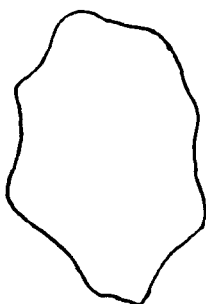
0 100 200 300 yards

FIG.7 KIMBERLITES OF THE U.S.S.R. (A) AND BASUTOLAND (B)
UDACHNAYA ZARNITSA

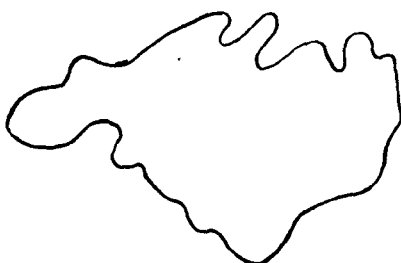
A.



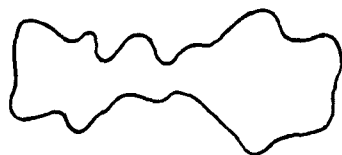
MIR



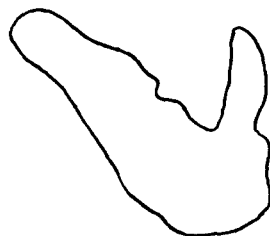
LENINGRAD



ZAPOLYARNAYA



NOVINKA



POLYRNAYA



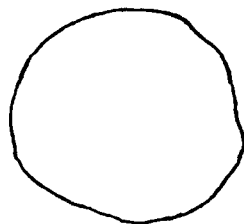
KAO 1



KAO 2



LIQHOBONG



THABA PUTSOA



SEKHAMENG



HOLOLO



0 100 200 300 yards



province, the Brukkaros vent down into the kimberlite and melilitite area of Bushmanland (Beetz 1933). The line has, however, no surface expression in the form of faults and does not coincide with earthquake zones (Korn & Martin 1950), but it might represent the beginning of a flexure in the Nama and pre-Nama rocks, which underlie the Kalahari Basin and curve upwards to form the highlands bordering the Great Escarpment.

(iii) Conclusions

The Gibeon kimberlite province comprises a group of rather small occurrences, of which many are fissures or fissure-pipes. The shape and elongation of the outcrops is influenced by the local joint pattern in the Nama sediments, while their distribution can possibly be related to a north-south line of weakness of more than local importance.

TABLE 2. Relative abundances of minerals in kimberlite concentrates

<u>Locality</u>	<u>concentrate</u>	<u>A</u>	<u>B</u>	<u>C</u>	<u>D</u>	<u>E</u>
O 1	fair	2	1	1	1	
O 2	poor	1	1	1	1	
O 3	good	3	1	1		
O 5	good	3	2	1		
O 6	fair	2	2	1	1	
O 7	poor	1	1	1		
B 10	fair	1	2	1		
B 11	fair	2	2	1		
L 1	good	4	2	1	2	
L 2	fair	3	1	1		1
L 5	poor	2				
L 7	good	3	2	1		
Di 1	fair	2	3	1	3	
Di 2	very good	1	3	1	3	
M 1	very good	2	3	2	2	
M 2	very good	2	3	2	3	2
AL 1	very good	4	2	2	3	
G 1	very good	4	1	1		
G 2	good	3	3	1		2
A 1	good	2	3	1	1	
A 2	good	3	2	2		1
DE 1	fair	3	1	1		1
DE 2	good	2	3	1	2	
Lo 1	good	4	2	3	3	
Da 1	fair	3	1	1		
Ha 1	very good	3	3	1	1	1
Ha 2	very good	3	2	2		
GT 1	good	3	2	1	1	
GT 2	fair	3	1	2		
GT 3	good	3	1	2		
GR 1	poor	2	2	1	1	
Do 1	fair	2	1	1		
KK 1	fair	2	1	1		
KK 2	fair	2	1	1		
R 2	poor	1	1			
Ht 1	fair	2	1			

1 = few 4 = abundant

A = pyrope garnet
 B = ilmenite
 C = chrome diopside
 D = phlogopite
 E = grass green pyroxene

(b) Chemistry and mineralogy

(i) Introduction

Kimberlites can be divided into several varieties, according to the main characteristic considered. A common division is based on the behaviour to weathering, viz yellow ground, blue ground and hardebank.

The bluish black hard, unweathered kimberlite occurring in the deeper zones of a vent is a compact, slightly carbonated, micaceous, serpentized peridotite, containing pyrope-garnet, pyroxene and ilmenite, and many nodular inclusions of several different kinds of rock. It usually changes to blue ground nearer to the surface by losing its compactness, while the colour changes to bluish or bluish-green. The result is a friable or clayey rock, from which inclusions can be easily separated. Some kimberlite, however, does not change into blue ground, but forms outcrops of hard brittle rock, called hardebank, at the surface of the vent.

Yellow ground is the completely weathered and oxidized variety of blue ground and usually forms the topmost layer of the vent. It consists of decomposed olivine-serpentine pseudomorphs and flakes of hydrated phlogopite held together by a friable or clayey mass of calcitic, zeolitic and limonitic composition. The inclusions are also

weathered and the surface of the vent becomes secondarily enriched with heavy minerals, derived from both kimberlite and inclusions.

Lewis (1888) divided kimberlites also in kimberlite-lava, -tuff or -breccia, but the three types grade into each other and a strict classification cannot be maintained. The main difference between kimberlites is that some contain very many inclusions, while others are rather homogeneous and can be described as porphyritic olivine-rich peridotites or picrite-porphyrries. This distinction is often useful in separating different intrusions in one pipe, which may be very important from an economic point of view.

Alternatively, Wagner (1914) has sub-divided kimberlites into : 1. basaltic varieties and; 2. micaceous or lamprophyric varieties. Strictly speaking the basaltic variety is wrongly named because plagioclase is not present and olivine is the main constituent (50% or more) though phlogopite may be present. This is the most common type in kimberlite pipes and in most of the dykes. Phlogopite is the main constituent in the second variety which is found in some dykes.

(b) Chemical features

All of the occurrences in the Gibeon province contain basaltic kimberlite, only 8 out of 46 pipes contain

phlogopite in any quantity (see table 2). The basaltic hardebank is generally black or dark greyish-green and the density, measured on 6 specimens, ranges from 2.76 to 2.87. It usually contains much calcite. Thin calcite veins traverse the hardebank and in fissure-hardebank they are extensive and trend parallel to the sides of the fissure. Cavities, lined with calcite and specks of fluorite are common in hardebank.

Comparison of the Gibeon kimberlites with the average basaltic kimberlite given by Nockolds (1954) shows that the former have a higher CaO - and volatile-content and a lower SiO₂-, Al₂O₃, MgO and alkali-content (see table 3). In this respect (calcium richness) they are closer to kimberlites from the Siberian Platform, which are also comparable in having a similar low alkali-content (see table 3).

When plotted in a von Wolff diagram it is seen that some of the Gibeon kimberlites and the Siberian kimberlites trend towards the calcite corner and fall partly outside the actual kimberlite field (compare figures 8 and 9).

For comparison, some peridotitic dykes from other areas (Pennsylvania, Quebec and Alno) are shown, which have been described as kimberlites, but they cannot be considered to represent true kimberlites.

The trace element composition of the kimberlites conforms to the pattern discussed by Dawson (1962) for

kimberlites of Basutoland.

The amounts of Ca, Cr, Cu, Ni and Sc and the Co/Ni ratio are typical for ultrabasic rocks; while the amounts of Ba, Ga, La, Li, Mo, Pb, Rb, Sr, V, Y and Zr and the K/Rb and Ga/Al ratios are typical for a late magmatic differentiation (see table 4).

TABLE 3. Analyses of kimberlites

	R21	F13	A1	GR21	Hal2	1	2	3
SiO ₂	33.5	33.0	30.67	33.0	30.0	35.02	36.33	29.57
TiO ₂	1.01	1.15	0.82	1.37	1.77	1.22	1.89	1.31
Al ₂ O ₃	2.0	2.2	2.34	3.4	2.7	3.90	5.09	3.48
Fe ₂ O ₃	7.57	6.27	6.28	5.27	9.69	5.15	7.43	5.04
FeO	3.59	4.19	2.47	5.05	1.89	4.14	3.40	2.63
MnO	0.18	0.19	0.15	0.18	0.19	0.06	0.10	0.11
MgO	27.0	27.0	20.4	29.5	27.0	31.29	26.63	26.26
CaO	10.03	12.49	16.94	7.5	11.1	6.80	6.78	11.92
Na ₂ O	0.19	0.30	0.21	0.29	0.33	0.34	0.37	0.25
K ₂ O	0.17	0.70	0.18	1.80	0.30	1.05	2.43	0.54
H ₂ O ⁺	10.23	7.61	9.51	10.76	13.79	7.43	7.25	
P ₂ O ₅	0.38	0.90	1.10	0.40	0.40	0.87	0.66	0.45
CO ₂	4.89	5.52	10.76	3.44	1.17	2.73	1.64	18.06*
	102.74	101.52	101.83	101.96	100.30	100.00	100.00	100.30
S.G.	2.79	2.87	2.81					

R21 surface-hardebank, Rietkuhl 2. Analyst G. H. Hornung

F13 surface-hardebank, Gibeon Reserve 2. " " " "

A1 surface-hardebank, Amalia 1. " " " "

GR21 blueground, Gibeon Reserve 2. " " " "

Hal2 blueground, Hanaus 1. " " " "

1. Average chemical composition of basaltic kimberlite, 10 analyses (Nockolds 1954).
2. Average chemical composition of micaceous kimberlite, 4 analyses (Nockolds 1954).
3. Average vein kimberlite, 210 analyses (Lebeder 1964).

18.06* = total loss on ignition

TABLE 4. Trace element composition of some kimberlites from the Gibeon province

	Ba	Be	Co	Cr	Ga	La	Li	Mn	Mo	Nb	Ni	Pb	Rb	Sr	Sc	Ti	V	Y	Zr
DE10	>1000	<3	25	15	13	<100	45	2300	4	25	<10	10	320	200	40	>3000	240	85	280
Ha19	1000	<3	40	400	17	<100	5	1800	<3	<20	90	10	65	400	85	>3000	380	<30	80
Ha12	1000	<3	55	>1000	<10	<200	10	2000	<3	200	1100	50	300	350	15	>3000	110	50	250
Ht16	>1000	<3	35	>1000	<10	<200	17	2500	<3	150	1100	25	350	600	15	>3000	200	<30	160
F13	>1000	<3	60	>1000	<10	<200	5	2000	7	250	1300	30	100	700	10	>3000	200	30	190
A1	>1000	<3	45	>1000	<10	<200	50	3000	<3	200	1200	10	200	800	10	>3000	120	<30	160
A3	500	<3	10	190	<10	<100	30	2700	<3	65	190	30	125	550	10	1800	50	50	40
B1	220	3	60	700	13	450	10	2000	5	240	450	10	70	1000	20	>1000	110	65	200

Spectrographer : Miss J. M. Rooke

DE10 syenitic inclusion in kimberlite, Deutsche Erde, S.W.A.

Ha19 basalt inclusion in kimberlite, Hanaus 1, S.W.A.

Ha12 blue ground from kimberlite, Hanaus 1, S.W.A.

Ht16 calcareous hardebank from kimberlite, Hatzium, S.W.A.

F13 hardebank from kimberlite fissure, Gibeon Native
Resefve, S.W.A.

A1 hardebank from kimberlite, Amalia 1, S.W.S.

A3 kimberlitic-carbonatitic dyke, Amalia, S.W.A.

B1 monticellite-peridotite from Mt. Brukkaros, S.W.A.

Explanation of symbols of figure 8.

- A = alnoite (von Eckermann 1948)
- AP = average alkali peridotite (Nockolds 1954)
- BK = average basaltic kimberlite (Nockolds 1954)
- GPK = average garnet peridotite nodule in kimberlite
(table 18)
- KA = kimberlite Alnö (von Eckermann 1958)
- KP = kimberlite Pennsylvania (quoted in Dawson 1960)
- KQ = kimberlite Quebec (quoted in Dawson 1960)
- MK = average micaceous kimberlite (Nockolds 1954)
- MP = monticellite peridotite (table 6)
- OM = average olivine melilitite (Nockolds 1954)
- P = average peridotite (Nockolds 1954)
- PB = average peridotite nodule in basalts (table 18)
- PK = average peridotite nodule in kimberlite (table 18)
- VK = average vein kimberlite (table 3)

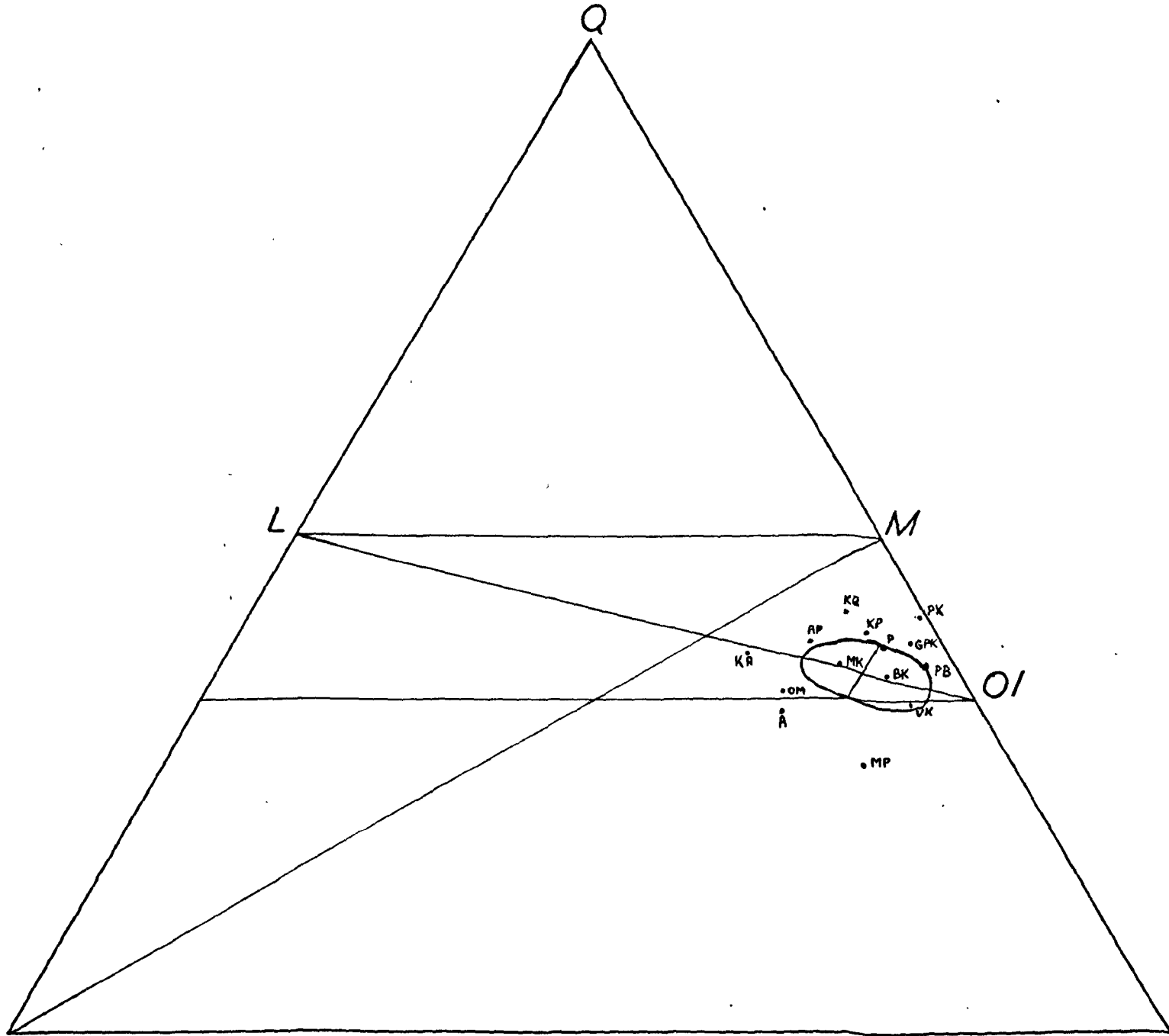


Fig. 8. The average composition of some ultrabasic rocks.

(iii) Mineralogical features

Minerals

In thin section kimberlites consist of phenocrysts of olivine and phlogopite, embedded in a turbid green groundmass of microcrystalline serpentine and calcite. In contrast to the more calcitized hardebank in which the groundmass looks more like a smooth grey paste. Small laths of phlogopite, small black crystals of ilmenite, minute black octahedra of magnetite and small brown equant crystals of perovskite are also contained in the groundmass.

Olivine is the main constituent of the kimberlite and occurs both as phenocrysts and as very small crystals in the groundmass. It is always serpentinized to a large extent, but in some kimberlites the groundmass contains small euhedral olivines, which are only partly replaced (cf. Nixon et al 1963). The outlines of the phenocrysts are more irregular, embayments and resorption characteristics are frequent. The olivine has been completely replaced by serpentine in most kimberlites in the pipes, while in some fissure-kimberlites large cores of unaltered olivine are still present. The initial alteration is mainly along cracks and rims to produce chrysotile, but in later stages the whole olivine-crystal may be altered to antigorite with the original chrysotile-cracks still intact. The unaltered olivine is always bi-axial positive, with a $2V$ near to 90° ,

which indicates a forsterite-content of ca 90%. The olivines show mostly a faintly undulose extinction, indicating mechanical stress.

Discussing South African and Basutoland kimberlites, Williams (1932) and Dawson (1962) suggested that the fissure-kimberlite did not reach the surface and was not subjected to the same sudden drop in pressure as in most kimberlites, consequently the serpentinization of the olivine only reached the first stage.

Phlogopite also occurs in two grain sizes. It occurs in the groundmass, forming a part of the turbid mass of serpentine and calcite and it also forms larger flakes or small books noticeable in hand specimen. The phenocrysts are distinctly pleochroic with a very small 2V. The ends of the flakes are usually frayed and bent, indicating mechanical stress. The outline of the crystal shows frequently resorption embayments where the phlogopite is altered to chlorite. A rim of exsolved magnetite surrounds the larger flakes. The stress- and exsolution- indications make it appear likely that they have formed before the kimberlite was emplaced.

The groundmass mica does not possess rims of exsolved magnetite and has a lower birefringence. It probably formed as a secondary alteration from serpentine (Dawson 1962). When the groundmass is rich in mica, it is also rich in calcite.

Alterations of the phlogopite to a dull bronze coloured vermiculite is common. Vermiculite occurs as small books or flakes or as single large flakes in the blue- and yellow-ground, but several vents also contain glimmerite nodules (nodules consisting of vermiculite and serpentine) which are probably accidental inclusions of a micaceous kimberlite. Occasionally vermiculite is an important constituent of the olivine-bearing nodules; on weathered surfaces it tends to form small ($\frac{1}{4}$ inch) nodular aggregates. An X-ray diffraction pattern of a small aggregate showed four strong peaks of similar intensity at d-values of : 14.42; 7.21; 4.80 and 3.59. These values are significantly larger than the ones given in the A.S.T.M. (1961) index (vermiculite : 14.2; 7.1; 4.59 and 3.52) which indicates a smaller cell-size, probably caused by a predominance of magnesium in the crystal lattice.

Ilmenite. Tiny black spots (0.05 mm.) in the groundmass are probably ilmenites; this is confirmed by X-ray diffraction patterns. It also occurs as black opaque patches in perovskite.

Perovskite is a typical constituent in the groundmass of kimberlites. It occurs as nearly isotropic, dark-brown equant crystals up to 0.5 mm. diameter. With secondary alteration some of the perovskite is altered to light-brown tiny fragments, while black opaque patches (ilmenite?)

occur in the larger crystals.

Magnetite occurs in kimberlites as very small black octahedra (ca 0.01 mm.). The relatively high content of Fe_2O_3 in the chemical analyses of unweathered kimberlite already confirm its presence. It is an important constituent in many weathered kimberlites, derived from exsolution of olivine and phlogopite.

Apatite has not been detected in thin section, but chemical analyses show its probable presence. It is frequently enriched in yellow ground.

Clinopyroxene. The presence of small euhedral clinopyroxene in the groundmass of kimberlites has been reported by Wagner (1914), Williams (1932) and Nixon et al (1963), but it has not been observed in the Gibeon kimberlites.

Groundmass

The above mentioned minerals are all typical constituents of the groundmass of kimberlites. The remainder of the groundmass is formed by a turbid mass of serpentine and calcite. This calcite-serpentine-(phlogopite) groundmass is a fundamental characteristic feature of kimberlites even in the deepest levels of the Kimberley Mines (Williams 1932).

Various authors have expressed opinions upon the original composition of the groundmass of kimberlites. Three possibilities are usually put forward -

1. ultrabasic glass
2. olivine + melilite
3. olivine + monticellite

Du Toit (1954, p. 420) thought it was "an ultrabasic glass, as in the limburgites"; von Eckermann (1948, p. 98) writes "the original meaning of the term kimberlite is a biotite-melilite-peridotite", however, the kimberlitic dykes of Alno do not fall within the kimberlite field when plotted in a von Wolff diagram (see figure 8).

Frankel (1956) described an extensively calcitized kimberlitic dyke from Mukorob (South West Africa) and postulated the original presence of melilite from the assumption that short prismatic laths in the groundmass were calcitic pseudomorphs after melilite. A similar dyke, but without inclusions, has been found near the old farmhouse on Arietites-West. However, owing to the usually extensive secondary alteration of this type of rock, petrological determinations are rather uncertain and the presence of unaltered melilite in kimberlite has still to be verified. In contrast, monticellite has been recorded from several localities and could equally account for the calcium richness of the groundmass. Wagner (1929) has reported monticellite in the groundmass of basaltic kimberlite from South Africa and Verhoogen (1938) described the occurrence of this mineral as rims around serpentized olivine

phenocrysts together with its presence in the groundmass of micaceous kimberlites from Katanga. Small euhedral crystals of a mineral that could be monticellite have been reported by Dawson (1962) from Basutoland kimberlites.

From theoretical considerations monticellite, rather than melilite, might be expected to form in kimberlites. Kushiro and Yoder (1964) found that forsterite and merwinite ($3 \text{ CaO} \cdot \text{MgO} \cdot \text{SiO}_2$) combined to form monticellite below 9 kb and 1400°C , and akermanite (ca-melilite) formed from diopside and merwinite below 15 kb and 1400°C . But, since diopside-bearing varieties are rare, and forsterite is the main constituent in kimberlites, the calcium-bearing mineral in the groundmass is more likely to be monticellite.

(iv) Conclusions

The kimberlites of the Gibeon province are all of the basaltic variety and can be described as serpentized, slightly micaceous, calcium-rich peridotites in various stages of calcitization and oxidation.

By analogy with other regions (Katanga, Verhoogen 1938; South Africa, Wagner 1929; and Basutoland, Dawson 1962) and from theoretical considerations it may be that the calcium richness of the groundmass of kimberlites is due to monticellite.

(c) Inclusions in kimberlite

(i) Introduction

Inclusions are a characteristic feature of kimberlites. They can be divided in : (1) accidental inclusions and (2) cognate inclusions.

Amongst the accidental inclusions, there are angular fragments of sedimentary or metamorphic rocks, derived from the adjacent host rocks of the intrusions and from subsurface lithologies.

In contrast, a second variety of inclusions is represented by nodular xenoliths of deep-seated origin and of basic or ultrabasic character. A controversy rages about the question of whether these inclusions are accidental (picked up from the host rock during ascent of magma) or cognate (derived from a common parent magma by earlier consolidation).

To avoid these problems the following subdivision is proposed :

1. Near-surface inclusions of angular fragments of host rock;
 2. Deep-seated inclusions of monomineralic and composite nodules;
- and 3. Deep-seated inclusions of polymineralic nodules.

(ii) Near-surface inclusions of host rock

Sedimentary fragments

The near-surface inclusions have been acquired at

relatively shallow depth, they are always angular and have been derived from the host rocks which are sediments in most cases; they have an obviously accidental origin. They can be divided into two groups :

1. fragments of strata, early in the regional succession, which have been brought up to higher levels,
2. fragments of strata (which may have been eroded already) which have sunk in the vent to lower levels than their original deposition.

The Gibeon kimberlites contain many small angular fragments of sandstone and shale, derived from the Nama formation. The originally red sandstone and shale have been changed into a whitish to pale greenish friable rock with a slightly hardened rim. Larger fragments and coherent masses of Dwyka rocks, mudstones and shales are found in two kimberlites (Lichtenfels 7 and Hatzium) very near to the present Nama-Dwyka boundary.

Basalt and dolerite fragments

The most common larger fragments in kimberlites are basaltic and doleritic rocks derived from surface lava flows, similar to those in the Kub-Hoachanas area, 50 miles north of Mariental (figure 4).

In hand specimen the basalts have a bluish-black to

purplish colour with light green specks of chlorite. Many specimens are crowded with amygdules, coated with dark green earthy chlorite and filled with clear calcite and natrolite. The natrolite is usually fibrous; however, massive or nodular forms are common in fragments in kimberlite from Gibeon Townlands 2.

In thin section the rocks are seen to have a hypocrystalline intersertal to sub-ophitic texture. Small laths of subhedral plagioclase are partly enclosed by larger equant anhedral pyroxene. In places a brown stained glassy base is present.

Plagioclase is present in two grain sizes: (a) small laths of twinned and unweathered (0.4 x 0.03 mm.) labradorite (An 55), and (b) larger short prisms (0.9 x 0.7 mm.) of rather weathered labradorite (An 65). A few large plagioclase oikocrysts are also present which have a strongly zonal extinction, An 42 - 70.

Pyroxene is present in two grain sizes: (a) short prisms (0.7 x 0.7 mm.) of colourless to very slightly pink augite ($2V = \text{ca } 56^\circ$); and (b) large equant anhedral crystals (up to 2.5 mm.) which act as oikocrysts for small plagioclase in the rocks with a more poikilitic texture.

Olivine. A few subhedral crystals of olivine occur and are partly resorbed and altered to chlorite with rims and cracks altered to hematite. The optical properties

of the olivine, particularly its 2V, which is 82° to 84° , indicates a Fo-content of ca. 70%, i.e. chrysolite.

In addition to these principal rock-forming minerals, interstitial brown glass with black specks of magnetite are present. Sericite, chlorite and hematite are also present as secondary minerals.

The amygdules contain calcite, chlorite and natrolite.

The relative amounts of plagioclase and augite vary a little, but usually there is twice as much plagioclase as augite.

In some fragments pigeonitic augite with a low 2V (ca 20°) was noticed, and the lavas on the whole belong to the tholeiitic group (see table 5) with a few percent of olivine and orthopyroxene in the norm. Two fragments from Hanaus 1, however, have a rather high sodium content and nepheline appears in the norm, but this may not be an inherent characteristic of the basalt, because many basalt fragments in other vents show distinct signs of alkali-metasomatism.

The fine grained hypocrySTALLINE basalt fragments grade into coarser ophitic dolerites with similar mineralogical and chemical composition. The dolerites occur as continuous coherent masses in the vents in the Ovas area, but nodular fragments of similar dolerite occur in many vents in other areas. The olivine content in some doler-

ites reaches 4% (see table 7). The coarser dolerites grade into gabbros with a grain size of up to 3.5 mm. Comparable hand specimens and thin sections of the Kub-Hoachanas lava were not obtained, as good exposures were not found and the basalt was extremely weathered. According to their mineralogy and chemical analyses, however, the fragments in the kimberlite are similar to the rocks of the Stormberg volcanics in other parts of Southern Africa.

TABLE 5. Analyses of basaltic and doleritic inclusions

	Dall	021	Ha21	Ha19	C1	L53
SiO ₂	51.0	50.8	49.6	49.5	47.33	49.5
TiO ₂	0.77	1.47	0.95	0.95	0.95	1.40
Al ₂ O ₃	14.2	14.45	14.0	14.2	14.26	12.8
Fe ₂ O ₃	5.76	1.67	5.81	2.14	5.20	3.29
FeO	4.15	10.30	4.41	8.40	4.40	9.99
MnO	0.10	0.17	0.14	0.16	0.16	0.17
MgO	8.1	5.2	8.6	6.4	6.90	8.1
CaO	9.81	8.00	9.46	8.60	10.28	8.59
Na ₂ O	3.53	3.02	2.37	4.20	4.43	2.24
K ₂ O	0.88	1.85	1.47	0.60	0.72	0.62
H ₂ O ⁺	0.99	1.55	1.40	3.06	2.42	2.31
H ₂ O ⁻	0.53	0.21	0.94	0.16	0.81	0.81
P ₂ O ₅	0.05	0.32	0.19	0.24	0.18	0.29
CO ₂	n.d.	n.d.	n.d.	n.d.	1.96	n.d.
BaO	n.d.	0.09	0.09	0.12	n.d.	0.02
SrO	n.d.	0.05	0.07	0.05	n.d.	0.02
	99.87	99.15	99.50	98.78	100.00	100.15

Analyst : Dr. G. Hornung, except where stated.

Dall basalt from feeding duct, Diamantkop, S.W.A.

021 dolerite from feeding duct, Ovas 2, S.W.A.

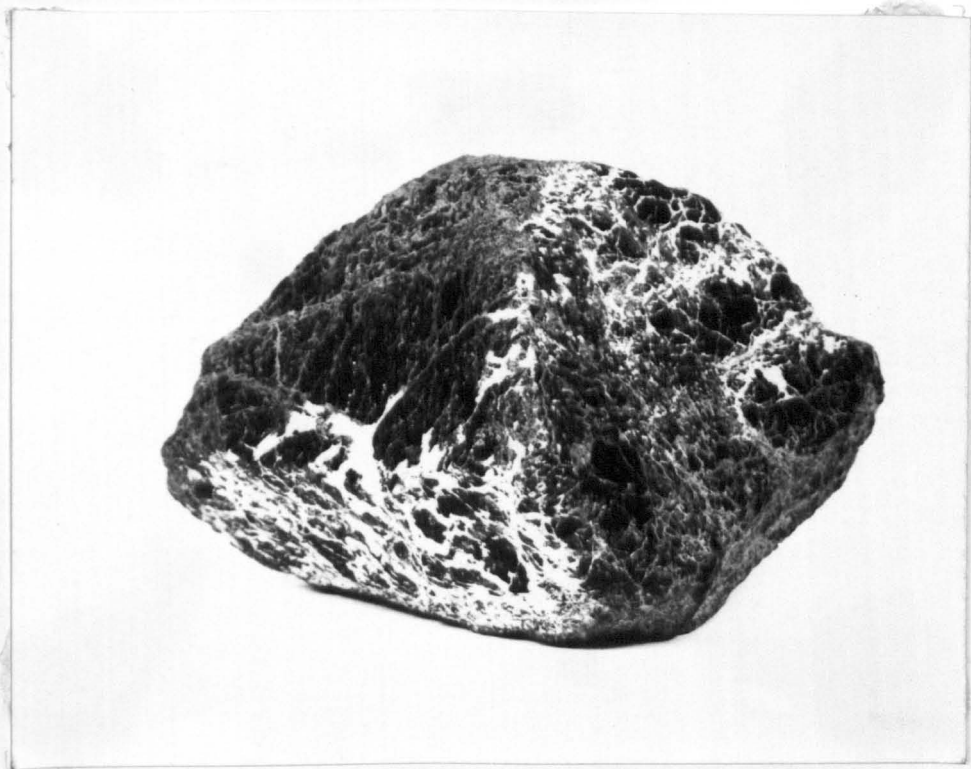
Ha21 basalt from feeding duct, Hanaus 2, S.W.A.

Ha19 basalt fragment from kimberlite vent, Hanaus 1, S.W.A.

C1 basalt fragment from kimberlite vent, Hanaus 1, S.W.A.
Analyst : Mrs. H. Kerr.

L53 dolerite, nodular inclusion in kimberlite,
Lichtenfels 1, S.W.A.

Plate 8. Garnet nodule in kimberlite, Hanaus 1
with remnants of crystal faces
(natural size).



(iii) Deep-seated inclusions of monomineralic and composite nodulesMonomineralic nodules

The monomineralic nodules are transported crystals or discrete nodules of garnet, pyroxene, olivine and ilmenite enclosed in the kimberlite matrix. They are not true phenocrysts, but seem to have existed as individual entities. In general, they are of larger grain size than the minerals of the enclosing kimberlite. However, they do not possess distinct crystal faces, but they are rounded, abraded or drawn out to an elongated shape. Commonly, they are separated from the kimberlite matrix by a skin or reaction rim, which is usually stripped off in the mineral concentrates on the surface of the vent.

Garnet nodules. The garnet, which occurs as discrete nodules in the kimberlite matrix is a red brown variety of pyrope. It occurs as typically rounded grains, which are often cracked and drawn out to an elongated shape (a flattened ellipsoid), but occasionally large garnets are found which still possess remnants of crystal faces (see plate 8). They range in size from a few millimeters to more than ten centimeters and they are usually traversed by numerous fractures and cracks, lined with kelyphite and calcite.

Where present, the kelyphitic rim around the garnet

is usually quite wide and consists of brown opaque, optically unresolvable material, which changes into a narrow outer zone of dark, granular appearance. Nixon (et al, 1963) found that Basutoland kelyphites consist of spinel granules, phlogopite, chlorite or amphibole. In some cases the brown opaque zone is separated into a light brown semi-opaque inner zone, which is anisotropic in first order colours and a dark brown opaque outer zone.

Clinopyroxene nodules. Grass-green diopside and emerald-green diopside occur as discrete nodules in kimberlite. They are tabular and are of similar size to garnet nodules but they are not so common. They are usually cracked and the fractures and outlines are coated with a white alteration product.

Orthopyroxene nodules. Smoky brown orthopyroxene has been found on kimberlite outcrops in rather large grains, but it has not been observed in situ.

Olivine nodules. Pale, olive-green forsterite occurs as discrete nodules in kimberlite. The nodules have a rounded tabular shape and are very much cracked and usually surrounded by a darker alteration rim. Many olivines have been completely serpentized, but rather large olivines exist with only slight alteration rims.

Ilmenite nodules. Ilmenite occurs as dull metallic

black ellipsoids which are characterized by "striations, pluck marks, flat soles, indicating abrasion during intrusion" similar to those described from Basutoland by Nixon (et al 1963). Some grains contain cylindrical channels or spherical cavities, lined with a white substance, which in the Basutoland ilmenites consists of secondary perovskite, goethite, hematite and calcite (Nixon et al 1963). Particularly strongly corroded ilmenite occurs in slightly micaceous blue ground from Dickdorn 1 and Deutsche Erde 2.

Composite nodules

In addition to the monomineralic nodules there exist small nodules of a composite nature. They consist of two minerals, often the one enclosing the other and have the same characteristics as the monomineralic nodules in that they are also surrounded by reaction rims and do not possess crystal faces. Variable combinations of ilmenite + diopside, ilmenite + pyrope, ilmenite + olivine and pyrope + diopside, have been reported by Wagner (1941) and Frankel (1956) and Nixon (1960). Only ilmenite + olivine nodules have been observed in the Gibeon kimberlites.

(iv) Deep-seated inclusions of polymineralic nodules

The polymineralic nodules are composed of mineral combinations which are stable at greater depth under very high pressure and temperature. The minerals are pyrope, forsterite, pyroxene and plagioclase in various proportions

and they present valuable clues for the composition and PT conditions in the lower crust and the upper mantle.

The deep-seated inclusions in the Gibeon kimberlites can be divided into two main groups:

A. Pyroxene bearing nodules

Rocks without olivine in which pyroxene plays an important role in combination with plagioclase or garnet. These rocks are noritic or pyroxenitic in composition and belong to the granulite- or eclogite-facies.

B. Olivine bearing nodules

Rocks in which olivine plays an important role in combination with garnet and pyroxene.

Group A : Pyroxene-bearing nodules

Representatives of this group are the most frequently observed inclusions in the Gibeon vents, because only the surface outcrop was available for sampling and these rocks are more resistant to weathering than the olivine-bearing nodules. The rocks are of three types : granulitic (noritic), garnet pyroxenitic and (retrograde) eclogitic.

Granulitic (noritic) nodules

These rocks are composed of variable proportions of basic plagioclase, orthopyroxene and clinopyroxene. Magnetite, ilmenite and titanite are accessory minerals.

They range from anorthosites, leuco-norites, norites, pyroxene-gabbros to plagioclase-free pyroxenites (see

table 9, modal analyses).

The plagioclase ranges from labradorite to bytownite, the composition varying from An 65 in the norites to An 80 in the anorthosite. Some antiperthite is present in the less basic type.

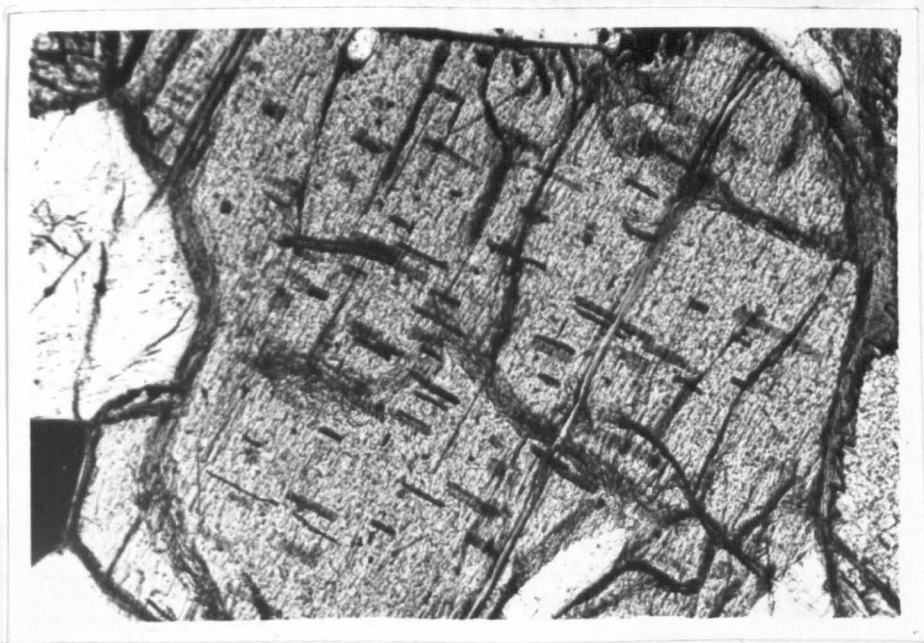
A few plagioclase crystals contain very fine needles of clinopyroxene(?) at random orientation.

The orthopyroxene is a distinctly pleochoric variety with X = pink to Z = pale green. It is optically negative with $2V = \text{ca } 70^\circ$. The variety is bronzite or hypersthene and the En-content varies from 80 % to 69%. Schiller structures caused by small brown flakes of rutile(?) are very common (see plate 9). More frequent, however, are sagenitic structures of very fine needles in two directions at 60° angles, which are symmetrical to the main cleavage and extinction directions; the needles show oblique extinction and positive elongation and have a slightly higher R.I. than the orthopyroxene.

The Clinopyroxene is a colourless variety. Diallage and salite structures are very common, often in the same crystal, while some crystals have the typical "herring-bone" structure. It is optically positive with a $2V$ of ca. 59° . Sagenitic structures are again very common, but tend to take the form of fine dust or very small rods, while a clear zone is preserved along the rim of the crystal.

Plate 9. Photomicrograph of thin section F 10.018
(033) (128x). Schiller structure in
orthopyroxene in a hypersthene granulite
from Ovas 3.

Plate 10. Photomicrograph of thin section F 9882
(DE13) (13x). Clinopyroxene needles
in zonal plagioclase in a pyroxene
granulite from Deutsche Erde 1.



In some rocks the orthopyroxene is surrounded by coronas of granular and needle-like clinopyroxene. Large sheafs of pyroxene needles lie between the orthopyroxene crystals and traverse the intersertal plagioclase. The plagioclase is completely xenomorphic and has a strongly zonal extinction where it encloses the pyroxene fibres. The fibres have a high relief, positive elongation and generally a straight extinction (see plate 10).

Titanite with ilmenite rims and magnetite are accessory minerals.

The texture of the rock is mostly granular and xenomorphic. The crystals are often cracked, especially the plagioclase. The cracks are sericitized and extend through various crystals. As the rocks occur as separate nodular fragments, it is not clear if these rocks are intrusive (norites or gabbros) or metamorphic (granulites), however, their texture is more characteristic of a basic granulite of basaltic (noritic) composition. (They are not basic charnockites - endebites - as they do not contain quartz or potash-feldspar).

TABLE 6. Modal analyses of granulites, amphibolites and dolerites

	DE12	G21	033	DE13	L92	032
Plagioclase	92	67	53	41	59	-
Orthopyroxene	-	26	44	26	-	-
Intergranular fibrous pyroxene	-	-	-	33	-	-
Clinopyroxene	8	7	-	-	34	13
Hornblende	-	-	-	-	-	51
Olivine	-	-	-	-	4	-
Garnet	-	-	-	-	-	6
Titanite	P	P	-	-	-	2
Apatite	-	-	-	-	-	1
Opaque minerals	-	-	3	-	3	2

P = present

- DE12 anorthosite nodule from Deutsche Erde 1.
- G21 granulite (norite) nodule from Gruendorn 2.
- 033 hypersthene-granulite nodule from Ovas 3,
Berseba Reserve
- DE13 pyroxene granulite nodule from Deutsche Erde 1.
- L92 dolerite nodule from Lichtenfels 5.
- 032 eclogite-amphibolite nodule from Ovas 3,
Berseba Reserve.

TABLE 7. Analyses of granulitic (noritic) inclusions

	DE12	M25	O33	M21	DE13	O22	M26
SiO ₂	46.6	48.0	47.7	47.7	48.3	42.5	44.5
TiO ₂	0.05	0.25	1.60	0.12	0.14	0.27	3.12
Al ₂ O ₃	28.0	15.0	14.8	21.7	17.4	9.7	15.0
Fe ₂ O ₃	0.26	9.98	6.77	2.27	7.31	5.30	8.76
FeO	1.98	7.15	8.72	5.26	4.72	7.83	7.15
MnO	0.02	0.11	0.25	0.11	0.12	0.17	0.19
MgO	2.5	10.0	9.4	7.6	10.6	11.4	9.0
CaO	17.00	8.67	5.30	12.30	9.34	14.00	5.70
Na ₂ O	3.38	1.88	1.99	1.91	1.72	2.35	0.41
K ₂ O	0.32	0.48	0.82	0.38	0.21	0.80	1.13
H ₂ O ⁺	1.08	0.85	2.46	0.80	0.61	4.11	5.20
P ₂ O ₅	-	-	-	-	-	0.80	0.45
							1.0
							(=SO ₃)
							0.14
							(=BaO)
	101.19	102.37	99.81	100.15	100.47	99.23	99.75
s.g.	2.78	3.01	3.11	2.97	3.22	3.15	2.95

Analyst : Dr. G. Hornung

- DE12 anorthosite nodule from Deutsche Erde 1.
M25 granulite nodule from Mukorob 2.
O33 hypersthene-granulite nodule from Ovas 3.
M21 granulite nodule from Mukorob 2.
DE13 pyroxene granulite from Deutsche Erde 1.
O22 amphibolite (retrograde eclogite) from Ovas 2.
M26 altered nodule from Mukorob 2.

Garnet pyroxenite nodules

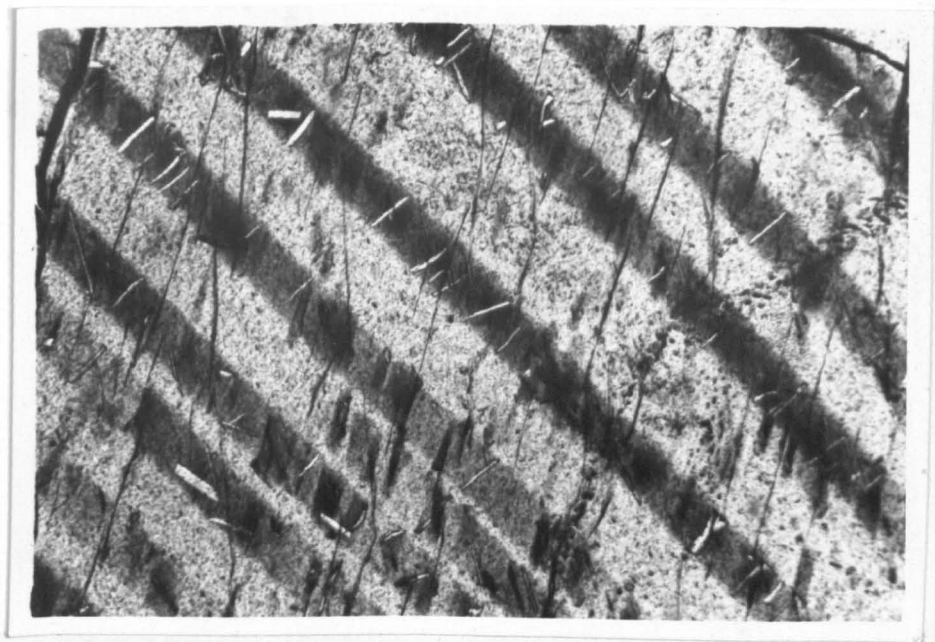
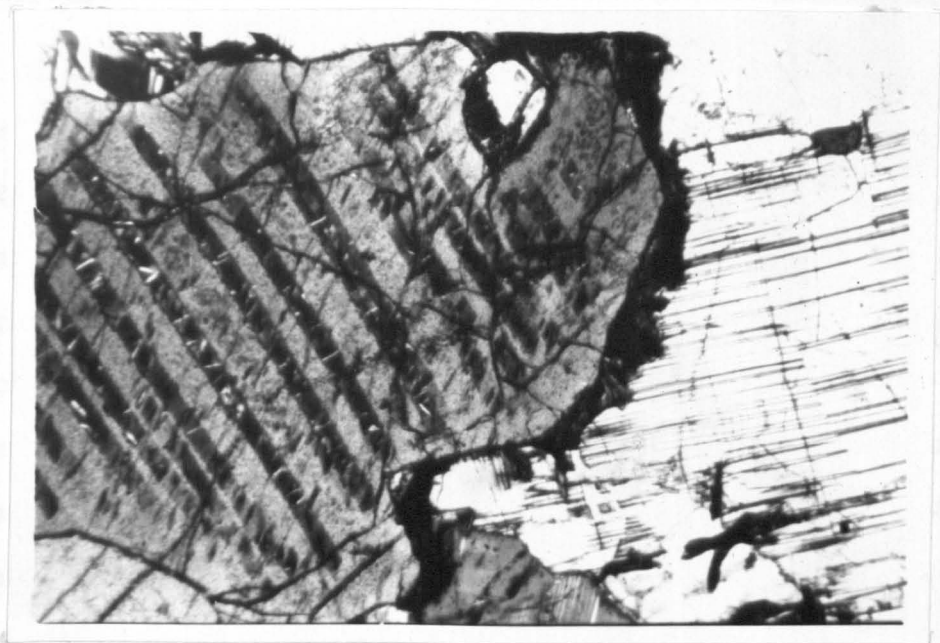
The garnet pyroxenite nodules are mainly composed of variable proportions of dark green clinopyroxene and orange-red garnet. Locally a little basic plagioclase may be present. A large nodule from Hanaus 1 consists mainly of orthopyroxene (bronzite) with small amounts of clinopyroxene, enclosing lamellae of garnet (see plate 13) and a very small amount of plagioclase. (Ha 17; table 8). Another nodule from Deutsche Erde 1 contains a pale pink garnet (lime pyrope), two varieties of clinopyroxene (an emerald green chrome diopside and a light green omphacitic chrome-poor diopside), olive green enstatite and black spinel (DE 15; table 8).

However, the garnet pyroxenite nodules are essentially biminerally with a medium- to coarse-grained xenomorphic texture and a very high density, ca. 3.4 (table 9).

The clinopyroxene is colourless in thin section with a general appearance similar to diopside. It contains lamellae of another pyroxene with a slightly higher R.I., together with small rodlike inclusions of an unknown mineral (see plates 11 and 12). Lamellae of pink garnet without reaction rims and flakes of an opaque mineral (goethite ?) are enclosed in a coarse-grained clinopyroxene (over 4 mm. across) from Kaitzub and Kaudus 2. Locally reaction rims of a clear isotropic substance are formed

Plate 11 Photomicrograph of thin section
F 10.621 (Hal6). Clinopyroxene
with pyroxene lamellae and small
rodlike inclusions.

Plate 12 Detail of plate 11.

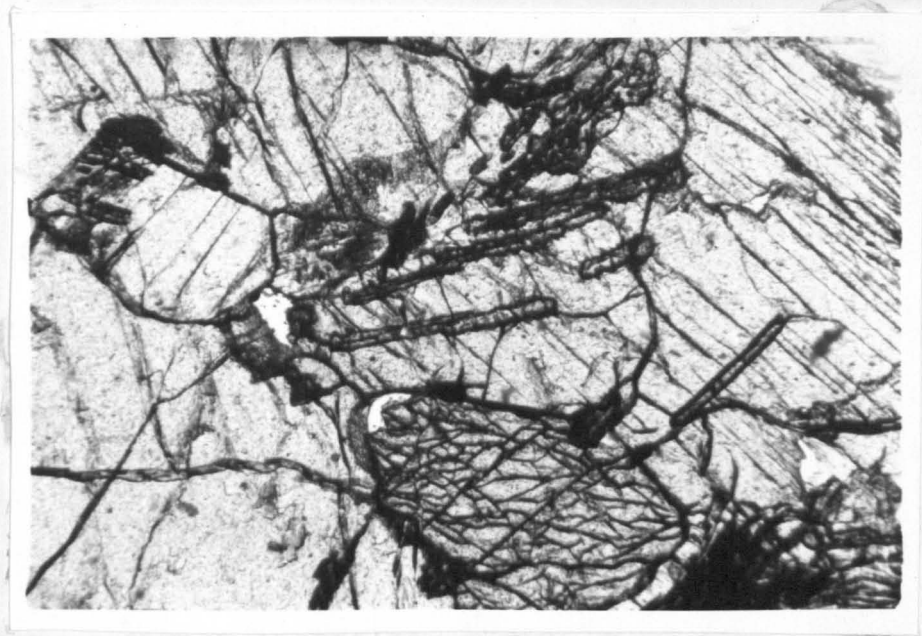


on the boundaries between the pyroxene crystals (see plate 14).

The garnet is slightly pink or pale brown in thin section. It is sometimes granulated or encloses small pyroxene crystals and it generally shows slight anisotropic features. The density is over 3.8 and the R.I. is ca. 1,766, indicating an almandine-rich pyrope. Rounded grains generally have a narrow rim of brown fibrous minerals, sometimes separated from the unaltered garnet by a clear isotropic rim (see plate 14). Inclusions of short brown rods are common.

Plate 13. Photomicrograph of thin section F9888
(Hal7). Clinopyroxene with garnet
lamellae.

Plate 14 Photomicrograph of thin section F9884
(Dol2). Light brown garnet with pale
kelyphitic rims, embedded in clino-
pyroxene. Clear isotropic reaction
rims occur on the boundaries of the
pyroxene crystals.



giant-invertebrate muscle from
(Nixon et al 1963)

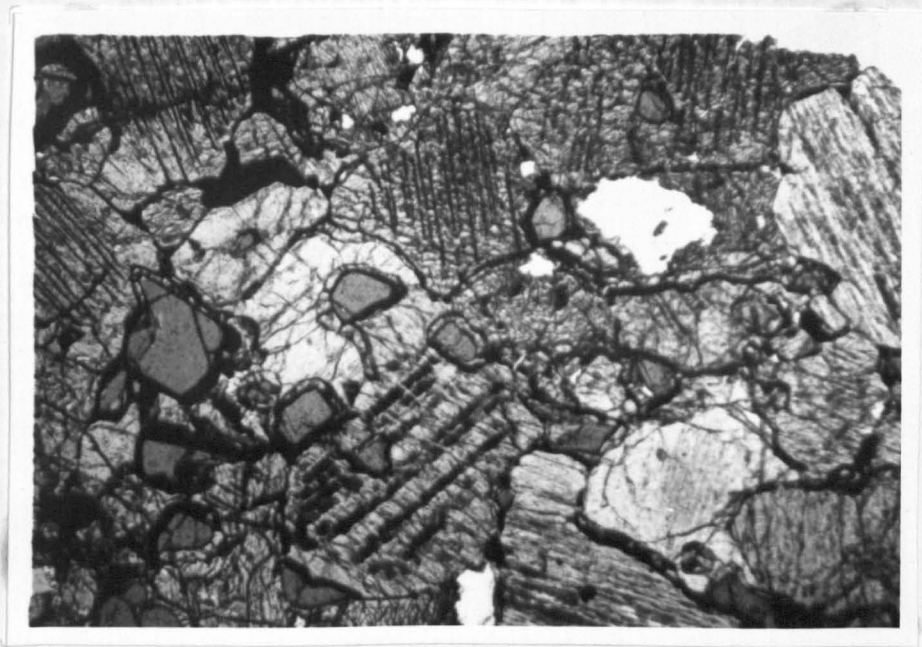


TABLE 8. Modal analyses of pyroxenitic inclusions

	DE15	Dol2	KK20	KK21	E11	Hal7
Garnet	39	32	37	28	6	} 22
Clinopyroxene	52	68	49	67	17	
Orthopyroxene	6.5	-	-	-	12	78
Plagioclase	-	-	14	-	-	
Olivine	-	-	-	-	65	
Spinel	2.5	-	-	-	-	
Brown opaque flaky mineral	-	-	-	5	-	

DE15 garnet-pyroxenite nodule from Deutsche Erde

Dol2 garnet-pyroxenite nodule from Docheib

E11 garnet-lherzolite nodule from Louwrensia
(Nixon et al 1963).

KK20 garnet-pyroxenite nodule from Kaitzub & Kaudus.

KK21 garnet-pyroxenite nodule from Kaitzub & Kaudus

Hal7 bronzitite nodule from Hanaus l.

TABLE 9. Analyses of pyroxenitic and peridotitic inclusions

	KK25	KK21	Hal7	Dol2	KK14	DE15	Loll
SiO ₂	47.3	47.5	48.0	47.0	45.8	42.5	42.49
TiO ₂	0.13	0.78	0.14	0.44	0.18	0.05	0.18
Al ₂ O ₃	14.3	7.4	10.9	9.0	8.1	8.2	2.88
Fe ₂ O ₃	7.3	8.40	2.12	2.70	2.01	5.70	2.47
FeO	6.5	4.9	6.02	4.59	5.14	1.99	5.27
MnO	0.10	0.12	0.18	0.12	0.18	0.08	0.12
MgO	9.7	12.4	17.8	21.3	24.0	23.5	40.17
CaO	13.2	16.16	12.0	13.5	12.6	16.44	1.76
Na ₂ O	1.27	1.14	1.30	0.88	0.75	0.80	0.18
K ₂ O	0.13	0.05	0.25	0.27	0.17	0.02	0.06
H ₂ O ⁺	1.58	0.65	0.67	0.51	0.90	0.59	4.51
P ₂ O ₅	0.08	-	-	-	0.05	0.11	0.04
	101.59	99.50	99.38	100.31	99.88	99.98	100.13
s.g.	3.24	3.44	3.35	3.38	3.39	3.41	n.d.

Analyst : Dr. G. Hornung

- KK25 retrograde eclogite nodule from Kaitzub & Kaudus 2.
 KK21 garnet pyroxenite nodule from Kaitzub & Kaudus 2.
 Hal7 bronzitite nodule from Hanaus 1.
 Dol2 garnet pyroxenite nodule from Docheib 1.
 KK14 garnet pyroxenite nodule from Kaitzub & Kaudus 1.
 DE15 garnet pyroxenite nodule from Deutsche Erde 1.
 E11 garnet lherzolite nodule from Louwrensia
 recalculated without H₂O⁻ (Nixon et al 1963).

Retrograde eclogites (amphibolites and eclogite-amphibolites)

Several nodules have been found which have distinct retrograde characteristics. In thin section the gradual transition of eclogite into amphibolite can be seen.

The omphacitic pyroxene breaks down into a nearly isotropic greyish paste of low relief, which changes into a diopside-plagioclase symplectite or into an amphibole. The diopside-plagioclase symplectite encloses quartz and kyanite needles. Small relicts of clinopyroxene are still present and consist of a non-pleochroic pale green variety, which is biaxial positive and free of inclusions.

The amphibole is distinctly pleochroic with X= yellow green and Z= bluish green and has become nearly opaque with sagenitic inclusions of fine brown needles. X-ray data showed it to be actinolitic in character.

The garnet is still relatively unaltered, but it has been broken up into irregular elongated aggregates and is partially enclosed in the amphibolite. Kelyphitic rims are narrow.

Unaltered eclogites have not been found in the Gibeon kimberlites; however, the presence of diopside-plagioclase symplectites suggests that omphacite did originally exist in the rock.

Group B.: Olivine bearing nodules

Inclusions of this group weather rather more easily than the ones from group A, and so tend to be rejected for sampling. They are, however, more abundant than the

pyroxene-bearing nodules and form conspicuous nodules in surface hardbank.

The nodules are composed of variable proportions of olivine, garnet and pyroxene. They are often rather coarse-grained and xenomorphic in texture.

Garnet-peridotites and garnet lherzolites.

These rocks are composed of variable proportions of a blood-red pyrope garnet and olivine or serpentine with smaller amounts of enstatite and emerald green chrome diopside. They form strikingly colourful green and red nodules.

The olivine is biaxial positive forsterite and is altered to serpentine only around the rim and along cracks. Faint twinning and undulose extinction are common. The crystals form an interlocking mosaic of xenomorphic crystals in which slightly granoblastic rounded garnet are embedded. A brown alteration of the serpentine fibres is very common.

The garnets are colourless in thin section. They have a typically rounded appearance although some of the larger crystals still have remains of previous crystal faces. Most garnets are surrounded by a narrow brownish grey kelyphitic rim with small phlogopite flakes along the outer rim.

The orthopyroxene is a colourless to very pale green variety. It is biaxial positive enstatite with a medium

relief and a 2V near to 90° . It does not contain inclusions.

The clinopyroxene is non-pleochroic and pale green in thin section and emerald green in hand specimen. It is free from inclusions or lamellae.

The olivine and garnet are the main constituents and are rather coarse-grained, especially the garnet. Ortho- and clino-pyroxene are usually present in much smaller size and abundance and the rocks range from garnet peridotites to garnet lherzolites. The olivine alters easily to serpentine minerals, and some olivine nodules have completely changed into serpentinite nodules, whereas other nodules form a skeleton of hard calcite with cavities, filled with the remains of few serpentized olivines and relatively unaltered crystals of chrome-diopside and a lilac garnet.

(v) Alteration of the nodules

Heat. Most of the inclusions in kimberlites are unaffected by pyrometamorphism. Only some of the accidental inclusions of host rock (shales and sandstone) show the effects of heat in that they are surrounded by a narrow hardbaked rim (see place 6).

Mechanical deformation. The majority of the mono-mineralic nodules have long, drawn out, elongated shapes and the nodules are often cracked. This is evidence for mechanical deformation during intrusion of the kimberlite. Undulose extinction, granulation and cracks are often observed in the olivines and garnets of the garnet peridotite

nodules. Assuming that they are accidental in origin these features could, however, represent relict textures, inherent in the original rocks from which they were derived.

Chemical alteration. Serpentinization is the most common type of chemical alteration in kimberlites and it has affected all the olivine-bearing inclusions in a greater or lesser degree. The serpentinization is accompanied by the formation of phlogopite and Dawson (1962) reports that in the Basutoland kimberlite the phlogopite has formed from the serpentine. The majority of the garnets, occurring either as monomineralic nodules or contained in polymineralic nodules, are surrounded by kelyphitic rims of fibrous minerals, amongst which phlogopite can be recognized. Rims and coatings of calcite often surround various mono- and poly-mineralic nodules. Inclusions of dolerite and basalt show signs of alkali-metasomatism. Some dolerite nodules contain considerable amounts of epidote, quartz and calcite, while the basalt fragments in Gibeon Townlands 2. are replaced by masses of calcite and natrolite in needlelike, massive and nodular habit.

(vi) Discussion of results

Discrete nodules of garnet can consist of both varieties, red brown or blood red, although it is noticed that the red brown varieties are much more altered. The same can be said for clinopyroxene; grass green or emerald

green varieties occur as discrete nodules, the grass green one being the more altered. The presence of relatively unaltered olivine nodules beside very altered ones is also very marked.

It is suggested that the unaltered nodules have been derived from broken up olivine-bearing inclusions during intrusion of the kimberlite.

The main difference between the basic granulites ("norites") and the garnetiferous pyroxenites is the presence of basic plagioclase and the absence of pyroxene lamellae in the first group while pyroxene lamellae are typical in the second group and plagioclase is absent or only present in very small quantities. Sagenitic inclusions are common in both groups, but they are more frequent in the norites.

Sagenitic inclusions in garnet and pyroxene and lamellae in pyroxene have been described from many rocks in the granulite and pyroxenite facies (Davidson 1943; Knorring and Kennedy 1958; Ross et al 1954). They are considered indications of high temperature (Poldervaart & Hess 1951). Descriptions of these phenoma from eclogites (where high pressure predominates) seem to be lacking.

Noritic or basic hypersthene - granulite inclusions have been described from kimberlites in Russia (Bobrievitch et al 1959) and Katanga (Verhoogen 1938). Some Russian

kimberlites contain a series of inclusions which show a gradual change from hypersthene-schists, similar to those occurring in the crystalline basement of the Siberian Platform, into plagioclase-eclogites (Bobrievitch et al 1959). Associations of basic granulites, eclogites and anorthosites have a world wide distribution in Archean formations (numerous examples quoted by Davidson 1943, p. 103). The Gibeon kimberlites also show a range of inclusions from anorthosite, "norite" or basic granulite, hypersthene granulite, garnet pyroxenite to eclogite, although unaltered eclogites have not been found. It seems reasonable to suppose that all these pyroxene-bearing inclusions are accidental in origin and derived from high grade metamorphic rocks in the lower basement of Southern Africa.

Olivine-bearing inclusions are found in nearly all the vents. Usually they can easily be separated from the soft blue ground or top soil but some are tightly contained in surface hardbank, notably in Anis-Kubib and Gibeon Townlands 2 (figure 4). Olivine-bearing nodules from different kimberlite occurrences are all very similar.

The positions of the analysed kimberlites and nodules have been plotted on a von Wolff diagram (figure 9).

Three distinct groups can be recognized. The first group, near to the position of the average tholeiitic basalt,

norite and pyroxene-gabbro (Nockolds 1954) contains the basalt and dolerite inclusions, i.e. Da 11, Ha 19, Ha 21, L 53 and O 21 (table 5) plus the basic granulites, i.e. DE 13, M 21, M 25 and O33; De 12 is an anorthosite and KK 25 is a retrograde eclogite (tables 7 and 9).

The second group contains the garnet pyroxenites i.e. KK 21, Ha 17, DE 15, Do 12 and KK 14 (table 9); O 22 is an amphibolite, a retrograde eclogite.

It is seen that the garnet pyroxenites fall just outside the eclogite field, (compare figure 12, page 165).

The third group contains the olivine-bearing inclusions E 3, E 11, and the kimberlites A 1, F 13, GR 11, Ha 12 (compare figure 8, page 81 and table 3); the transition from kimberlites to carbonatites is represented by the trend in the direction of the calcite corner, i.e. Ht 16, Ht 15 and A 3 (table 17).

(vii) Conclusions

Summarizing it can be concluded that the Gibeon kimberlites are characterized by containing :

1. numerous garnet peridotite nodules in every vent,
2. many nodular inclusions of basic granulite,
3. many nodular inclusions of garnet pyroxenite,
4. few nodular inclusions of retrograde eclogite,
5. many monomineralic nodules of garnet, clinopyroxene, ilmenite and olivine.

The garnet peridotites consist of : forsterite, blood red garnet (pyrope) and a little emerald green clinopyroxene (chrome diopside) and enstatite.

The basic granulites consist mainly of : basic plagioclase, orthopyroxene (bronzite) with sagenitic inclusions and some clinopyroxene, (with diallage or salite structures).

The garnet pyroxenites consist mainly of : orange red garnet (almandine-pyrope) and dark green clinopyroxene (omphacitic).

The retrograde eclogites contain : partly decomposed clinopyroxene (omphacite,) orange red garnet, amphibole (actinolitic) and a little sodic plagioclase, quartz and kyanite.

The monomineralic nodules are : altered brownish red garnets with kelyphitic rims, clean blood red garnets, grass green clinopyroxenes with alteration rims, clean emerald green clinopyroxenes, altered ilmenite and olivines both with and without alteration rims.

Another characteristic of the Gibeon kimberlites is the presence of many angular inclusions of basalt and dolerite fragments, derived from the Stormberg volcanics.

The inclusions have been little affected by the effects of heat and mechanical deformation.

Chemical alteration has taken place under the

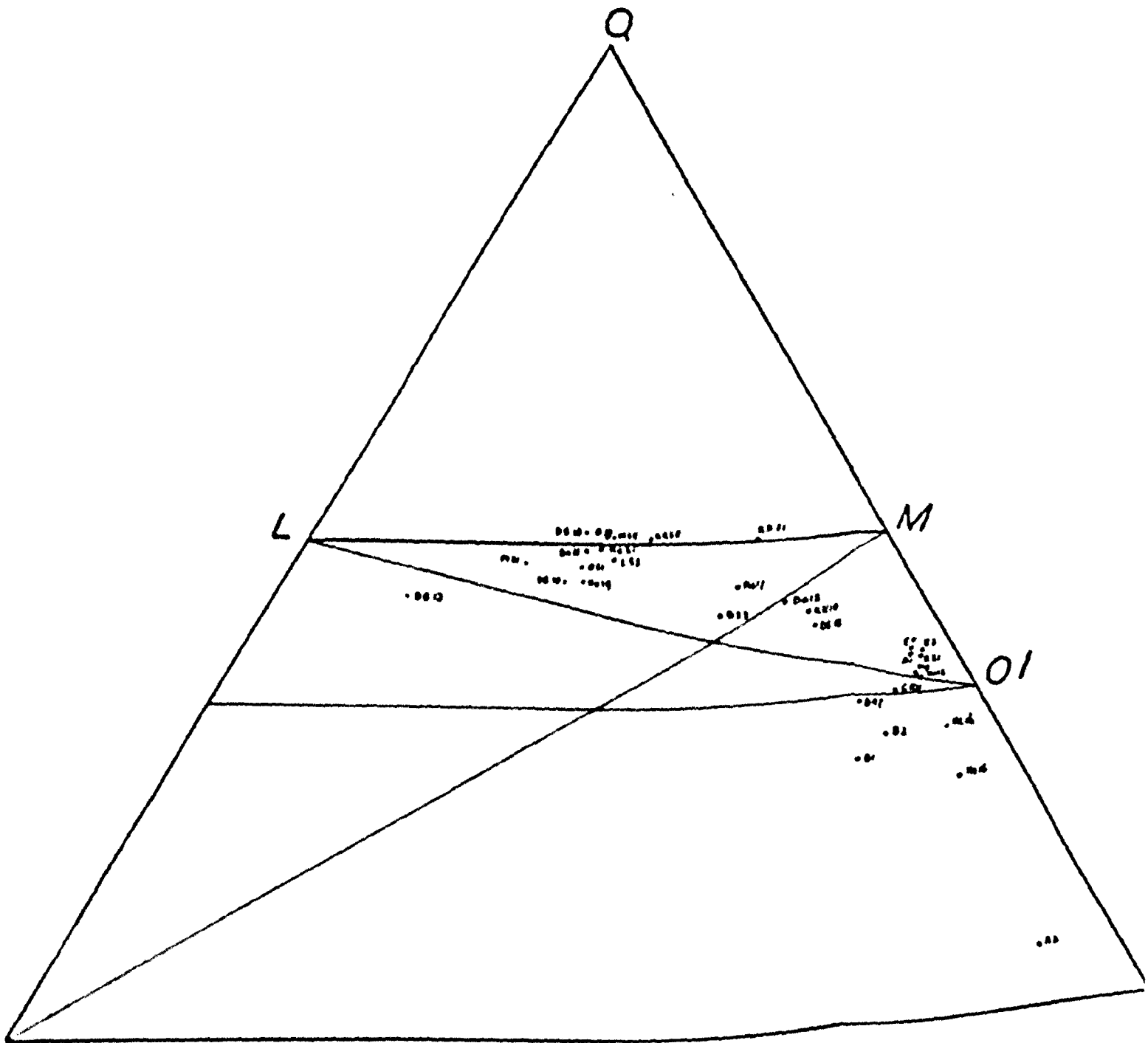


Fig. 9. Von Wolff diagram. Composition of the Gibeon meteorite breccias and related rocks (for explanation of symbols see page 112).

influence of agents rich in H_2O , CO_2 , CaO and alkalies.

(d) Mineral chemistry(i) Garnets

Several varieties of garnets, distinguishable by colour differences occur in kimberlite heavy mineral concentrates. Earlier writers (van Lingen 1928, Williams 1952) have published analyses of garnets without considering colour varieties or mode of occurrence and considered that garnets containing unusually high amounts of magnesia and chromium, were kimberlitic.

Following the work of Nixon (Nixon 1960; Nixon et al 1963) the examination of chemical analyses, X-ray diffraction patterns and optical data have made it possible to define two main varieties :

- (1) chrome pyrope, a crimson (blood red) or lilac variety, derived from garnet-lherzolite inclusions.
- (2) pyrope-almandine or almandine-pyrope, an orange-red variety, derived from garnet-pyroxenite inclusions.

A more indistinct variety consists of :

- (3) titanium-bearing chrome pyrope, a red brown variety, occurring as discrete nodules in kimberlite.

For recalculations of the chemical analyses the

structural formula of Menzel (1928) was adopted, R_3^{2+} R_2^{3+} $(SiO_4)_3$ with $R^{2+} = Mg^{2+}, Fe^{2+}, Mn^{2+}, Ca^{2+}$ in 8-fold co-ordination and $R^{3+} = Al^{3+}, Fe^{3+}, Ti^{3+}, Cr^{3+}$ in 6-fold co-ordination. The garnet end member molecules were calculated in the order : andradite, uvarovite, grossularite, spessartine, almandine and pyrope. Fermor's molecules, koharite and skiagite were not considered, but in one case it was necessary to calculate hanléite, $3MgO \cdot Cr_2O_3 \cdot 3SiO_2$ as there was not enough calcium to combine with the chromium.

Chrome pyrope. (blood red). Two new analyses of crimson garnets, GT350 and Hal3 (table 10) derived from lherzolite inclusions give additional evidence to the data of Nixon et al (1963) and confirm the presence of chrome-rich pyrope in the peridotitic inclusions in kimberlite (see table 10).

Typically this garnet contains circa 20% MgO and 2% or more Cr_2O_3 , which corresponds to over 70% of pyrope end member and 6% or more of uvarovite end member. When the Cr_2O_3 percentage increases, the MgO and Al_2O_3 decrease, with Al_2O_3 diminishing more than MgO; CaO also increases slightly.

The X-ray and optical data are given in table 11. The rate of change between the weight percentages of Cr_2O_3 and the R.I. seems to be linear at these low values (see figure 10, diagram after Nixon et al 1963). Figure 10 shows how

the crimson chrome-pyropes all fall on a nearly straight line, while the red brown pyropes (A1, L20) and the orange red pyrope-almandines (KK21, Kbl, E15) cannot be connected by a single curve.

The Frietsch diagram (figure 11) shows that the chrome-pyropes can be delimited to a special field, although pyropes with exceptionally high Cr_2O_3 values cut right through the eclogite and granulite field. It is probably the slight increase in CaO, which is connected with the Cr_2O_3 increase, that influences the cell size so much.

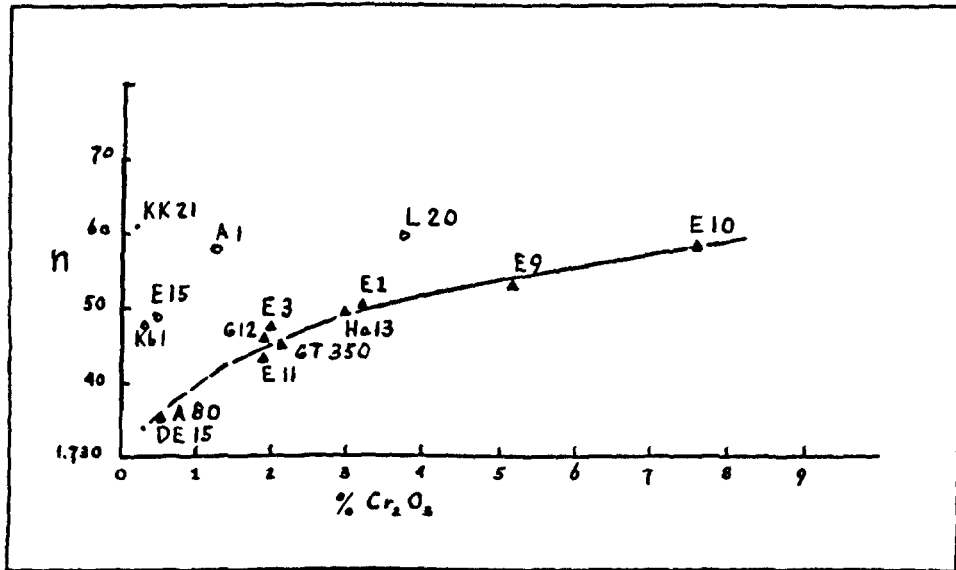


Fig. 10. Diagram of weight percentage of Cr_2O_3 in pyrope garnets (after Nixon, et al, 1963).

▲ = bloodred chrome pyrope

● = brownish red titanium-bearing chrome pyrope

◦ = orange red almandine pyrope

Explanation of symbols of figures 10 and 11:

A80, E1, E2, E3, E4, E5, E6, E7, E8, E9, E10, E13, E15, E39, K44 = garnets from Basutoland (Nixon, et al, 1963).

G12, K61 = garnets from Kimberley (Nixon, et al, 1963).

E11, GT350, H13, L20 = garnets from S.W. Africa, table 10.

A1, DE15, KK21, = garnets from S.W. Africa, table 12.

M22 = garnet from S.W. Africa, table 11.

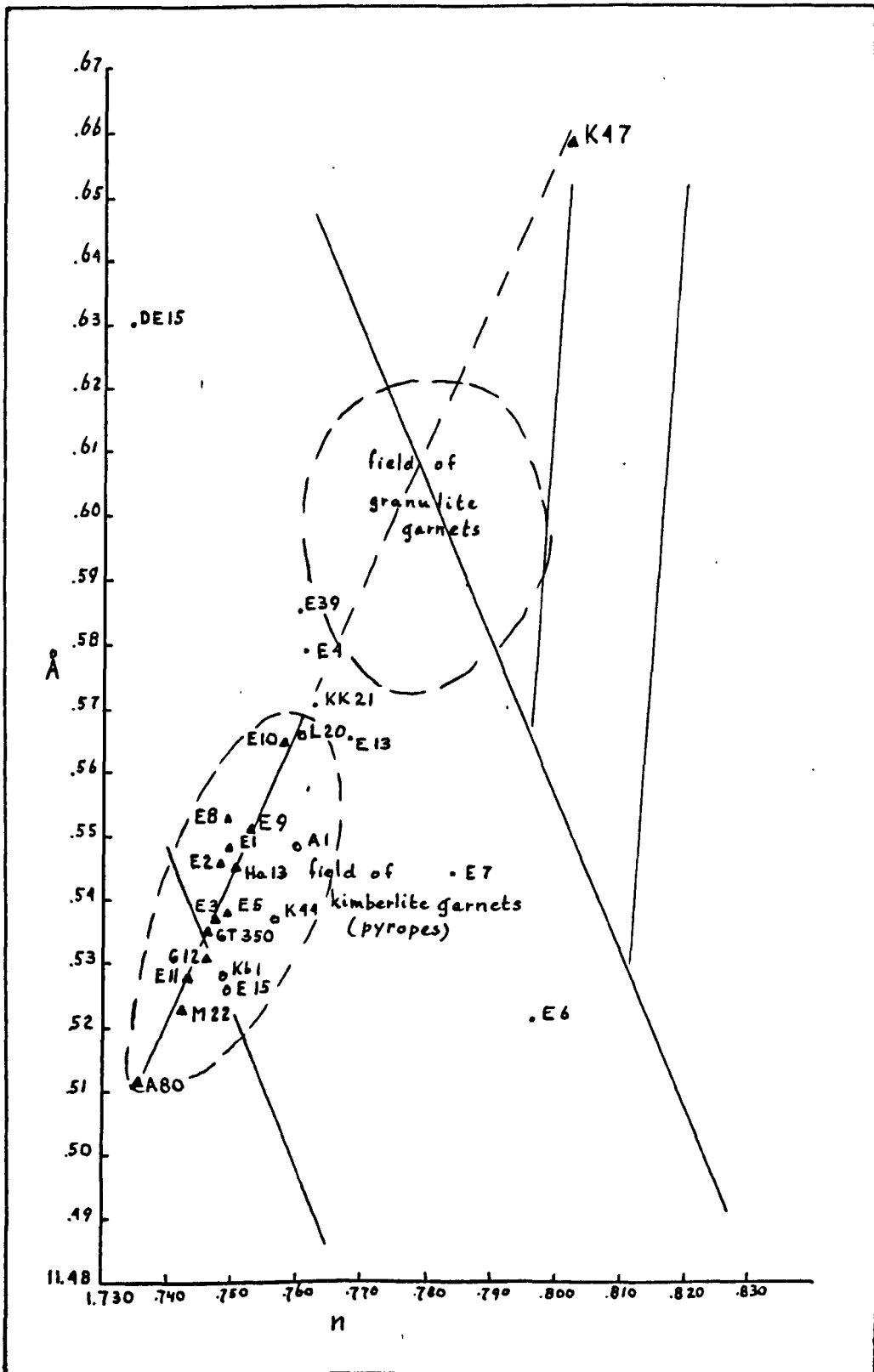


Fig. 11. Diagram after Frietsch (1957) showing unit cell size and refractive index of garnets.

TABLE 10. Analyses of chrome pyropes

	E11	GT350	Hal3	L20	E10
SiO ₂	42.77	42.44	42.25	42.32	41.90
TiO ₂	0.30	0.26	0.23	0.80	0.11
Al ₂ O ₃	21.91	21.40	21.10	18.87	16.92
Cr ₂ O ₃	1.90	2.07	2.71	3.67	7.52
Fe ₂ O ₃	1.25	0.97	1.00	1.38	1.24
FeO	6.79	7.62	6.86	6.79	6.17
MnO	0.26	0.35	0.37	0.29	0.59
MgO	20.70	20.31	20.19	19.92	19.64
CaO	4.65	4.75	5.05	5.64	6.27
	<u>100.53</u>	<u>100.17</u>	<u>99.76</u>	<u>99.69</u>	<u>100.36</u>

Analyst : Dr. O. von Knorring

Percentage composition in terms of garnet end member molecules

Andradite	3.3	3.3	3.3	6.0	3.3
Uvarovite	5.4	8.8	7.6	8.7	12.8
Hanleite	-	-	-	1.9	8.6
Grossularite	3.1	-	2.2	-	-
Speccartine	0.6	0.7	0.7	0.6	1.2
Almandine	13.9	15.1	14.2	12.5	12.4
Pyrope	73.7	72.1	71.8	70.3	61.7

- E11 chrome-pyrope (blood red) from lherzolite inclusion, Louwrenzia, S.W.A. (Nixon et al 1963).
 GT350 chrome-pyrope (blood red) from lherzolite inclusion Gibeon Townlands 2, S.W.A.
 Hal3 chrome pyrope (blood red) from lherzolite inclusion Hanaus 1, S.W.A.
 L20 chrome pyrope (brownish red) discrete nodule Lichtenfels 2, S.W.A.
 E10 chrome pyrope (blood red) from altered inclusion Basutoland (Nixon et al 1963).

TABLE 11. Physical properties of garnet from kimberlites

<u>No.</u>	<u>Occurrence & locality</u>	<u>n</u>	<u>aA</u>	<u>colour</u>
<u>Pyropes</u>				
A1	discrete nodule, Amalia 1	1,759	11,548	red brown
A32	discrete nodule, Amalia dyke	1.756	11,548	red brown
Ha31	discrete nodule, Hanaus 1	1,760	11,557	red brown
Ha32	discrete nodule, Hanaus 1	1,759	11,556	red brown
<u>Chrome-pyropes</u>				
Ha13	lherzolite, Hanaus 1	1,750	11,545	crimson
L5	garnet-peridotite, Achterfontein	1,748	11,540	crimson
L20	discrete nodule, Lichtenfels 2	1,760	11,566	brownish red
GT10	garnet peridotite, Gibeon Townlands 1	1,746	11,534	crimson
GT350	lherzolite, Gibeon Town- lands 3.	1,745	11.535	brownish red
A31	discrete nodule, Amalia dyke	1,746	11,529	lilac
GT351	lherzolite, Gibeon Town- lands 3.	1,744	11,529	lilac red
M22	weathered lherzolite, Mukorob 2.	1,742	11,523	lilac
<u>Almandine-pyropes</u>				
KK14	garnet pyroxenite, Kaitzub & Kaudus	1,766	11,569	orange red
KK20	- do -	1,763	11,571	- do -
KK21	- do -	1,762	11,570	- do -
KK22	- do -	1,766	11,567	- do -
KK23	- do -	1,769	11,566	- do -
KK25	- do -	1,766	11,566	- do -
<u>Grossularite pyropes</u>				
DE15	garnet pyroxenite, Deutsche Erde	1,734	11,630	pale pink

Titanium-bearing chrome pyrope (brownish red). Two new analyses are presented for brownish red garnets (Al and L20, table 12 and 10), extracted from the kimberlite matrix. These data and the X-ray and optical data from several others (table 11) show that they cannot be distinguished from the chrome pyropes in the Frietsch diagram. They have the same amount of MgO as the chrome pyropes, but a slightly higher ferrous iron content instead of chromium, increases the R.I. and brings the brownish red pyropes into the right side of the kimberlite garnet field. The small amount of titanium probably causes the brownish red colour.

Almandine-pyrope (orange red). One new analysis has been made of an orange red garnet (KK21, table 12), extracted from a garnet pyroxenite; taken in conjunction with data from Nixon (et al 1963), this analysis again demonstrates the variability of garnets from eclogites and garnet pyroxenites (see figure 11). The R.I. and cell sizes vary considerably depending on the iron and calcium percentages respectively. The density of the almandine-pyropes is circa 3.8 and higher, while the pyropes and chrome-pyropes have a density of circa 3.7.

Grossularite-pyrope (pale pink). An unusually light pale pink garnet, (DE15, table 12) ($G = 3.58$) has been extracted from a garnet-pyroxenite from Deutsche Erde. The X-ray and optical data show a very large cell size (high CaO) and

a low R.I. (low FeO). The chemical analyses show it to be a grossularite-pyrope (see table 12) which falls in the immiscibility gap between the pyralspite and the ugrandite series (see Winchell & Winchell 1951, page 484).

TABLE 12 Analyses of pyropes and almandine-pyropes

	Al	KK21	1	2	DE15
SiO ₂	42.13	41.30	41.82	41.52	42.58
TiO ₂	0.89	0.18	0.04	trace	0.08
Al ₂ O ₃	20.56	21.79	21.60	23.01	22.60
Cr ₂ O ₃	1.23	0.20	0.04	0.22	0.32
Fe ₂ O ₃	1.70	1.79	2.05	1.22	0.95
FeO	8.10	13.86	18.99	12.86	4.86
MnO	0.32	0.44	0.39	0.33	0.18
MgO	19.95	15.40	9.36	16.64	16.19
CaO	5.30	5.38	5.86	4.71	12.58
	<u>100.18</u>	<u>100.34</u>	<u>100.15</u>	<u>100.51</u>	<u>100.34</u>

Analyst : Dr. O. von Knorring

Percentage composition in terms of garnet end member molecules

Andradite	7.3	5.5	7.6	3.4	2.8
Uvarovite	3.4	0.7	1.2	0.6	0.9
Grossularite	2.5	8.1	8.3	8.3	28.5
Spessartine	0.6	0.9	1.0	0.7	0.4
Almandine	16.0	28.4	42.6	26.3	9.7
Pyrope	70.2	56.4	38.3	60.7	57.7

-
- Al discrete nodule from kimberlite Amalia, S.W.A.
 KK21 almandine-pyrope from garnet-pyroxenite,
 K aitzub & Kaudus, S.W.A.
 1 pyrope-almandine from diamond-bearing eclogite,
 Mir pipe (Bobrievitch et al 1959).
 2 pyrope from eclogite in olivine rock,
 Almklovdalen, Norway (Eskola 1921) H₂O content 0.16.
 DE15 grossularite-pyrope from garnet pyroxenite,
 Deutsche Erde, S.W.A.

(ii) Clinopyroxenes

Clinopyroxenes, like garnets, occur in several varieties in the heavy mineral concentrates from kimberlite (see table 14). New data are given below for clinopyroxenes, extracted from garnet pyroxenite - and garnet peridotite - nodules. Clinopyroxenes from eclogites contain considerable amounts of alumina and alkalis, which can be recalculated as jadeite. Clinopyroxene with 8 or 9% Al_2O_3 and 4 to 8% Na_2O is called omphacite. The emerald green chrome diopside, occurring in garnet peridotites and garnet pyroxenites from the Gibeon province, contains small amounts of aluminium and sodium, lower than those normally occurring in omphacites from eclogites. Non-chromium bearing clinopyroxenes, also containing small amounts of aluminium and sodium, exist as well in the Gibeon province.

Hence it is possible to distinguish between three varieties :

1. Omphacitic chrome diopside
2. Omphacitic diopside (chrome-poor)
3. Omphacite

Omphacitic chrome diopside. Two new analyses of emerald green clinopyroxene are given in table 13. The optical properties (table 13) are in agreement with the data of Nixon (et al 1963), but the mode of occurrence is

not confined to one category. Chrome diopside is associated with chrome pyrope in peridotitic inclusions, but emerald green diopside occurs as discrete nodules in kimberlite and has been extracted for analyses from a garnet pyroxenite from Deutsche Erde. The optical data are similar to the diopside end member, although the R.I. and 2V are rather higher, due to the influence of the jadeite or aegirine end member. The X-ray patterns of chrome diopside DE15 and diopside KK21 are nearly identical.

Omphacitic diopside (chrome-poor) Two new analyses of light green or grass green clinopyroxenes, extracted from garnet pyroxenites, in addition to data from Nixon (et al 1963) and Williams (1932), confirm the existence of diopsides, containing amounts of aluminium and sodium lower than in "normal" omphacite (table 13). There are no data to state that this diopside is similar to those occurring as discrete nodules in kimberlite.

Comparing the omphacitic diopsides with the omphacitic chrome diopsides it is seen that the amount of alkalis is of the same order, but part of the aluminium is replaced by chromium.

Omphacite. True omphacites have not been found in the Gibeon province.

Table 13. Analyses of omphacitic diopsides and chrome diopsides

	DE151	KK21	DE152	M22
SiO ₂	53.20	51.71	54.06	53.47
TiO ₂	0.10	0.60	0.17	0.10
Al ₂ O ₃	4.34	4.53	2.05	2.70
Cr ₂ O ₃	0.21	-	1.29	1.33
Fe ₂ O ₃	0.19	3.41	1.32	1.23
FeO	1.52	1.93	0.96	1.87
MnO	0.02	0.07	0.06	0.08
MgO	15.90	14.57	16.81	16.61
CaO	22.66	21.77	21.92	20.33
Na ₂ O	1.57	1.71	1.54	1.96
K ₂ O	0.04	0.05	0.01	0.03
	<u>99.75</u>	<u>100.35</u>	<u>100.19</u>	<u>99.71</u>

Analyst : O. von Knorring

n _x	1,674	1,670	1,675	1,677
n _y	1,680	1,675	1,683	1,685
n _x	1,698	1,693	1,701	1,702
2V _z	59°	64°	68°	70°

DE151 grass green diopside from garnet pyroxenite, Deutsche Erde, S.W.A.

DE152 emerald green diopside from garnet pyroxenite, Deutsche Erde, S.W.A.

KK21 dark green diopside from garnet pyroxenite, Kaudus, S.W.A.

M22 emerald green diopside from weathered peridotitic nodule, Mukorob, S.W.A.

DE151 = Ca_{14.5} Na_{1.8} Mg_{14.1} Fe_{0.8}²⁺(Fe³⁺, Ti, Cr, Al_{2.8}) 3.0
Al_{0.3} Si_{31.7} O₉₆ percentage Al in Z = 0.9%,
surplus Al in Y = 1.4

DE152 = Ca_{13.5} Na_{1.7} Mg_{14.5} Fe_{0.5}²⁺(Fe³⁺, Ti, Cr, Al_{0.4})1.6
Al_{1.0} Si_{31.0} O₉₆ percentage Al in Z = 3.2%

KK21 = Ca_{13.5} Na_{1.9} Mg_{12.5} Fe_{1.0}²⁺(Fe_{1.5}³⁺, Ti, Cr, Al_{1.0})2.7
Al_{2.1} Si_{29.9} O₉₆ percentage Al in Z = 6.7%

M22 = Ca_{17.5} Na_{2.2} Mg_{14.3} Fe_{0.9}²⁺(Fe³⁺, Ti, Cr, Al_{0.6}) 2.2
Al_{1.3} Si_{30.7} O₉₆ percentage Al in Z = 4.0%

(iii) Orthopyroxenes

Two types of orthopyroxene are found in the kimberlite mineral concentrates, pale green enstatite and smoky brown bronzite. Discrete nodules of orthopyroxene have not been found in the Gibeon kimberlites, therefore a conclusion about the nature of the orthopyroxene in kimberlite, if any, cannot be drawn here.

Using the mineralogical data of the kimberlite inclusions it is assumed that the enstatites are derived from the granulites and garnet pyroxenites.

(iv) Olivines

Two types of olivines are found in the mineral concentrates, i.e. forsterite and chrysolite. X-ray and optical data show that the olivines from kimberlites and from the garnet peridotite nodules range from F090 to F094. There are not yet enough data to decide whether the forsterites from the kimberlite are similar to those occurring as discrete nodules or those occurring in the garnet peridotite nodules. The more fayalitic olivines in the concentrates could be derived from the basalt and dolerite fragments of the Stormberg volcanics. However, Nixon (1960) suggested that the chrysolites were derived from the kimberlite matrix.

(v) Ilmenite

Chemical analyses of ilmenite nodules show a very high

percentage of MgO. (Nixon et al 1963 : 8.65%; Wagner 1914 : 8.87%; Williams 1932 : 8.00%). This leads to the conclusion that the typical variety occurring in kimberlite is a micro ilmenite.

The ilmenite in the nodules with a composite nature has also been shown to be a micro ilmenite (Frankel 1956).

(vi) Discussion of results

Nixon (et al, 1963) divided the garnets from kimberlite concentrates into three groups : 1. pyropes, 2. chrome pyropes and 3. almandine-pyropes, derived respectively from the kimberlite, the garnet peridotite nodules and the eclogite nodules. However, figure 11. shows that two definite fields, distinctly separating chrome-rich and chrome-poor pyropes cannot be recognized. Both types of pyropes, the blood red and the brownish red, can be more or less rich in chromium. A distinction between the two types can be made, however, according to their titanium content and their amount of alteration.

The titanium-bearing brownish red pyropes are always surrounded by thick kelyphitic rims and always occur as discrete nodules in the kimberlite matrix.

The blood red chrome pyropes are contained in the garnet peridotite nodules and occur occasionally as discrete nodules without alteration rims in the kimberlite matrix. In this case they are considered to be derived from broken-

up garnet peridotite nodules.

The almandine-rich pyropes have quite variable properties. Their colour, however, is quite distinctive orange red.

Den Tex and Vogel (1962) have established a field of granulite-garnets for garnets with rather high proportions of the grossularite and almandine end members. The field of eclogite-garnets lies probably between that and the field of the peridotite-garnets.

Comparing the data from Nixon (Nixon, 1966; Nixon et al 1963), Bobrievitch et al (1959), and Eskola (1921) it seems that there are :

- 1) pyrope-almandines, in which the pyrope end member ranges from 30 to 50%, and grossularite + almandine are over 50%;
- and 2) almandine-pyropes, which contain over 50% pyrope end member and grossularite + almandine ranges from 30 to 50%. They also contain some chromium (less than 0.5%).

Garnets from eclogites in metamorphic rocks belong to the first type, while garnets from garnet pyroxenites or eclogites "which are associated with the kimberlitic magma" (Bobrievitch et al, 1959) or which are considered intrusive (Eskola 1921) belong to the second type.

Garnet KK 21 (table 12) belongs to the second type.

In the opinion of the writer insufficient data are available for any recognition of the fundamental differences in the composition of garnets derived from various eclogites; nor is it known if definite boundaries exist between the garnet stability fields of granulites, garnet amphibolites, eclogites or garnet pyroxenites.

The clinopyroxenes yield a similar picture as the garnets. Grass green clinopyroxene with alteration rims occur as discrete nodules in the kimberlite matrix, while emerald green and light green clinopyroxenes without alteration rims are contained in the garnet pyroxenites. Emerald green chrome diopsides without alteration rims are likewise considered to be derived from broken-up nodules.

The fact that the omphacitic pyroxenes contain unusually low amounts of alumina and alkalis, could mean that the PT conditions were too low to form normal omphacites. The percentages of Al in the four-fold coordination is rather high and in the case of KK 21 (see table 13) it is comparable with the garnet-pyroxene-hornblende-scapolite gneiss from Ghana (Knorring and Kennedy 1958); Al in Z = 7.5%) which suggests that this type of rock is formed in a PT field between the amphibolite or pyroxenite facies and the eclogite facies.

On the other hand, the fact that minerals like plagioclase and hornblende are not present in the garnet pyroxenite nodules, shows that there was no surplus of alumina and alkalies to form normal omphacite. All the alumina and alkalies that could go into the pyroxene structure did so. It seems then that the original ultrabasic bulk composition of the rock from which the nodules were derived and not the PT conditions, was the main criterion for the Si - Al and alkali relations in the clinopyroxene (see also Kushiro 1960).

(Compare figure 8 and figure 12, the positions of the garnet pyroxenites fall to the right of the main eclogite field).

Laboratory experiments have shown that the magnesium end members of the minerals under discussion are stable under higher pressures than the iron end members (Boyd and England 1959). Therefore, the minerals pyrope, forsterite and enstatite are indicative of higher pressure conditions than almandine-pyrope, omphacite, pyroxene or bronzite.

When the mineral associations chrome pyrope + forsterite (garnet peridotite), almandine-pyrope + omphacitic pyroxene (garnet pyroxenite) and pyroxene + plagioclase (granulites) are considered it is seen that the various PT conditions are reflected in the role played by aluminium.

It is seen that with increasing pressure, aluminium goes from the plagioclase via the pyroxene into the pyrope structure. In the pyroxene structure some aluminium can proxy for silicium, but with increasing pressure all the aluminium is in the 6-fold co-ordination position of the pyrope-structure.

(vii) Conclusions

Garnets from kimberlite concentrates can be divided into two main types :

1. chrome pyropes (blood red and brownish red)
2. almandine-pyropes (orange-red).

In the chrome pyropes two varieties can be recognized :

- 1a. blood red chrome pyrope, derived from garnet peridotites (or garnet lherzolites)
- 1b. brownish red chrome pyrope (titanium bearing), derived from the kimberlite matrix itself.

The orange red almandine-pyropes are derived from garnet pyroxenites or from eclogites.

The clinopyroxenes can be divided into two types :

1. omphacitic chrome diopsides (emerald green)
2. omphacitic chrome-poor diopsides (grass green and dark green).

Both varieties contain appreciable amounts of alumina and alkalies, but lower than in the omphacites from eclogites.

In the first variety chromium can replace aluminium.

From the comparison of the specific mineral associations of the granulitic, pyroxenitic and peridotitic inclusions it is concluded that these nodules reflect a range of variable PT conditions. The peridotitic nodules are formed under the highest pressure conditions.

A recapitulation of the results on the mode of occurrence of the heavy minerals in kimberlite concentrates is given in table 14.

TABLE 14. Mode of occurrence of the heavy minerals in kimberlite concentrates

<u>Minerals in concentrate</u>	<u>1</u>	<u>2</u>	<u>3</u>	<u>4</u>	<u>5</u>	<u>6</u>
olivine : forsterite	X		X			X
chrysolite		X				
phlogopite	X					X
ilmenite	X		X			
perovskite	X					
magnetite	X					
apatite	X					
pyrope var. red brown			X			
blood red			X			X
orange red					X	
clinopyroxene var. diallage				X		
grass green	?		X			
dark green					X	
emerald green			X		X	X
orthopyroxene : enstatite			?			X
bronzite/ hypersthene				X	X	
spinel					X	

1. microscopic crystals in the kimberlite groundmass and true phenocrysts in kimberlite (forsterite and phlogopite)
2. minerals derived from included basalt and dolerite fragments.
3. monomineralic nodules ("discrete nodules").
4. noritic nodules.
5. garnet pyroxenite nodules
6. garnet lherzolite and garnet peridotite nodules.

2. Calcium-rich rocks with kimberlitic affinities

(a) Introduction

As already briefly mentioned on page 77, the Gibeon kimberlites have a higher CaO - and volatile - content and a lower SiO₂-, Al₂O₃-, MgO - and alkali - content than the average kimberlites. Various examples of calcium-rich kimberlites and carbonatitic-kimberlitic dykes can be found in the vents and fissures on the farms Hatzium, Mukorob and Amalia (see figure 4).

In South West Africa, an occurrence of a monticellite-bearing peridotite was recognized by the author. This rock is not directly connected with a kimberlite vent, but it occupies a vent of its own, the Blue Hills vent (see map 4). The distance to the nearest kimberlite vent is 5 to 6 miles.

(b) Hatzium vent

The outcrop of the vent at Hatzium is mostly occupied by dark greyish-green hardebank. The hardebank is of the breccia-type and contains many inclusions of country rock. The outcrop is nearly circular and a dyke enters the southeastern part, which is occupied by a large irregular mass of carbonated dull grey hardebank (see table 16; Ht16). This hardebank is more homogeneous and contains small nodules of garnet and ilmenite. The density of this hardebank is 2.76. The dyke rock (density 2.96) is composed of compact grey calcite with lenses of light coloured crumbly granular

calcite and irregular masses of calcitic rock (density 2.72) which is traversed by intricately lobed spherical surfaces of denser calcite, probably remnants of reaction rims around previous nodules.

The dyke-rock is crowded with ellipsoidal cavities, mostly empty but occasionally lined with black ilmenite with a little magnetite or filled with black, shiny ellipsoidal nodules (see plate 16). In thin section the nodules are seen to be filled with calcite, enclosed in two concentric shells of opaque black ilmenite, separated by a thin film of calcite (see plate 17).

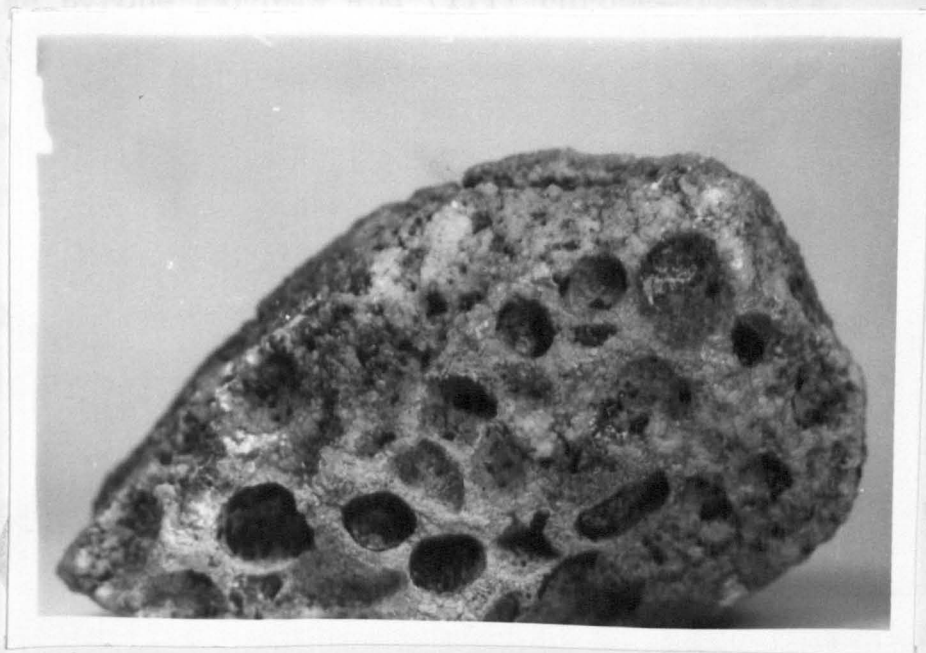
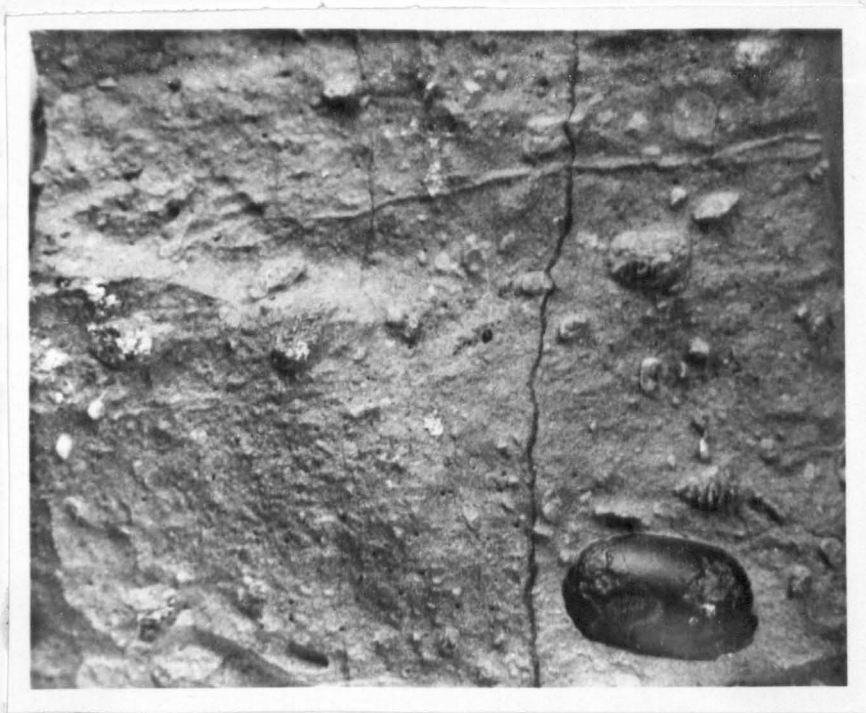
In the centre of the vent a soft friable rock occurs, it contains many magnetite octahedra set in a yellow earthy mass, which X-ray diffraction proved to be apatite (see table 16; Htl5). Ilmenite-encased cavities are also frequent in this rock.

(c) Mukorob dyke

Frankel (1956) has described a calcitized dyke which he calls an inclusion-bearing olivine melilitite, occurring near the kimberlite (M2) on the farm Mukorob. The dyke is not visibly connected with the kimberlite, but a genetic connection was assumed. The dyke consists of compact grey calcite and contains inclusions of country rock and nodules of diopside-ilmenite and diopside-garnet. The most common inclusions are black, shiny ellipsoidal inclusions, composed of a core of pale brown or creamy substance, surrounded by concentric shells of ilmenite (see plate 15).

Plate 15. Mukorob dyke, with ilmenite encased
olivine nodule (right-bottom corner)
natural size).

Plate 16. Granular calcitic rock from Hatzium 1
with empty cavities of previous ilmenite-
olivine nodules (natural size).



The pale brown substance was originally olivine, later replaced by serpentine, in turn replaced by quartz. These nodules are similar to the ones in Hatzium. The kimberlites of Mukorob and Hatzium are, moreover, both rich in apatite. Apatite has been recorded in the Mukorob pipe by Scheibe (1906) and the P_2O_5 content in Ht16 is rather high (table 16).

(d) Amalia dyke

A further example of the transition between kimberlite and carbonatite is provided by the dyke which connects the two kimberlites on the farm Amalia (see plates 18 and 19).

The dyke-rock is completely calcitized and is composed of pale brown yellow earthy calcite with many inclusions of (i) country rock (Dwyka mudstone); (ii) red-brown and lilac pyrope garnets and (iii) chrome-diopside. In addition large ellipsoidal nodules of ilmenite are present in large quantities.

(e) Other dykes

Nine calcitized dykes occur in the Ovas area where kimberlite minerals can be observed in situ in the rubble on the outcrop.

Many other dykes exist (e.g. Arditites-dyke) which consist of antigorite phenocrysts after olivine in a calcitic groundmass.

Kimberlite minerals cannot always be observed in the rock, but streams draining the outcrop directly, contain kimberlite minerals.

Plate 17. Photomicrograph of thin section F.9890
(Ht13). Concentric limonite shells
around calcitized olivine (X15).

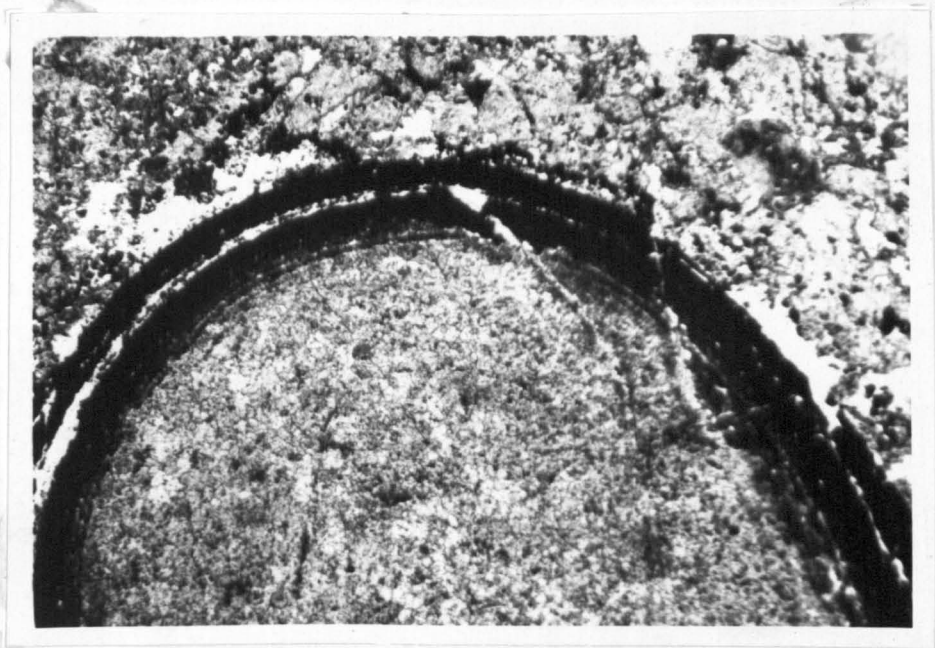


TABLE 15. Analyses of calcium-rich kimberlites and related rocks

	Ht16	Ht15	1	2	A3	B78
SiO ₂	25.0	17.0	13.30	7.29	4.6	2.93
TiO ₂	1.17	0.86	2.03	0.86	0.49	0.69
Al ₂ O ₃	2.4	2.7	8.98	1.04	3.5	0.68
Fe ₂ O ₃	7.69	4.37	2.94	2.23	1.08	9.69
FeO	0.99	2.52	2.15	1.58	2.41	0.00
MnO	0.15	0.08	0.18	0.35	0.25	0.33
MgO	26.0	6.3	13.78	3.74	9.4	0.79
CaO	15.9	37.0	29.63	45.71	39.35	45.63
Na ₂ O	0.20	0.37	0.16	-	0.23	0.22
K ₂ O	0.41	0.11	0.03	-	0.07	0.03
H ₂ O ⁺	9.60	3.61	6.60	0.54	1.57	1.49
H ₂ O ⁻	-	-	2.34	1.24	-	0.72
P ₂ O ₅	1.40	17.0	-	0.67	1.0	2.53
CO ₂	11.63	8.38	17.10	34.88	36.87	34.29
	<u>102.54</u>	<u>100.30</u>	<u>99.22</u>	<u>100.13</u>	<u>100.82</u>	<u>100.02</u>

s.g. 2.76

Ht16 surface hardebank, Hatziun, S.W.A. Analyst Dr. G. Hornung
Ht15 yellow ground, Hatziun, S.W.A. " " " "
1 carbonatitic lava from Igwisi Craters, Central
Tanganyika (Bassett 1956, quoted in Garson 1962),
BaO = 0.14, total = 99.36.
2 carbonatite dyke, Premier Diamond Mine, Transvaal
(Daly 1925).
A3 kimberlitic-carbonatitic dyke, Amalia, S.W.A.
Analyst : Dr. G. Hornung.
B78 calcitized dyke, near vent F west of Mt. Brukkaros,
S.W.A. Analyst : Miss J. Bandwin.

Plate 19. Detail of plate
18. Light brown kimber-
litic carbonatite with
veins of calcite and
inclusions of grey
mudstone.

Plate 18. Kimberlitic-
carbonatitic dyke on farm
Amalia.



(f) Monticellite peridotite of the Blue Hills

(i) Description of the vent

The monticellite peridotite is exposed in a vent on the lower slope of Mt. Brukkaros, about 3 miles south of the southern rim of the mountain. The principal rock type in the vent is a porphyritic ultrabasic rock, containing phenocrysts of olivine and flattened nodular aggregates of magnetite (up to $\frac{1}{2}$ inch diameter), set in a very fine grained granular groundmass. The colour is dark bluish grey; the rock is very tough and breaks with a splintery fracture. The density is 3.17.

The intrusion is situated in a short row of low hills (named the Blue Hills) and forms an outcrop about 900 yards long and 200 yards wide. The surface is covered by a 3 feet thick layer of calcrete. "Islands" of baked greyish-black shale protrude through the calcrete. A grey crumbly phlogopite-calcite rock is exposed in pits through the calcrete and in little gulleys on the south side of the hills. On the west side of the hills a tough bluish-black porphyritic rock is exposed in contact with steeply upturned shales and flagstones (ca 80° dip); the shales on the east side are slightly dipping inwards for a short distance. Contact metamorphism is slight; the colour of the maroon shales is changed to blue green for a distance of up to 10 feet and, nearer to the contact, they are slightly

baked. The shale-intrusive rock contact has been offset for a distance of about 70 yards by a small E-W fault.

Thin sills of variable thickness (1" - 9" approx.) surround the hills on the northeast and east sides. They are often lenticular and transgress from one bedding plane to another. They consist of altered basic igneous rock, greenish-blue when comparatively fresh but mostly completely weathered to a yellow-brown mass. Phenocrysts of large phlogopite flakes (up to $\frac{1}{4}$ inch) are common.

A $4\frac{1}{2}$ " - 5" wide yellow weathered dyke containing brecciated shale fragments is exposed on the south-east side of the hills.

(ii) Mineralogy

Under the microscope the monticellite-peridotite is seen to consist of perfectly fresh phenocrysts of olivine embedded in a fine-grained granular mosaic of colourless minerals, consisting of monticellite, nepheline and olivine.

Idiomorphic crystals of magnetite and perovskite are scattered throughout the mosaic. Ghost structures of altered phenocrysts, revealed by concentrations of very small magnetite crystals are also present.

The modal analyses of the peridotite is :

Forsterite phenocrysts	27%
ghost phenocrysts	4%
magnetite	9%

perovskite		5%
phlogopite	} in groundmass	2%
calcite		2%
groundmass		51%

Olivine is almost completely unaltered. Some phenocrysts show very little alteration to serpentine along cracks and others contain inclusions of small laths of colourless phlogopite.

The phenocrysts are up to 2 mm. diameter, but usually in the order of 0.5 to 0.7 mm, the outlines are perfectly idiomorphic in most cases and the crystals do not show indications of strain.

The olivine is biaxial positive, $2V_z$ equals 87° to 88° ; $n_x = 1.651$, $n_y = 1.667$ and $n_z = 1.684$ which indicates an Fo content of 92% to 94%.

Small xenomorphic olivine crystals are present in the groundmass.

Magnetite occurs as black idiomorphic crystals up to 0.1 mm. diameter in the groundmass and as very small specks in altered phenocrysts. It also forms flattened nodular aggregates in hand specimen.

Perovskite is present as brown idiomorphic crystals up to 0.1 mm. diameter. The crystals have a very high relief and are nearly isotropic. Complex twinning is commonly observed. The identification of this mineral was confirmed by X-ray diffraction patterns. The high Nb-content

in the trace element composition of the monticellite-peridotite (see B.1, table 4) suggests that the perovskite is fairly rich in niobium.

Ghost structures are formed by concentrations of very small grains of magnetite which reveal the presence of altered phenocrysts with olivine outlines. The phenocrysts consist of aggregates of magnetite, phlogopite, calcite and olivine. The phlogopite is colourless, $2V$ equals zero, and X-ray data point to a high Mg-content. The ghosts are thought to represent unstable phenocrysts of monticellite, containing a little alumina and alkalies.

The thin section also contains a rounded inclusion of a rock with a slightly different texture and composition. The nodule is 5 mm. in diameter and is separated from the host rock by a thin rim of calcite.

The included rock consists of a mosaic of olivine crystals (0.3 mm.) which contain many very fine grains of magnetite. The mosaic is interspersed by many small laths of colourless phlogopite and patches of calcite. The olivine has a very low birefringence compared with the olivines of the host rock, it is also biaxial positive. Perovskite is not present. The texture is aphyric.

This inclusion could be the result of alteration and recrystallization of a previously existing unstable subhedral

monticellite crystal.

The groundmass-mosaic of the monticellite-peridotite is extremely fine-grained, the average grain size is 0.03 to 0.04 mm, the texture is holocrystalline-granular.

Small olivine crystals are present in the groundmass together with many grains with a lower refractive index, which could be monticellite and/or nepheline and several small laths of phlogopite and small patches of calcite. Several unsuccessful attempts were made to separate the individual minerals of the groundmass. Separated fractions did, however, yield X-ray evidence for the presence of monticellite, forsterite, perovskite and nepheline. The determination of the olivine by the method of Yoder & Sahama (1957) gives an Fo-content of 94%. The determination of the nepheline by the method of Smith & Sahama (1954) gives a potassium content of 30% $\left(\frac{K}{K+Na+Ca}\right)$

(iii) Calcite-phlogopite rock within the monticellite-peridotite

Grey phlogopite-calcite rock occurs as lenses in the peridotite. In thin section it consists essentially of calcite and 2 mm. long fibrous laths of colourless phlogopite. Brown-stained pseudomorphs of antigorite after olivine-phenocrysts are also present, together with bleached perovskite and magnetite. The phenocrysts, magnetite and perovskite are of the same order of size as in the peridotite. The modal analyses of the phlogopite-

calcite rock is :

calcite - antigorite groundmass	32%
phlogopite	30%
antigorite-phenocrysts	24%
magnetite	9%
perovskite	5%

Except for a rather high CaO content, possible caused by contamination from the overlying calcrete, the calcite-phlogopite rock is similar to a micaceous kimberlite (see B2 and 1, table 17).

(g) Discussion of results

The presence of minerals and inclusions, characteristic of kimberlites, combined with a high CaO- and volatile-content place the calcium-rich kimberlitic rocks in an intermediate class between kimberlites and carbonatites. In the field, a connection between high calcite- and high ilmenite- content is noted, although this is not evident from the chemical analyses (see table 15).

Transitions between kimberlites and carbonatites also occur in other areas, notably at Igwisi, Central Tanganyika (Bassett 1956, quoted in Garson 1962). Garson (1962, p. 208) considers that the lava from the Igwisi craters represents a top fraction of the differentiates in a kimberlite vent, which with further differentiation would have produced dolomitic and sövitic carbonatites. He envisages a kimberlite vent as having a top fraction

enriched in volatiles, which through differentiation and diffusion acquires a carbonatitic composition. This would also explain the absence of kimberlitic extrusives, which would be carbonatitic in composition, according to this theory. Likewise, hypabyssal dykes and veins of kimberlite, which did not reach the surface would retain their calcium- and volatile-rich fraction and thus are richer in calcite, and sometimes phlogopite, than the kimberlites in the vents.

Various transitions from calcium-rich kimberlite to calcitized dyke are given in table 15. The analyses show the desilification and the growing predominance of calcium over magnesium, but unfortunately the exact nature of these rocks is obscured by extensive secondary alteration through weathering, which causes calcretization.

In contrast, the monticellite peridotite of the Blue Hills is completely unaltered and is characterized by the almost complete absence of volatiles. Occurrences of similar rocks, called porphyritic picrites by the Russian geologists, have been found in kimberlite vents of the northeastern Siberian Platform (Milashev, et al, 1963). They do not occur as inclusions in kimberlite, but form separate intrusions in the vents. These rocks, known as wesselite, contain streaks and lenses of monticellite-bearing varieties. Milashev (et al, 1963) considers

that the intrusions of wesselite are younger than kimberlites for two reasons: (i) they have a perfectly fresh appearance; and (ii) the kimberlite breccia in the same vent does not contain inclusions of wesselite.

The analyses of the monticellite peridotite shows its similarity to the Siberian monticellite picrites (see table 16). The interesting feature about these rocks is their calcium-rich ultrabasic character, low SiO_2 , high MgO, high CaO, combined with a high alkali- and a low Al_2O_3 content. The sodium- and calcium-content of the South West African rock are even higher than those in the Siberian rocks (see table 16).

Because of the overlying calcrete cover it is very difficult to decide if the calcite-phlogopite rock represents cognate inclusions which are more prone to weathering. Comparing the modal analyses of the monticellite peridotite and the calcite-phlogopite rock it is seen that the amounts of magnetite and perovskite are the same and the amount of olivine phenocrysts is nearly the same, but that the monticellite-nepheline-forsterite groundmass is represented by a mixture of calcite-phlogopite-antigorite. Beginning stages of phlogopitization and calcitization can be observed in the monticellite peridotite, but it is obvious that the difference cannot be caused by simple weathering.

An even greater problem is the origin of the monticellite peridotite itself. Comparing the monticellite peridotite with kimberlite the following points are noted: (i) They are similar in their olivine, magnetite and perovskite mineralogy and in the fact that the host rocks around the vents are upturned but only slightly metamorphosed; (ii) they are dissimilar in that the monticellite peridotite does not contain deep-seated inclusions and is characterized by an unaltered groundmass; and (iii) the chemical analyses (see B1 and 2, table 17) are similar in general, except for a higher CaO- and Na₂O-content and a lack of volatiles in the monticellite-peridotite.

A possible explanation is that the monticellite peridotite represents the crystalline phase of a liquid portion of the top fraction of a kimberlite vent, which has been enriched in CaO and alkalies, but which lost its volatiles. The calcite-phlogopite rock could then represent small volatile-rich portions, trapped in the liquid, resulting in a micaceous kimberlite. It is, however, very difficult to understand how the monticellite peridotite was emplaced, without causing not more than a slight metamorphism of the host rock.

TABLE 16. Analyses of monticellite-bearing picrites and peridotites

	B1	1	2
SiO ₂	31.16	33.13	34.02
TiO ₂	3.44	2.78	5.52
Al ₂ O ₃	5.63	7.41	5.98
Fe ₂ O ₃	7.32	5.04	5.27
FeO	9.04	8.29	8.48
MnO	0.27	0.22	0.23
MgO	20.18	21.11	20.15
CaO	17.09	14.82	12.82
Na ₂ O	2.12	1.09	1.00
K ₂ O	1.52	1.81	3.08
P ₂ O ₅	0.28	0.84	0.66
H ₂ O ⁺	1.45))	
H ₂ O ⁻	0.15)	3.49)	2.54
CO ₂	0.62)	(1.0.1.)	(1.0.1.)
	<u>100.27</u>	<u>100.03</u>	<u>99.75</u>

- B1. monticellite-peridotite from Mt. Brukkaros, S.W.A.
Analyst : Miss J. Baldwin.
1. monticellite-bearing picrite, Siberian platform
(Milashev et al 1963). 3.49 = loss on ignition,
of which H₂O = 1.21 and CO₂ = 0.38
2. monticellite-bearing picrite, Siberian platform
(Milashev et al 1963). 2.54 = loss on ignition,
of which H₂O = 0.63 and CO₂ = 0.93

TABLE 17. Analyses of micaceous kimberlites and related rocks

	B1	B2	1	2	3
SiO ₂	31.16	28.0	27.93	30.13	27.30
TiO ₂	3.44	2.28	2.73	3.60	3.68
Al ₂ O ₃	5.63	3.8	4.47	4.72	8.95
Fe ₂ O ₃	7.32	8.18	7.04	8.15	8.87
FeO	9.04	2.37	5.12	6.68	7.01
MnO	0.27	0.22	0.23	0.12	0.27
MgO	20.18	19.0	25.42	25.87	12.34
CaO	17.09	20.3	10.01	7.05	17.18
Na ₂ O	2.12	0.44	0.21	0.45	0.38
K ₂ O	1.52	2.71	1.18	0.96	2.99
H ₂ O ⁺	1.45	5.53	7.89	6.96	3.95
H ₂ O ⁻	0.15	0.61	0.68	1.55	-
P ₂ O ₅	0.28	n.d.	1.07	0.34	2.90
CO ₂	0.62	8.12	5.61	5.32	2.17
	<u>100.27</u>	<u>101.56</u>	<u>99.55</u>	<u>100.38</u>	<u>97.99</u>

- B1. monticellite-peridotite from Brukkaros, S.W.A.
Analyst : Miss J. Baldwin.
- B2. calcite-phlogopite rock from Brukkaros, S.W.A.
Analyst Dr. G. Hornung.
1. micaceous kimberlite, Robert dyke, Basutoland
(plus F = 0.89, total 100.44, less O for F,
0.38 = 100.06) (Dawson 1962).
2. dyke kimberlite, Troynoga, Olenek district,
U.S.S.R. (Krutoyarsky 1958, quoted in Dawson 1962).
3. alnöite, from Alnö, Sweden (von Eckermann 1948)
(plus BaO = 0.25, Cr₂O₃ = 0.07, S = 0.33,
F = 0.17 total 98.81).

3. Petrogenetic considerations

Petrogenetic conclusions on the origin of kimberlite must take into consideration (a) the origin of the nodules in kimberlite and (b) the origin of the kimberlite itself.

(a) The origin of the nodules in kimberlite

The nodules include : (i) monomineralic and composite nodules; (ii) olivine-bearing and pyroxene-bearing nodules; (iii) diamonds. It is understood that diamonds are, in fact, monomineralic nodules but in view of their great importance and significance in discussions of kimberlite genesis, it is thought that they warrant a separate section.

(i) Monomineralic and composite nodules

The minerals, which are contained in the kimberlite as discrete nodules, occur in two varieties : (1) minerals exhibiting partial or total alteration and (2) minerals which are comparatively unaltered.

The minerals in the first group include : titanium-bearing pyrope, diopside, picro-ilmenite and forsterite.

Smirnow (1959) has described the systematic distribution of colour differences in pyrope garnets from kimberlites in the U.S.S.R. and this indicates that they are diagnostic of individual kimberlites, i.e. they have crystallized in the kimberlite vent and are cognate.

Research of this kind has not been done on the other altered minerals but it is assumed that the alteration points to a common origin and all the minerals of group (i) are considered cognate. Additional evidence is given by the fact that the cognate pyropes are titanium-bearing, the diopsides are often subcalcic and the ilmenite is very rich in magnesium. These chemical features point to a kimberlitic origin.

The composite nodules are also considered cognate because they have the same characteristics as the minerals of group (i).

The minerals of the second group, chrome pyrope, chrome diopside and forsterite were derived from the disintegration of the olivine-bearing inclusions, the question of their origin thus depends on the origin of these inclusions.

(ii) Olivine-bearing nodules

The three main characteristics of the olivine-bearing nodules in kimberlites are as follows :

1. garnet-peridotites (or lherzolites) are the predominant deep-seated inclusions in kimberlites;
2. they have a remarkable constant chemical composition, regardless of the type of kimberlite in which they occur;

and 3. they have a mineral assemblage indicative of formation under high pressure (e.g. pyrope).

Constant chemical composition is also a characteristic feature of the olivine nodules, which occur in various undersaturated basalts. This led many authors to believe that the olivine nodules have been derived from a world-wide ultra-basic zone, i.e. the peridotite zone of the mantle; a review of the opinions of many authors has been discussed by Ross (et al 1954) and Wilshire and Binns (1961). Frechen (1948) and O'Hara and Mercy (1963) have presented arguments that according to their mineralogical composition the olivine nodules in basalts cannot be unmetamorphosed representative fragments of the upper mantle, but that they are of igneous origin. However, from their study of the nodules of the 1800-1801 alkalic basalt lava flow (Kaupulehu) of Hualalai volcano, Hawaii, which are of undoubted igneous origin, Richter and Murata (1961) have shown that the minerals of these nodules have a quite different composition than those of the average olivine nodules in basalts. O'Hara and Mercy (1963) consider that the garnet peridotite nodules in kimberlites represent relatively unaltered fragments of mantle material.

Certain olivine-bearing nodules in kimberlite contain only forsterite as their main constituent and little or no

garnet. The relative amounts of garnet and forsterite being variable, certain nodules could represent garnet peridotite fragments with a local absence of garnet. On the other hand, some of these peridotite nodules are quite large, while their bulk chemical composition shows, compared with the garnet peridotite nodules, considerable difference in the TiO_2 content, the K_2O content and the Na/K ratio (see table 18). It seems then that the peridotite nodules in kimberlite are fragments of a distinct rock type.

Comparing the average olivine nodules in basalts with the garnet peridotite nodules in kimberlite it is seen that their TiO_2 content and their K_2O content are more similar, but the olivine nodules have a considerably lower SiO_2 content and a higher Na_2O content. There are also important mineralogical differences. The main difference is the role played by aluminium, which is ⁱⁿ a 6-fold coordination in minerals of kimberlite inclusions, hence the presence of garnet. This suggests that they have originated under high pressure conditions, at least within the stability curve of pyrope (Boyd and England 1959). The obvious place to look for these conditions is the upper mantle. The argument for the origin of kimberlites follows the same lines, the presence of diamond in some

kimberlite from other areas points to a derivation from regions under very high pressure conditions.

It does not matter in this argument if the garnet-peridotites and the diamonds are cognate or accidental. In both cases the kimberlite must have either originated under very high pressure or moved from deeper levels through regions under very high pressures. (Regarding this last part of the previous sentence Davidson (1943, 1957) suggests that all inclusions in kimberlite are accidental and derived from the lower crust, see discussion below).

Williams (1932) and others, have suggested that garnet-peridotites were cognate. But the results of this study, the data of Nixon (et al 1963), O'Hara and Mercy (1963), Wagner (1914), Holmes (1936), and others, suggest that they are, in fact, accidental inclusions.

The arguments against a cognate origin are as follows:

1. Bulk chemical difference. The SiO_2 -content of the peridotite nodules is appreciably higher than that in the kimberlites, which is contrary to what would be expected of cognate nodules.
2. Mineralogical differences. The pyrope of the garnet-peridotite nodules contains more chromium and has a lower Fe/Fe+Mg ratio than in the kimberlites. The diopside is rich in chromium in the peridotites. Perovskite and

TABLE 18: Average composition of peridotites

	1	2	3	4	5
SiO ₂	46.12	47.59	43.29	43.87	41.96
TiO ₂	0.11	0.32	0.09	0.82	1.35
Al ₂ O ₃	2.37	0.45	1.81	4.02	7.59
Fe ₂ O ₃	1.54	3.64	3.00	2.53	4.46
FeO	5.43	4.09	6.65	9.91	9.46
MnO	0.12	0.18	0.16	0.21	0.26
MgO	42.21	41.47	42.23	34.28	25.32
CaO	1.47	1.53	1.83	3.49	7.45
Na ₂ O	0.16	0.03	0.46	0.56	1.10
K ₂ O	0.11	0.27	0.15	0.25	0.65
P ₂ O ₅	0.02	0.02	0.03	0.05	0.40
Cr ₂ O ₃	0.21	0.20	0.34	n.d.	n.d.
NiO	0.14	0.21	n.d.	n.d.	n.d.
average	4	5	24	23	12

1. average garnet peridotite nodule in kimberlite.
2. average peridotite nodule in kimberlite
3. average olivine nodules in basalts
4. average peridotite (Nodkolds, 1954).
5. average alkali-peridotite (Nockolds, 1954).

ilmenite are not present in the peridotites.

3. Textural characteristics. The minerals in the peridotite are xenomorphic and cataclastic and occur often in orientated fabrics. This does not favour the igneous origin.

4. Equilibrium characteristics. Compositions of coexisting pyroxenes do not suggest temperatures of crystallization much greater than 900° (O'Hara and Mercy 1963). The olivine Fe/Fe+Mg ratio is higher than that in the coexisting pyroxene. O'Hara (1963) considers that this is an argument against an igneous origin.

On these data, it is concluded that the garnet peridotites in the kimberlites are accidental inclusions.

Considering that there are so many inclusions of garnet peridotite in kimberlite it is clear that they must have been derived from a quite large body of garnet peridotites. Measurements of the velocity of earthquake waves suggest that it is unlikely that large masses of garnet peridotite exist in the crust. Therefore it is concluded that the garnet peridotite nodules in kimberlites are derived from the mantle.

(iii) Pyroxene-bearing nodules

In contrast to the olivine-bearing nodules the pyroxene-bearing nodules do not show a constant chemical composition. As stated earlier, the nodules can be

divided into basic granulites, garnet pyroxenites and retrograde eclogites, all of widely different chemical composition, Davidson (1943) has pointed out the world-wide distribution of the assemblage basic granulites (or charnockites) - eclogites - anorthosites - (and often peridotites) in Archean rocks and believes that these rocks, including eclogites, are derived from deep-seated sediments by prograde metamorphism under dry conditions. This assemblage of high-grade metamorphic rocks is similar to that found in the kimberlites of the Gibeon province and other areas and it suggests that all the pyroxene-bearing nodules are accidental in origin and, moreover, that they are derived from crustal layers (Davidson 1943).

Bobrievitch (et al, 1959) describes the gradual change of basement hypersthene schists into plagioclase-eclogites, and he distinguishes between this crustal metamorphic plagioclase-eclogite and (mantle? igneous?) "eclogites" which are associated with the kimberlite magma" and it is in this last type a diamond was found.* It seems then that he has in mind the possibility of two types of

* This is not definitely stated, but it can be deduced from the contents of the paper; the eclogite contains phlogopite, hornblende, clinopyroxene and decomposed clinopyroxene, no plagioclase.

eclogite formation. One type in the lower crust, resulting in plagioclase-eclogites and probably rocks like the scapolite gneiss from Ghana (Knorring and Kennedy 1957) and other similar rocks in folded Archean complexes. The second type, not containing primary plagioclase or hornblende, has been brought up from deeper levels (mantle?) in a kimberlite vent. However, before discussing the place of origin of the eclogitic or garnet pyroxenitic nodules it is necessary to discuss the exact definition of the term "eclogite".

The classical theory, developed by Becke and Grubenmann, stated that eclogites were products of iso-chemical metamorphism of basic igneous ^{rocks} in great depth, under especially high static pressure which forced the main components to join into a mineral combination of the smallest possible specific volume, i.e. almandine-pyrope and omphacite; minerals present in accessory amounts may include hornblende, hypersthene, plagioclase, scapolite, kyanite, quartz and rutile.

Subsequently, Eskola (1921) adhered to this theory in his mineral facies hypothesis, but claimed the possibility that eclogites could also crystallize directly from basic magma. Rocks in the eclogite mineral facies included then (1) metamorphic eclogites, formed by very high-grade

metamorphism from basic igneous rocks or basic sediments (greywackes or basic tuffs); and (ii) igneous eclogites (named griquaites by Becke), crystallized from basic magma under very high PT-conditions.

Many geologists and geochemists envisaged a continuous shell of eclogite in the earth, composed of a rock with a more or less constant basaltic composition, from which fragments in kimberlite vents have been derived. This opinion is inconsistent with the wide variability of the bulk composition of eclogitic nodules in kimberlites (see figure 12). However, eclogitic nodules are amongst the rarest inclusions in kimberlite. This is certainly the case in the kimberlites of the Gibeon province where the more common pyroxenitic nodules are garnet pyroxenites. Because of their ultrabasic bulk composition and subsequent low amounts of alkalies, the pyroxene in these nodules is not an omphacite but an omphacitic diopside. However, all the available alkalies and aluminium has been forced into the pyroxene- and garnet-structure, so that according to the classical definition, the garnet pyroxenites belong to the eclogite mineral facies.

Several attempts have been made by various authors to delimit the fields of true eclogitic garnet and pyroxene from that of garnetiferous pyroxenites, granulites

or charnockites (den Tex and Vogel 1962; Howie and Subramaniam 1957; Yoder and Tilley 1963) but sufficient data are as yet not available. From experimental results Yoder and Tilley (1963) obtained a stability curve for the eclogite facies under dry conditions and considered that regional hydrostatic pressures in the crust cannot be high enough to reach eclogitic conditions. They concluded that eclogites are the partial melting products of "mantle"-peridotite. This suggests that igneous rocks in the eclogite mineral facies are derived from the mantle. It must be considered, however, that laboratory experiments are only an approximation of natural conditions and that metamorphic eclogites could probably form under different conditions depending on the nature of multiphase systems with various catalysers.

From the very beginning of the classical theory of eclogite formation, various authors have put forward serious doubts as to the necessity of very great depth and high static pressures involved in eclogite formation. The occurrence of eclogites in rocks of variable grades of regional metamorphism, in granulites, migmatites, amphibolites, various gneisses and mica-schists suggests that instead of great depth and high static pressure, migmatization or differential, dynamic pressure was the main agent

(Backlund 1936 and many others). Smulikowsky (1960) states that in the Glatzer Schneegebirge (South Poland) eclogites were produced in the course of granitization of mica-schists by metasomatic recasting of some ultrabasic intercalations without intervention of notably increased pressures.

After studying and reviewing various possibilities Turner and Verhoogen (1960) came to the conclusion that eclogites were formed deep within or even beneath the crust, implying that the many low pressure occurrences described by others were all relict assemblages left by retrograde metamorphism. They stressed the fact that eclogites have the tendency to occur in areas "which bear the imprint of strong intrusive or tectonic transport of rock from the depths".

Assuming that the average alkali content of rocks diminishes with depth we can say that the garnet pyroxenites are derived from deeper levels than the metamorphic eclogites of a more common basaltic composition. Igneous eclogites of basaltic composition could be derived from the partial melting of mantle-peridotite at various deeper levels in the mantle. In the laboratory basaltic (tholeiitic) fractions were obtained from a peridotite at 1 atm. (Reay and Harris 1964), but partial melting of a

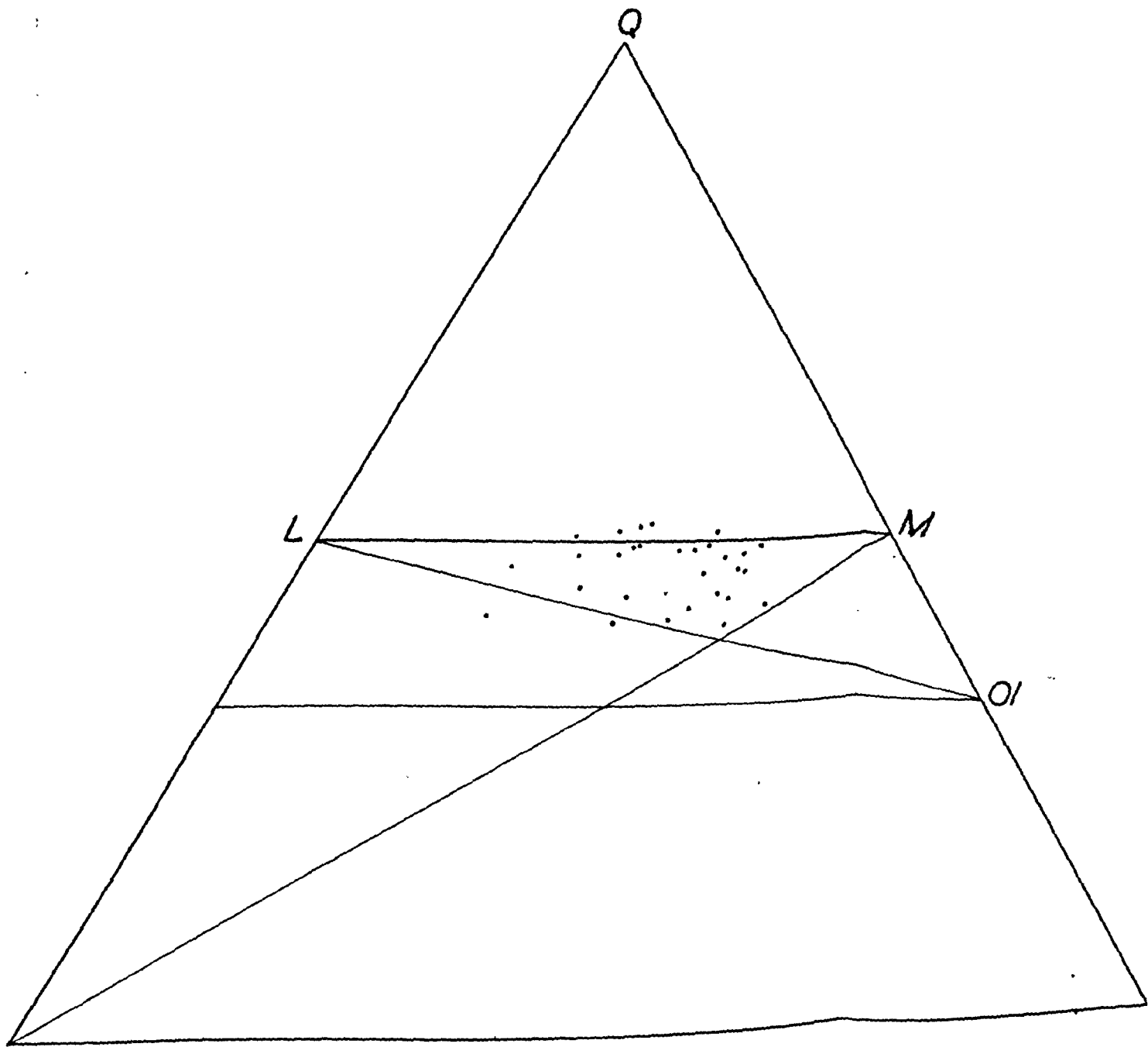


Fig. 12. Composition of kimberlitic eclogites from various localities.

peridotite under high PT conditions has not yet produced true eclogites.

It can be seen that the problem of the place of origin of eclogites has not yet been solved; moreover, the distinction between igneous and metamorphic eclogites cannot be determined from the inclusions of kimberlite.

(iv) Diamonds

Although no diamonds have been found in the Gibeon kimberlites, they have been found in many kimberlites in other areas. Their origin has therefore a bearing on the origin of kimberlites. Their presence can be explained in two different ways. On the one hand, diamond crystals indicate systematic differences in morphology, colour and abundance from pipe to pipe (Williams 1952). This suggests that they have crystallized from the kimberlite when the vent existed as a separate entity, i.e. they are cognate. On the other hand, diamonds occur sometimes in eclogitic nodules in kimberlite (Bonney 1899; Bobrievitch et al 1959). It is possible that diamonds are rare constituents of mantle rocks below 150 km. and that the breaking-up of fragments of mantle rock might provide a source of diamonds of accidental origin in kimberlites. Gardner Williams had 20 tons of nodules from Kimberley mine crushed to check this possibility, but no diamonds

were discovered. However, most of the nodules were garnet peridotites (Williams 1932) while the reported diamond-bearing nodules are eclogitic inclusions.

Like pyropes, diamonds occur in two different varieties, clear and coated (Grantham and Allen 1960). Not enough data are as yet available to connect this property with an accidental or a cognate origin.

The statement whether or not kimberlites, outside certain meteorites, are the only primary source rock for diamonds has also been questioned. Diamonds have been found near Pre-Cambrian high-grade metamorphic rock complexes in West Africa and the Urals, or in Pre-Cambrian conglomerates and gravels from Brazil, the Witwatersrand and India, in areas without known kimberlite occurrences. Some authors have stated or implied that the diamonds could have been derived from the eclogitic or peridotitic rocks, which occur in these complexes (Davidson 1943; 1957; Bobrievitch; et al 1959). It is perhaps possible that small diamonds can form under pressures generated by shearing stress or by shock waves near an earthquake focus. The fact that diamonds can be formed by shock is suggested by their occurrence in meteorites. Moreover, Eversole (1962; quoted in Guardini and Tydings 1962) reported diamond growth on diamond seeds at pressures ranging from

partial vacuum to 2kb. The diamonds produced were very contaminated with graphite and the process needed repeated cleaning of graphite skins, but the crucial fact is that it shows that diamonds can form at the low pressure side of its stability curve.

However, diamond finds in Pre-Cambrian rocks have recently been traced to kimberlite occurrences in India (Mersk 1952) and in Sierra Leone (Grantham and Allen 1960). It is also conceivable that the eclogitic or peridotitic rocks from which diamonds are supposed to be derived are in fact the ultra-metamorphic products of previous kimberlites.

(b) The origin of kimberlite

The main characteristics of kimberlites are :

- (1) Occurrence as intrusive rock in vents and fissures.
- (2) Absence of related extrusives.
- (3) Extraordinary richness in rounded deep-seated inclusions and in angular host rock fragments.
- (4) Richness in volatiles.
- (5) Absence of pyrometamorphism in inclusions and host rock, except for some slight baking effect on shale and sandstone inclusions.
- (6) Ultrabasic chemical bulk composition with :
 - a. calcium-poor phenocrysts
 - b. calcium-rich altered groundmass
 - c. high TiO_2 -, Fe_2O_3 - and K_2O - content compared with SiO_2 , Al_2O_3 and Na_2O .
- (7) Primary source rock for :
 - a. pyrope garnets (with over 70% pyrope end member or ca 20% and more MgO).
 - b. micro-ilmenite (with over 8% MgO).
 - c. diamonds.
- (8) Trace element composition with affinities to both
 - a. ultrabasic suite (Co, Cr, Ni).
 - b. late-magmatic suite (Ba, Sr, Li, Rb, La, Y, V, Zr.)

(1) Chemical nature

The close association in space and time between kimberlites, melilitites, carbonatites and alkalic basalts in general gave birth to the idea that all these rocks have been derived from a common parent magma or closely related magmas. Kimberlite is a volatile-rich calcium-rich alkalic ultrabasic magma type and represents an extreme differentiate in the alkalic basaltic trend, this would explain the small amount of kimberlite compared to alkalic basalts in general. Some workers consider that kimberlite is the primary magma from which carbonatites are derived (v. Eckermann 1958; Garson 1962), while others consider melilitite as the primary magma (Holmes 1936; Taljaard 1936).

The puzzling feature of kimberlites is their richness in potassium and volatiles. Oxburgh (1964) has postulated a volatile- and potassium-rich layer in the upper mantle, but this idea is extremely conjectural and hypothetical and it does not explain why kimberlites should be so much enriched compared with other rocks derived from that zone. Holmes and Taljaard have tried to show that the introduction of volatiles was sufficient to change a melilitite into a kimberlite. Holmes postulated the resorption of lherzolite nodules to account

for the change in MgO and the removal of Ca, Na and Al by the settling of eclogite-nodules, but refuted this theory later when he found that the eclogite nodules were much older than the kimberlite. However, resorption of nodules in kimberlite has never been observed, while the presence of melilite in kimberlite groundmass has never been substantiated.

Harris (1957) suggested that zone refining could explain many characteristics of alkalic basalt. By this process the alkalic basalts which are most enriched in volatiles and large cations such as K, Ba, rare earths etc., (i.e. kimberlites) might be derived from the deepest and hottest levels in the mantle. This is consistent with the seismological data of Kuno (1959; 1960; see below). This originally highly ultrabasic magma would presumably be subjected to zone refining for the longest time and resulting in the most extreme kind of alkalic basalt, i.e. kimberlites. Zone refining could also explain the combination of the ultrabasic and late magmatic suite of trace elements.

Garson's (1962) hypothesis that kimberlites may develop a volatile-rich top fraction which is enriched in calcium and alkalies is consistent with the many examples of transitions from kimberlites to carbonatites

noted at Alnö (v. Eckermann, 1958), Fen (Saether, 1957), Premier Diamond Mine (Daly, 1925), Igwisi Craters (Garson, 1962) and other localities. The exact mechanism of this process is unknown, but it is probable that light minerals, such as calcite, phlogopite and nepheline (?) would move upwards while inclusions and heavy minerals, such as olivine, garnet and diopside would stay behind or sink. Most kimberlites which occur in vents have lost this volatile-rich fraction by explosive action and are consequently less rich in CaO and volatiles than kimberlites in hypabyssal veins and fissures. An extreme differentiation could result in a pure gas fraction consisting of CO₂ and H₂O, which could cause a phreatic eruption leaving a calcium-rich alkalic peridotitic residue.

(ii) Physical state

The precise physical state of the kimberlitic magma is very difficult to estimate because the liquids and gasses involved are in a fluid state far above their critical pressure and temperature. The extraordinary richness of inclusions in kimberlite may be related to the abrasive character of a system composed of a fluid mixture of liquid and volatiles which acquired more inclusions of host rock than a liquid with a low volatile content. This highly mobile system should have been

brought quickly to the surface (in other words, quenched), otherwise the less basic inclusions would have reacted with the ultrabasic kimberlite matrix. The change in pressure conditions would cause the volatiles to expand and, subsequently, lower the temperature, resulting in the rapid crystallization of the kimberlite magma. The presence of large cognate nodular crystals and euhedral phenocrysts, embedded in a fine grained matrix suggest this course of crystallization. Nearer to the surface a volatile phase would separate from the crystallized kimberlite and form a gas-solid suspension of fragments of host rocks, nodular inclusions and kimberlite matrix. The surface expression would be a narrow vent, choked with fragments of adjacent host rock. Any material extruded would be fragments of near-surface host rock and very little kimberlitic rock; in this sense kimberlites are similar to the "Maare" in the Eifel (Germany). The rounding and polishing of the inclusions and the vertical striations in the wall rock are evidence for the gas-solid suspension hypothesis.

From a study of the kimberlites of Yakutia, Mikheyenko and Nenashev (1962) concluded that kimberlite was not molten during its intrusion, but was in the form of a low-temperature fluid phase. It was brought to this condition

by gravitational and tectonic pressure at great depth. Furthermore, the typical form of kimberlite is not an explosion vent, resulting from gaseous explosions or jet piercing, but it is a narrow vent, caused by a diapyrlic process resulting from contemporary conditions during subsidence in platform (or craton) regions of the earth's crust.

(iii) Place of origin

As already briefly mentioned in previous pages, it is necessary that kimberlites are brought quickly to the surface. The depth of the kimberlitic reservoir can be deduced from the pressure stability fields of pyrope (garnet peridotite being the predominant deep-seated inclusion in kimberlite) and in some cases of diamond. It is possible that all kimberlites originally contained diamonds, which have only been retained in cases where kimberlites have been quickly brought up from 120 - 150 km. depth (Bovenkerk, et al 1959; Bardet 1964). The stability field for pure pyrope is at 55 - 60 km. at 1500° (Boyd and England 1959), but as the pyropes in the garnet peridotites contain up to 30% of almandine and grossularite, the kimberlites containing them could probably be derived from higher levels (40 - 50 km?).

If we accept the chondrite model for the composition

of the earth as presented by Macdonald (1959) and take into consideration geophysical measurements on the velocity of earthquake waves we can arrive at the conclusion that orthopyroxene-bearing garnet peridotite is the most probable material in the upper mantle (Ringwood 1959). In contrast, large masses of garnet peridotite are not likely to exist in the crust according to geophysical measurements. The fact that the inclusions in kimberlite are predominantly orthopyroxene bearing garnet peridotite implies that the place of origin of the kimberlites is in the mantle.

An argument for the considerable depth of formation of alkalic and tholeiitic basalts has been given by Kuno (1959; 1960). From the general correspondence of the tholeiitic provinces of Japan with areas of shallow earthquakes and of the alkalic province with that of deeper earthquakes, he suggests that the tholeiitic magma is produced by partial melting of mantle peridotite at the earthquake foci shallower than 200 km, and the alkalic basalt magma by partial melting at foci deeper than this level.

Ringwood (1959) and Boyd and England (1960) have shown the probability that the lower mantle (below 400 km.) is composed of a spinel phase with the composition of

olivine. O'Hara and Mercy (1963) state that because spinel structures have not been found in alkalic basalts or kimberlites, a lower limit of 400 km. is set for the generation of alkalic basalts. This argument is not valid as the spinel structures are unlikely to survive the change in PT conditions.

From experimental evidence Yoder and Tilley (1963) have concluded that the composition of fractional melts from mantle peridotite depends mainly on pressure conditions. Alkalic basalts would be generated under higher pressure, i.e. deeper levels than tholeiitic ones. This is consistent with the geophysical evidence of Kuno.

O'Hara and Mercy (1963), however, suggest that alkalic basalt and melilitite basalt are generated by renewed fractionation of the residual peridotite after the tholeiitic fraction was removed. This is inconsistent with the data of Kuno, but it explains the close association of tholeiitic basalts with kimberlites in Southern Africa and the U.S.S.R. However, it is hard to understand why the second fractionation would be richer in alkalies than the first one.

(iv) Evidence of kimberlites on the Mohorovicic discontinuity and on the nature of the upper mantle

Two main types of deep-seated accidental inclusions occur in kimberlites, i.e. the pyroxene-bearing and the olivine-bearing inclusions. The pyroxene-bearing

inclusions reveal a gradual change in mineralogical and chemical composition from a low to a very high-grade metamorphic facies. The olivine-bearing inclusions, derived from the mantle, have a constant mineralogical and chemical composition, quite different from the pyroxene-bearing inclusions. This significant change in composition adds one more argument in favour of the Moho, being a chemical discontinuity.

Observing the fact that eclogites are rare in kimberlites, it is suggested that the upper mantle is mainly composed of garnet peridotite with small pockets of (igneous) eclogites, resulting from the partial melting of the mantle peridotite. Several small pockets at different levels may have been traversed by one kimberlite and this could explain the variable composition of the eclogite nodules in kimberlites (e.g. Roberts Victor).

(c) General conclusions

1. Kimberlitic magma has formed by zone refining from an original magma from a depth probably greater than 200 km.
2. Zone refining is a gradual process, depending on place and time; only under exceptional circumstances of prolonged stability can kimberlitic magma be generated by this process.
3. Theoretical calculations and laboratory experiments

place the upper level of diamond formation at 120 - 150 km. depth but do not exclude the formation of non-diamondiferous kimberlite at higher levels; it is also possible that diamonds in nature can be formed in higher levels by shock or impact pressure or dynamic shearing pressure.

4. The emplacement of kimberlites in the crust took place along the borders of very stable blocks where deep-seated fractures could reach into the mantle.
5. The typical form of kimberlites near the surface is a narrow vent, caused by the intrusion of a low-temperature fluid phase system.
6. Kimberlites may develop a volatile-rich top fraction enriched in calcium and alkalis, which will escape from the vents. Kimberlitic dykes and veins which did not reach the surface, and certain vents choked with fragments of near-surface host rocks, did not lose their volatile-rich top fraction and are consequently richer in calcium and volatiles than the kimberlite in the vents.
7. All polymineralic nodules, and the monomineralic nodules derived therefrom, i.e. diamond?, chrome pyrope, chrome diopside, forsterite are accidental inclusions.
8. The cracked, altered and coated monomineralic and composite nodules are cognate inclusions, i.e. diamond, titanium-bearing pyrope, diopside, forsterite and ilmenite.

9. The upper mantle is composed of (enstatite-bearing) garnet peridotite with small pockets of igneous eclogites.
10. The evidence from the chemical composition of the deep-seated inclusions in kimberlite is more consistent with the fact that the Moho. represents a chemical discontinuity.

IV GROSS BRUKKAROS

Plate 20. Aerial view of Mt. Brukkaros.



1. Physiography of Gross Brukkaros and the surrounding area

(a) Gross Brukkaros

Gross Brukkaros or Mount Brukkaros is a ring shaped mountain, containing a large breccia-filled vent. It is situated at $25^{\circ} 52'$ S. latitude and $17^{\circ} 50'$ E. longitude in the Berseba Native Reserve, ten miles north of the village of Berseba, and about 60 miles northwest of Keetmanshoop (see figure 1).

The Gross Brukkaros is an important landmark, rising for about 2000 feet above the general level of the Great Namaqualand Plain. The general level of the plain rises from an altitude of 3000 feet (970 m.) at Berseba village to 3300 feet (1000 m.) at the private airstrip on the farm Lichtenfels, 20 miles north of the mountain. The altitude of the trigonometric beacon on the highest part of the mountain is 5203 feet (1586 m.).

Most of the surrounding area is formed by the sandstones and shales of the Fish River Series. The beds are nearly horizontal with a very gentle dip to the east of 3° . The thickness of the Nama sediments is known from a deep borehole near the village of Berseba and amounts to a little less than 3200 feet. At about 10 miles east of Mt. Brukkaros they disappear beneath the tillites of the Dwyka Series. Small outliers of tillite, transgressively over-

lain by thin beds of Cave Sandstone form the small table mountains circa 5 miles to the east.

From afar, the Gross Brukkaros has the appearance of an extinct strato-volcano with a giant explosion-crater; forming a ring-shaped structure (see plates 20 and 21). Closer investigation shows that it is not built up by volcanic ashes or lava, but by domed, upwarped sandstone strata, which form the flanks of the ring-structure. The dome is 5 miles in diameter and has a central depression, which measures nearly $1\frac{1}{2}$ miles across. The central depression is underlain by inward dipping reddish brown, grey and buff coloured clastic rocks (microbreccias), resembling bedded tuffs, which do not belong to the Nama formation. About $1\frac{1}{2}$ miles from the mountain the flat-lying Nama sandstones begin to curve upward, dipping away from it. Nearer the ring the dip becomes less till they are horizontal at an altitude of 4300 feet and a horizontal distance of about 1100 feet from the ring. From here they begin to dip inwards and are then overlain by about 500 feet of maroon shales. Then follow 400 feet of hardened, silicified clastic rocks which form the high rim around the central depression. The floor of the central depression is flat and covered with debris and is about 1000 feet below the highest part of the rim. A

Plate 21. Mt. Brukkaros from the south across the mud flat east of Berseba. The barranco breaks through the southern side of the ring.

Plate 22. Mt. Brukkaros from the northwest with the "balcony" of fractured shale on the northwestern slope. Great Namaland Plain with maroon shales in the foreground. Large terrace to the north of Mt. Brukkaros.



narrow gorge, or barranco, cuts through the ring to the south, making two steps or waterfalls where it traverses the hardest clastic strata. The first and highest waterfall is formed where the outgoing stream crosses the innermost hardest layer; the plunge pool at the bottom of the waterfall has permanent water even in a very dry summer (see plate 23).

The area occupied by the clastic rocks (microbreccias) is roughly circular and measures about 2 miles in diameter. The rocks are stratified and dip inwards at rather steep angles (35° to 45°). They are composed of grey, buff, red brown or red beds, which consist of alternating layers of coarser or finer fragmental material of an entirely non-volcanic nature.

The contact of these inward dipping clastic rocks with the also inward dipping shales of the Fish River Series is well exposed in the sides of the barranco. The contact is concordant and nearly vertical at the bottom of the gorge, then bends outwards gradually following concordantly the slope of the inward dipping shale beds (see plate 20). In general it is a disconformity, but many local angular unconformities occur at many places along the ring.

(b) Linear structures

In a wide area around Mt. Brukkaros there are

distinct radial and tangential lineated structures. On the ground they are narrow anticlines (up to 15 yards across) with steep dips (see plate 24). Cross sections tend to show a flattening of the dips with depth.

The structures might be the amplified version of the joint pattern in the competent layers of the Fish River Series. It would seem that their anticlinal nature is due to hydration and subsequent swelling and calcretization of the shales near the surface. Where these structures cross sandy plains or pans they stand out as 4 feet high walls.

(c) Radial dykes

Near Mt. Brukkaros the radial structures are filled with a buff coloured carbonate and show up as long narrow dykes, 1" - 10" wide, which resist erosion and stand out amongst the shales and sandstones (see plate 25). The dykes can be roughly divided into 5 swarms of 10 dykes each. Individually they are mostly straight or only slightly curved, but some run zig-zag, branching out and coming together again, enclosing lenses of shale. The shales along the contact show steep dips, but where the dykes traverse flagstones or sandstones little disturbance is observed, except for a certain cracking of the rock in a so-called "chessboard" manner. Contact-metamorphism

Plate 23. The first waterfall on the border
of the central depression and the
barranco.



has not been recognized.

The buff dyke-rock contains usually only few very minute angular and sub-angular fragments of shale and sandstone, but near a satellite vent or "blow" (see below) the fragments become more numerous and coarser and also include fragments of various granitic gneisses, muscovite-granite, and granodiorites.

The buff matrix consists of an indurated mass of iron stained material of calcitic and dolomitic composition, which gives the rock a very tough character.

(d) Satellite vents

On the flanks and around the foot of Mt. Brukkaros are numerous smaller vents filled with a very coarse breccia of entirely non-volcanic rock fragments, impregnated and cemented by a calcitized groundmass. The cemented breccia is harder than the surrounding host rock and some of the vents form rather large necks. The largest one, on the north side of the mountain, is 300 x 100 yards and over 200 feet high. In all, there are 8 larger vents and 37 smaller ones, some not more than a few yards across. Many of them are located in a dyke-swarm, at the intersection of a tangential structure, forming not more than a local widening of a dyke, a so-called "blow".

The breccia contains many angular and sub-angular

Plate 25. Radial dyke of
ankeritic carbonatite 9
inches wide near vent F.
west of Mt. Brukkaros.

Plate 24. Linear structure
(narrow anticline) near
Geinaggas



Fragments of shale and sandstone of various sizes, with
 bleached boundaries. In
 angular fragments and
 cobbles and boulders of
 white, white quartzite, and a
 white and hornblende gneiss
 matrix. The first type
 colored rock, which is very
 of the dykes. The other type
 which contains quartzite

shales are extremely shaly
 (vent 7. map 1) they are 3
 miles around most of the v
 shales and the host rock 1
 (shaly rock)
 Several narrow zones
 stand out as low ridges, 3
 mountain. The shales are
 streaked with quartz-veins

fragments of shale and sandstone, of various sizes, mostly maroon or buff coloured, with bleached boundaries. In addition there are also abundant angular fragments and subrounded and rounded pebbles, cobbles and boulders of gneiss granite, muscovite-granite, white quartzite, and a few boulders of dolerite, biotite and hornblende gneisses and amphibolite.

There are two types of matrix. The first type weathers to a yellow brown coloured rock, which is very similar to the buff matrix of the dykes. The other type is a bluish-weathering rock, which contains flakes of biotite and altered phenocrysts of mafic minerals. This bluish variety might be described as an altered mica-lamprophyre.

The contact of the vents with the enveloping Nama rocks is varied. At one large neck (vent J. map 1) the shales are extremely shattered and brecciated, at another (vent F. map 1) they are dipping inwards to the vent, while around most of the vents the contact is hidden by debris and the host rock is apparently undisturbed.

(e) Fracture zones

Several narrow zones of fractured shale and sandstone stand out as low ridges, 4 yards wide, radiating from the mountain. The shales and sandstones are brecciated, crowded with quartz-veins and vugs lined with quartz-

crystals, and impregnated with calcite and limonite and contain inclusions of granite and granite gneiss and veins of the buff carbonate of the dykes.

The regularity of the ring-shaped mountain is interrupted on the N-W side by a large area of fractured shale sticking out to form a sort of "balcony" on the north slope of the mountain (see plate 22).

(f) Terrace deposits

Several terraces occur around Mt. Brukkaros. They are composed of boulder- cobble- and pebble-sized sub-rounded fragments of microbreccia and Nama sandstones, and small pieces of vein quartz, cemented by a 2 to 3 feet thick layer of calcrete. The surface slopes away from the mountain at a very low angle (see plate 22).

(g) Ring structures on Gründorner Fläche and the Hatziom dome

These two structures occur some distance from Mt. Brukkaros but possess some of its characteristics and might be related to it.

On the farm Gründorner Fläche two peculiar small ring structures occur at about 40 miles northeast of Mt. Brukkaros. They are situated along the Gründorner-Kaffir River, one on each side; they are about half a mile apart. They are roughly circular with a diameter of circa 200 yards. The host rock in this area is Dwyka tillite with

impersistent horizons of hard gritty sandstone.

The structures are formed by a narrow ringwall of steeply outward dipping gritty sandstones. Outside the ring the sandstone dips under the tillite and on the inside of the ring the sandstone slabs form a low cliff. The height of the ringwall and cliff is about 20 feet.

The inside of the ring is filled with river alluvium, branches of the river go in fact through both structures.

Two 20 foot deep holes were drilled and only silty sand and tillite gravel were met (Brink 1961).

On the boundary of the farms Hatzium 2 and Rosenhof, about 70 miles north of Mt. Brukkaros, occurs a dome shaped structure; it is about $1\frac{1}{2}$ miles in diameter and 600 feet high. The dome is built up of upwarped Nama sandstones without signs of faults or fragmentation and brecciation. A $2\frac{1}{2}$ feet wide, greenish grey weathering dyke is exposed in the centre of the dome at the top.

2. Structural relationships

(a) Microbreccias

(1) Bedding

Massive red microbreccias are exposed on the north side of the central depression, but everywhere else around the ring they are generally well bedded. All the beds dip inwards into the depression, starting at a low angle, which gradually becomes steeper inwards until a maximum of ca. 50° is reached. In many places along the rim the microbreccias lie horizontal and in one or two places they are found on the outside of the ring, dipping outwards and truncating inward dipping shales. In most places along the rim, however, the contact with the shales is concordant or nearly so (see plate 20).

The dips on the north side of the depression are generally a little less than those elsewhere and local tangential dips occur along the rim.

There is no evidence of large scale faulting or folding in the microbreccias but small step faults offset the inward dipping beds. The movement along the fault plane is slight, averaging 8" to 10". The fault planes are encrusted with quartz crystals and, where numerous, give the impression of false bedding planes. Due to this cause, an outcrop at the northwest side of the depression

has an apparent outward dip of 45° as a result of numerous fault planes; however, the true dip is 20° inward.

The thickness of the individual beds is variable and is in the order of tens of feet. There is a sharp, and in many cases, obviously discondordant break between succeeding strata (see plate 26).

Laterally, the lithological composition in the strata is quite variable, any one variety grades into another over short distances so that very few beds can be followed along the strike around the mountain for any great distance.

Slump structures are common in the microbreccias (see plate 27), and reveal small tangential movements. In addition, features similar to cross bedding, current bedding and graded bedding are common in the red microbreccias (plates 29 to 33). Various examples can be observed in the outcrop of steep dipping (ca 50°) microbreccia 100 yards upstream from the main waterfall. Spheroidal weathering was observed in the hard band of buff microbreccia above the first waterfall.

The general character of the microbreccias gives the impression that they have been formed by volcanic eruptions of a phreatic nature, and that they represent the remnants of a cover of clastic rocks, deposited around a large explosion vent. The reddish microbreccias are protected

Plate 26. Discordant contact between very fine
grained buff coloured microbreccia and
succeeding coarser layer.

Plate 27. Slump structures in the microbreccias.

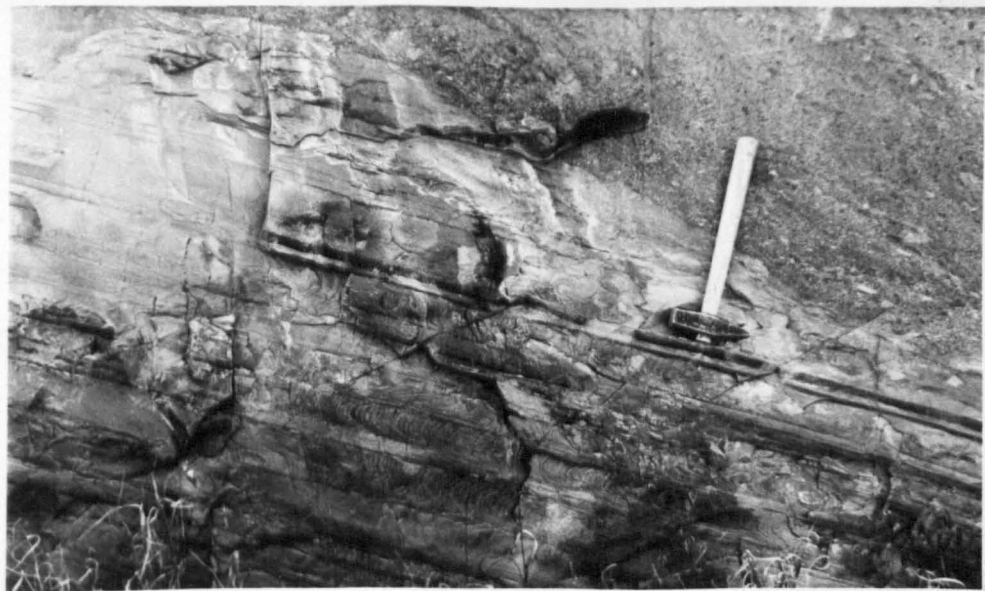
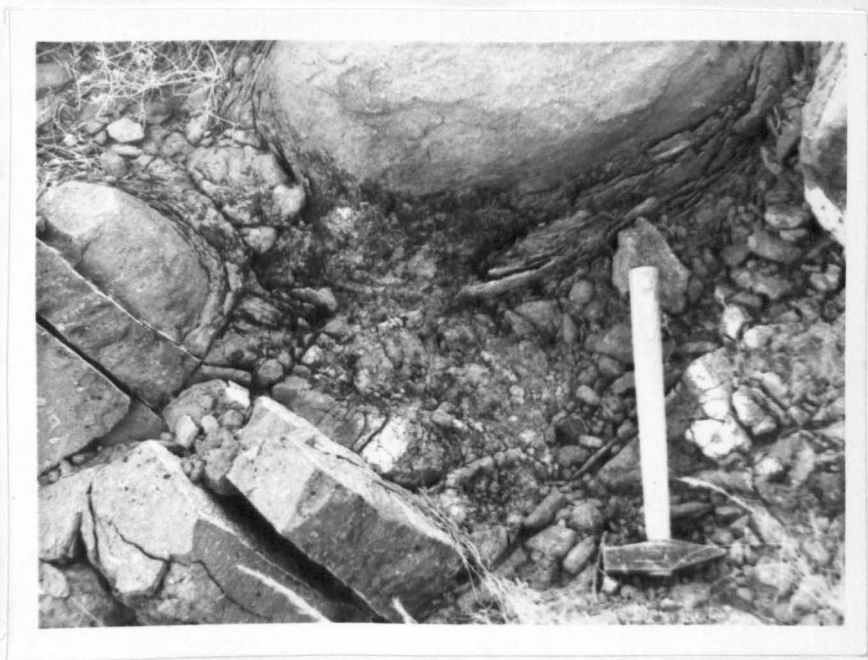


Plate 28. Spheroidal weathering in the hard
microbreccia, which causes the
first waterfall.

Plate 29. Cross bedding in microbreccia with
relatively large inclusion of very
fine grained microbreccia.



compared with those formed by deposition in water (Twenhofel 1939). The observed features are indeed rather irregular and wedge shaped (see plates 29 to 33), and it is believed that repeated outbursts in the same explosive stage account for these finer structural features in each layer of microbreccia. Graded bedding may have a similar origin since fragments thrown out by explosive activity will return to the surface in order of grain size. Eddy currents in the gas flow could account for the observed cross bedding.

(ii) Subsidence of central column

Whatever their mode of origin, it is clear that these fine structural features could not have formed in beds inclined at a 50° angle. The original dips of the beds must have been far less to nearly horizontal. Cloos concluded that the microbreccias had originally been deposited in horizontal position. He observed peculiar mudcracks, which he believed could be explained only by assuming that there were shallow depressions in a horizontal bedding plane, from which standing water slowly evaporated (Cloos 1937).

The present position of the beds has been caused by the slow subsidence of the microbreccias in the actual vent when the gas pressure decreased. The original horizontal microbreccias around the vent were bent down and at the same

Plate 30. Cross bedding in microbreccia.

Plate 31. Graded bedding in microbreccia.



time silica-rich fluids ascended and subsequent hardening of the beds took place.

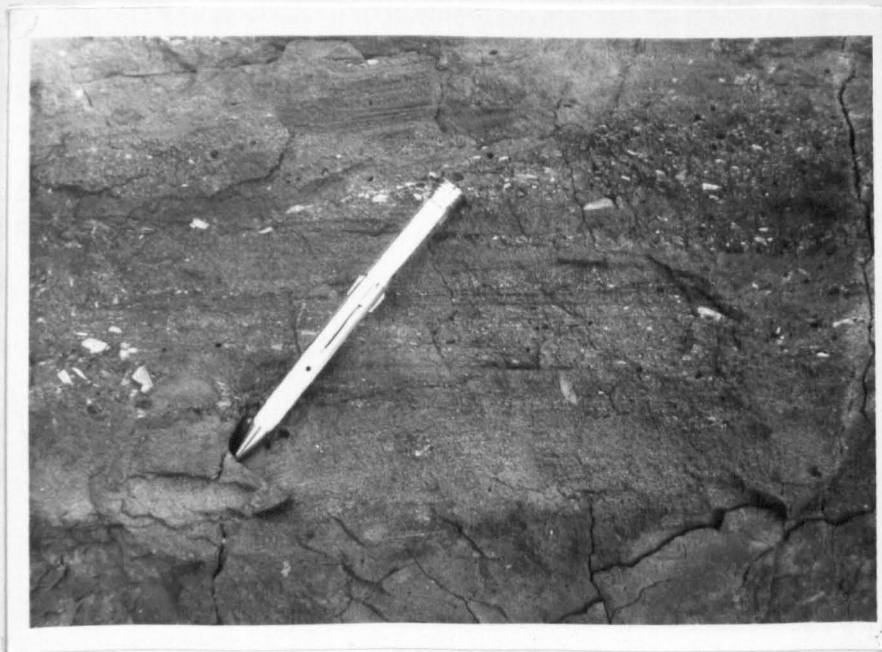
Joint planes and cracks in the microbreccias are usually coated with chalcedony or quartz. Small vugs occur with walls encrusted with clear quartz crystals or translucent opaline silica, hyaline (see plate 32). The rate of silicification increases towards the periphery of the microbreccias and extends into the shales around the vent and then quickly decreases. The result is a more or less conical column of hardened silicified microbreccia and shale - the ring- enclosing softer microbreccias.

Rogers suggested that "it appears likely, from the distribution of the hardened rocks, that the process of hardening was produced by liquids or vapours rising approximately along the walls of the vent, resulting in a more or less tubular column of hard rock enclosing loose rock." And the depression "is due entirely to the effects of erosion on a soft column of rock surrounded by harder rock". (Rogers 1915).

This statement cannot be entirely supported. The primary cause for the depression is the subsidence of the central column and the resulting inward dipping beds. Erosion is a very important secondary force in shaping the present saucerlike depression. There is no evidence of a

Plate 32. Cross bedding in microbreccia with
vug, coated with opaline quartz
and calcite.

Plate 33. Graded bedding and cross bedding
in microbreccia.



large ring fault or radial faults.

The unfractured and unfaulted condition of the hard microbreccia which forms the walls of the barranco shows that the gorge owes its shape to erosion mainly and not to a radial fault.

(iii) Contact with host rock of the Fish River series

The actual contact of the microbreccias with the host rocks is exposed in the sides of the barranco. The bottom of the barranco is slightly more than 1000 feet below the rim, and while the eastern-side is covered by screes, the western-side can be studied all the way and shows that the contact is generally concordant and curving with an increasing inward dip. Local angular unconformities occur at several places around the rim and at one place on the eastern-side the microbreccias are dipping outwards truncating inward dipping shales. At one locality in the barranco and at two places on the eastern and southern flanks of the mountain small discordant outliers of microbreccia probably represent apophyses of the main central vent. In general, however, the microbreccias rest concordantly on the maroon shales of the Fish River series (plate 20).

From a general point of view then Mt. Brukkaros could be considered to belong to the class of the enigmatic

cryptoexplosion (or cryptovolcanic) structures. When the classification of Lachman (1909) is followed we can refer to the Brukkaros vent as "a vent of the Fife type".

(b) Host rock (Fish River series).

The well bedded sandstones and shales of the Nama formation around the vent are relatively little disturbed. Large scale faulting is absent, but there are a few minor faults with small displacement.

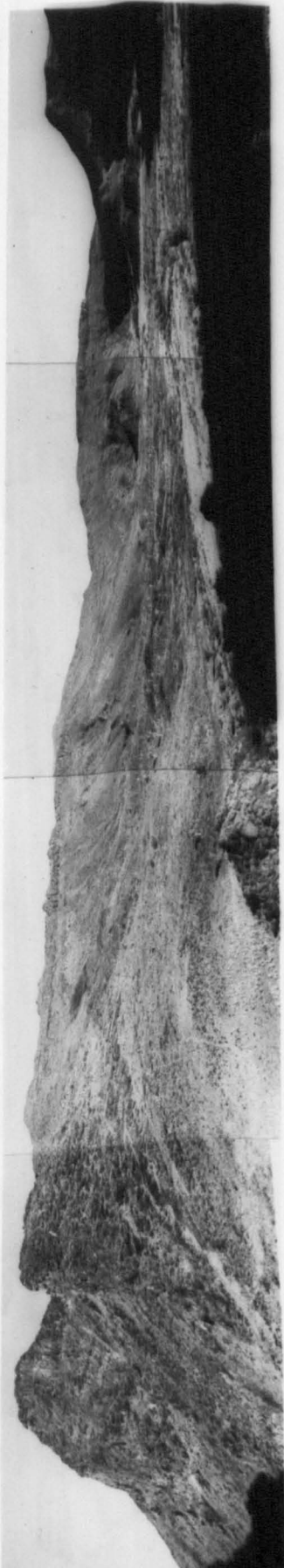
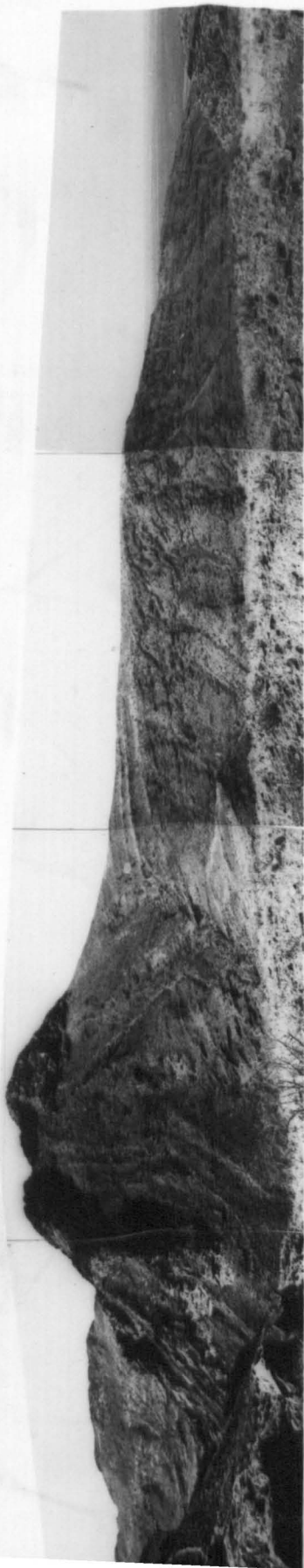
About $1\frac{1}{2}$ miles away from the mountain the shales and underlying sandstones begin to curve upward. At about 1 mile distance the shale thins out and the sandstone comes to the surface and forms the actual slopes of the mountain. The flanks of Mt. Brukkaros are stratigraphical slopes, essentially governed by the dip of the sandstone strata. Small flexures occur here and there in the outward dipping beds. Close to the vent the outward dip changes into an inward dip, and this change is accompanied by a certain amount of contortion and wrinkling in the sandstones (see plate 34). Normal maroon shales retake their position again, overlying the sandstones on the inward dipside.

The whole structure forms a sort of circular anticline. On the northwest side of the mountain, however, the regular outline of the circular anticlinal is interrupted and a smaller second anticline or tangential

Plate 34. East wall of the barranco, showing the
circular anticline and the inward dip.

Plate 35. The central depression, inside
Mt. Brukkaros.

194a



flexure, bounded by two radial flexures, exposes the sandstone again, while an erosion resisting mass of brecciated silicified shale is exposed in the enclosed syncline (see map 2). Many dykes and fracture zones fan out from this area.

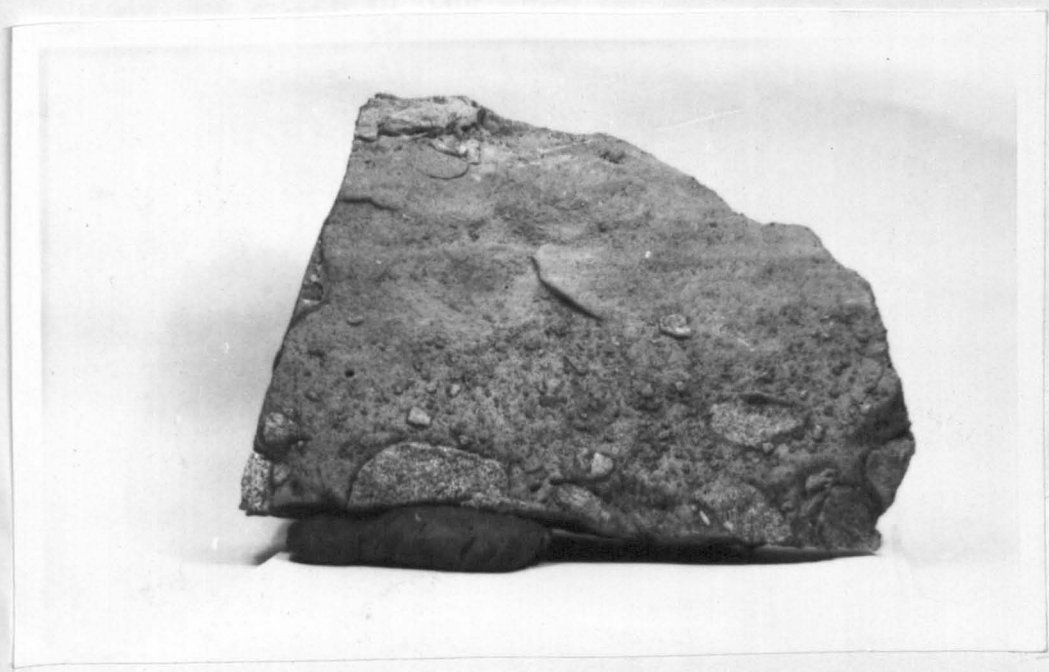
(c) Satellite vents.

In many places the sandstone strata are traversed by intrusive vents and dykes. The contact of the vents with the host rock is usually obscured by debris and scree, but where seen it is also clearly intrusive, although without much disturbance of the hostrock itself. The outcrop boundaries have a simple oval outline and according to the classification of Lachman (1909) they can be referred to as "vents of the Alb-type". Only one vent (vent F) is surrounded by inward dipping shales and is a "vent of the Fife type".

The material in the vents contains very many, mostly granitic, xenoliths, but usually there is a clear zone, about 1 to 2 inches wide, along the walls of the vent, which is free of inclusions (see plate 36). A similar phenomenon is noticed in some of the dykes. The centre of the dyke carries inclusions, while a zone, free of inclusions, exists along the walls. This zonal arrangement is another argument for the gas-solid streaming

Plate 36. Contact of satellite vent breccia T
with host rock showing border zone
free of inclusions ($X \frac{3}{4}$).

Plate 37. Radial dyke with muscovite granite
fragment near vent F ($X 1\frac{1}{2}$).



process. It seems that the gas phase moves slower near to the walls of the vent or dyke due to friction and only fine particles can stay in suspension.

(d) Radial dykes.

The dykes traverse the shale and sandstone around Mt. Brukkaros, but always stop at or near the contact with the vent. The contact of the dykes with the host rock is always sharp; small apophyses traverse and offset small sharp edged wedges of host rock (see plates 38 and 39). The satellite vents, when located on a dyke, always cut through the dykes, indicating that the dykes must be older than the vents.

(e) Faults.

The minor faults in the sandstone strata on the flanks of Mt. Brukkaros are younger than the dykes and the satellite vents. One case can be studied where a small dyke on the east flank has been offset by three or four very small faults and another case where a vent (vent I) is traversed by a fault.

Minor faulting also affects the contact between the main vent and the shale, especially on the west and east side.

(f) Age relationships.

The area around Mt. Brukkaros is formed by sediments of the Nama formation. The large Brukkaros vent, the

Plate 38. Yellow ankeritic carbon-
atite dyke cutting maroon
shales; near vent T.

Plate 39. Detail of dyke in plate.
38 showing intrusive
character of small apophyse
in host rock.

196a



satellite vents and the dykes cut through these sediments, indicating that the whole structure post dated the deposition of the upper part of the Fish River series. Horizons, younger than the maroon shales stage are exposed on the farm Hanaus and areas to the north and consist of a current bedded sandstone, forming an escarpment of local importance, ripple marked flagstones and soft red shales. Cave Sandstone beds, transgressing over Dwyka tillites on to Nama maroon shales at various small localities 5 miles east of Mt. Brukkaros, indicate that lower Karroo beds and uppermost Nama were eroded at the beginning of Cave Sandstone times. Elsewhere, for example on farm Gras, post-Cave sandstone lavas transgress from lower Karroo beds on to Nama shales. It is concluded that the micro-breccias were deposited on a surface from which rocks younger than the Fish River maroon shales were eroded and that the contact between the two formations represents a disconformity.

During the present field research one of the radial dykes (first mapped by J. A. Mills) was found to traverse the Cave Sandstone beds capping one of the small table mountains to the east of Mt. Brukkaros; this dyke is, moreover, cut off by a post-Karroo fault, which offsets the level of the Cave Sandstone beds. Assuming a genetic connection with these carbonate dykes, the Brukkaros

complex is then definitely of post-Cave sandstone age.

Two kimberlite outcrops occur near Mt. Brukkaros. One (B10) is situated at 6 miles northwest of the main vent, the other (B11) at 5 miles to the west. B10 consists mainly of blue ground and shale debris at the surface, but from an age point of view B11 is particularly important since the surface of the pipe consists of fragments of Brukkaros microbreccias and weathered pieces of a medium grained dolerite, embedded in blue ground. In view of this, it is concluded that this particular kimberlite erupted on a surface covered with microbreccia debris which has fallen or sunk into the vent and is therefore younger than the Brukkaros complex.

3. Petrography

(a) Fish River series (host rock)

(1) Sandstones

The sandstones of the Fish River series show a high degree of uniformity over large areas. Hard massive quartz-rich horizons alternate with softer laminated more micaceous layers. The grain size is generally 0.1 to 0.2 mm, and the colour is always red, brownish red, maroon or purple, caused by skins of iron oxides around the quartz-grains. Green or greenish-blue spots and layers are occasionally found in places where reduction of iron occurred.

The general pattern of the mineralogical composition of the heavy mineral content of the red sandstones is as follows : (determination Central Metallurgical Laboratories, Johannesburg).

magnetite	present to abundant
ilmenite, leucoxene) hematite and other iron oxides	abundant
monazite	trace to absent
rutile	trace
zircon	trace
epidote, pyribole) sericitic matter)	generally predominant
tourmaline	trace
staurolite	trace to absent

barite	trace
apatite	trace to absent
almandine/spessartine	trace
anatase, titanite	trace to absent.

At several places hard black magnetite-rich horizons are intercalated with the red sandstones. They are rich in magnetite, hematite, almandine/spessartine, epidote and zircon.

Microscopically the sandstones show a mosaic of interlocking articulated quartz grains. Kataclastic textures and undulose extinction are rare. The quartz is largely recrystallized but faint distinctions between the original subrounded quartz grains can still be seen. The microscopic texture is that of a quartzite.

Small anhedral grains of plagioclase, mostly twinned according to the albite law, are scattered amongst the quartz-mosaic. They are acid andesine (An_{32}) with $2V_x = 85^\circ$.

Small laths of clear muscovite are also present.

The modal analyses by point counting shows :

2 to 3% muscovite

6% clear unaltered plagioclase

64 to 79% clear quartz

28 to 12% ironstained quartz, ironstained altered feldspar.

(11) Shales

In hand specimens the shales are thinly laminated, hard, fissile rocks of maroon colour. Coarse varieties contain fine-grained quartz.

Microscopically they show a brownish-red irresolvable mass with occasional small angular quartz grains and muscovite flakes. Bands of sandy layers, composed of small angular quartz grains (size 0.02 mm.) alternate with clayey layers, composed of sericite, muscovite and crypto-crystalline clay-minerals, are common.

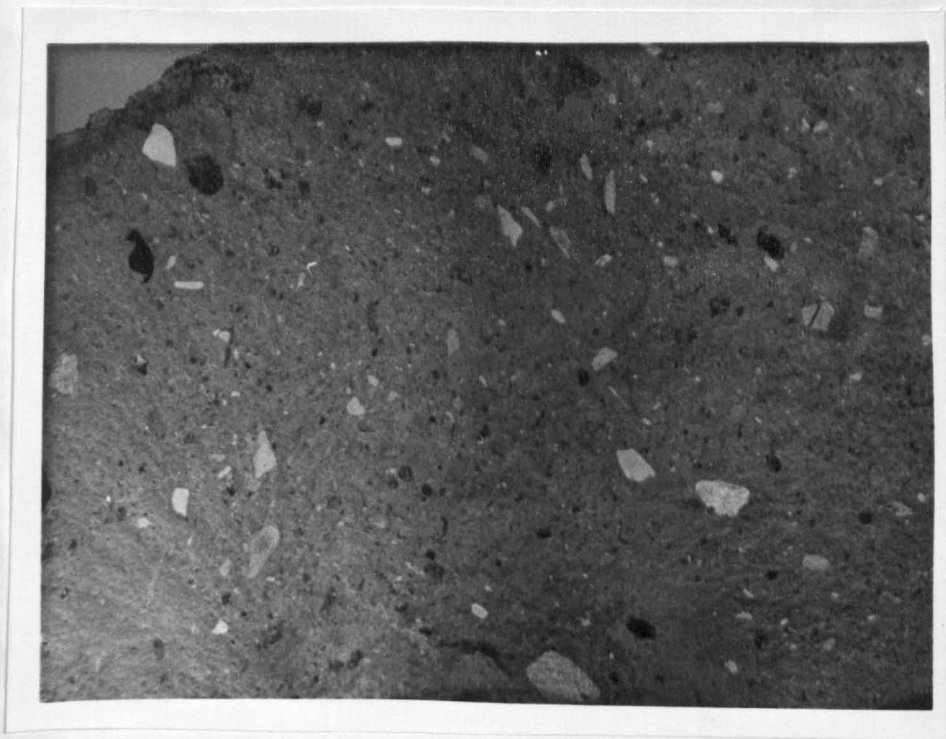
(b) Microbreccias of the central vent

(i) Nomenclature

The fragments in the clastic rocks of the central vent of Mt. Brukkaros are usually less than one inch in size (see plate 40). In contrast, the fragments in the material of the satellite vents are very coarse, usually boulder- or block-size; in one vent (vent H.2) an inclusion of blue baked shale of over 30 feet diameter was found (map 1).

Various names have been given to these rocks. The Brukkaros rocks have been called volcanic breccia, tuff-breccia, crystal tuff, porphyry tuff, quartz-porphiry, etc. The last three names are misleading since the quartz and feldspar crystals are inconspicuous and do not occur as phenocrysts. The name tuff breccia, synonym for lithic

Plate 40. Microbreccia of the central vent
(natural size).



tuff - a tuff containing many rock fragments of lava or scoriae (Schieferdecker 1959) - is equally unsuitable, because the material is non-volcanic. Nor is the term volcanic breccia justified since this name denotes a coarser type of clastic rock with fragments over 32 mm. (Pettijohn 1949).

Other names suggested to describe the Brukkaros rocks are either tuffites - according to Mugge a mixture of volcanic pyroclastic tuff and epiclastic detrital material (Schieferdecker et al 1959) - or tuffisites.

The name tuffite, however, is generally used for a normal tuff transported by water and mixed with sand or clay resulting in a tuffaceous sandstone or tuffaceous shale.

Cloos (1941) introduced the word "Tuffisiert", by which he meant that the large fragments of included host rock and the wall rock around the Swabian vents were crowded with little veins of intrusive tuff and seemed injected by tuff. This mixed rock he named tuffisite. The shales around the contact with the Brukkaros vent have been "tuffisiert" in this way (see plate 45). Recently the name tuffisite seems to have been applied in a wider sense to include all the various kinds of rock found in volcanic explosion vents (Reynolds 1957; Bucher 1963). Those vents usually contain lavas and tuffs of an alkaline

ultrabasic nature mixed with numerous accidental inclusions.

As the clastic rocks in the central vent do not contain volcanic material a non-committal name like microbreccia is used.

(ii) Description.

In handspecimen many of the microbreccias of the central vent have the appearance of sandstones or greywackes. The fine varieties are remarkably uniform in macrotexture and show many sedimentary structures, such as graded bedding and cross bedding. The colour of the rocks can be grey, buff, red-brown or red. The coarser varieties contain angular fragments of buff coloured shale or black chert in a grey, buff, red-brown or red matrix. Fragments of sandstones and quartzite are less common. Even rarer are fragments of igneous material but macroscopic inclusions of diorite and granite have been observed.

The microbreccias are moderately silicified. The greatest silicification occurs in, and is responsible for, the harder grey or buff coloured rocks of the highest parts of the rim. The softer, more feldspathic rocks, which are found around the central depression contain a large amount of ferruginous substance and are usually redbrown or red.

The silicified grey rocks are traversed by many

quartz veins which contain amethyst in places, and black chert veins. Less common are veins with parallel banded chalcedony or translucent opaline quartz, translucent nodular calcite and composite veins of quartz-calcite-dolomite-barite. Tiny specks of chalcopyrite have been observed in a few places.

Under the microscope the rocks show a clearly clastic texture. Fragmented crystals of quartz, plagioclase, pyroxene and alkaline feldspar are embedded in a matrix of finely comminuted material, consisting of quartz- and feldspar-dust, secondary silica, calcite, dolomite and limonite usually forming a redbrown-stained, irresolvable mass.

Three different textures (A, B and C) can be distinguished:

Texture A. is formed by a mosaic of angular fragmented grains in a greater or lesser amount of matrix, the grains are still interlocked or touching each other, the matrix fills the interstices or forms little veinlets. The highly silicified grey rocks belong to this type.

Texture B. is formed by a network of matrix, enclosing rounded fragmented grains, totally surrounded by matrix (see plate 43).

Texture C. is formed by a featureless smooth paste of redbrown stained material in which fragmented grains

are embedded at random (see plate 44). The ferruginous red fine varieties belong to this type.

True tuff textures are missing; glass shards or flow banding have not been observed, and there are no features which suggest welding. Although a low temperature is indicated by these data small shale and chert inclusions have bleached boundaries which indicate some kind of thermal reaction (see plates 41 and 42).

(iii) Mineralogy.

The mineral content of the microbreccias is as follows:

Quartz is usually predominant amongst the fragments and occurs as large clear rounded grains up to 1 mm. diameter and as angular fragments of an average size of 0.2 - 0.3 mm. It is always strained, cataclastic and shows undulose extinction. In one case it was seen to be bi-axial positive with a very small 2V. (F.9758). It is present in the matrix in greater or lesser amounts as cryptocrystalline quartz and chalcedony.

Plagioclase is present in two varieties. One variety is fairly fresh or only slightly sericitized with a grain size up to 1 mm. and an An content of 37%. Most grains are twinned according to the albite or pericline law; they are all slightly cataclastic. The second variety consists of very clouded feldspars (see plate 43).

Pyroxene is usually fairly altered and is optically positive clinopyroxene with a very faint pleochroism from yellow-green to light green and $Z' \wedge (100)$ of ca 40° . It may be a ferroaugite or hedenbergitic diopside. The alteration product is a red-brown and yellow opaque mineral, probably limonite. Bleached boundaries are common.

Alkaline feldspar is less common. It has a large 2V and shows the microperthitic texture of microcline. Myrmekitic intergrowths with quartz are not rare.

Epidote is present as light green, faintly pleochroic crystals and as rims around pyroxene.

Calcite is present in small amounts filling microscopic cavities in thin sections or forming part of the matrix. Macroscopic veins are also lined with calcite in many places. X-ray patterns determining the position of the main line d.211 (Goldsmith & Graf, 1958) show that it is a magnesian calcite with ca 10% Mg CO₃ in solid solution. The calcite in the veins is 100% Ca CO₃.

Dolomite occurs as small rhombohedra (average 0.05 mm.) in thin section and forms part of the matrix. It is also the main constituent of many composite veins. According to the method of Goldsmith & Graf (1958) it is a calcarian dolomite (ca. 65% Ca CO₃) in all cases.

Limonite is always present as alteration products of

pyroxene and as a red brown stain in the matrix.

Rock fragments in the microbreccia. In addition to the crystal fragments the microbreccias also contain fragments of quartzite, sandstone, shale, chert, clouded-feldspar rock and plagioclase-pyroxene rock. The sandstone-quartzite fragments consist of more or less rounded grains, cemented by secondary silica. They are very similar to the Nama sandstones and they are undoubtedly derived from them. The average grain size of the quartz grains in the sandstone-quartzite fragments (up to 1 mm.) is larger than that in the sandstones around Mt. Brukkaros (average 0.12 mm) This suggests that they have been derived from sandstones from lower Nama horizons, which are coarser grained.

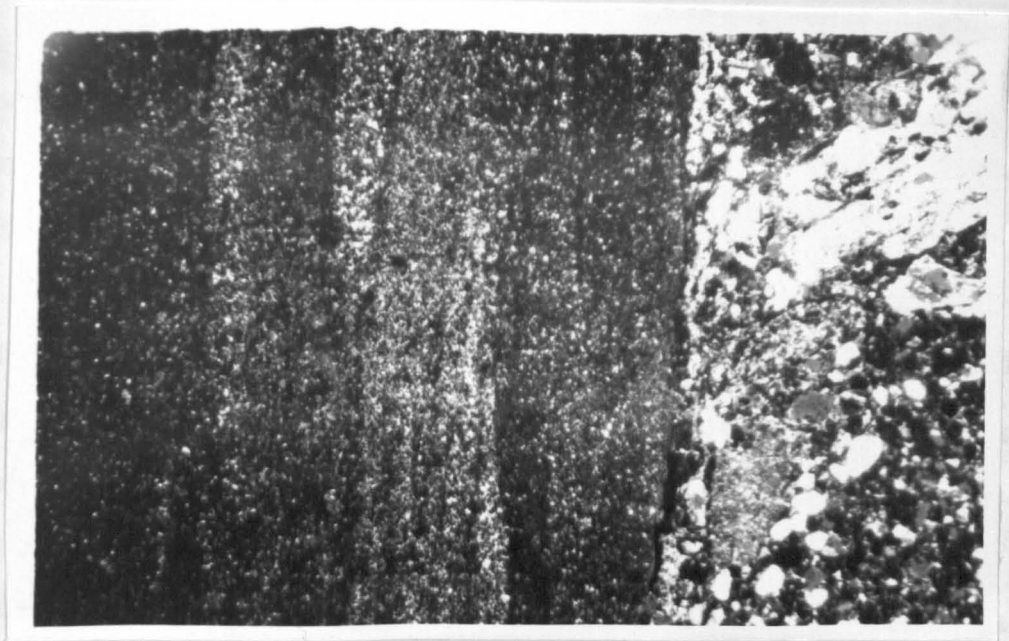
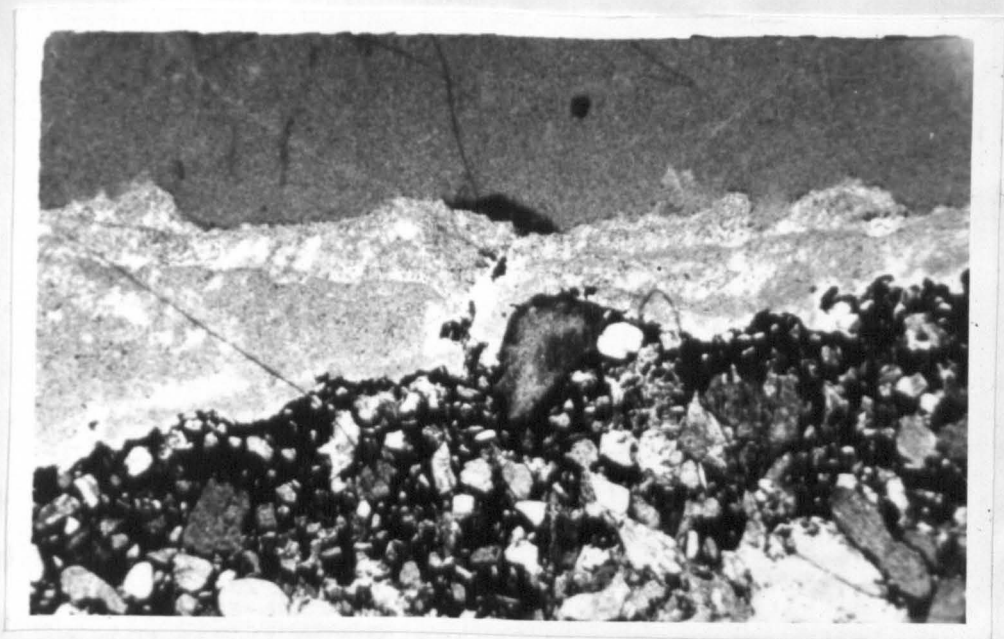
The shale fragments consist of very fine quartz, feldspar, muscovite, sericite, clay minerals which are all uniformly stained with calcite, dolomite and limonite. A clear unstained zone of circa 1 mm. occurs along the periphery of the fragments, while the contact with the matrix of the microbreccia is marked by a very thin film of calcite (see plate 41).

The chert fragments show a 1 mm. wide zone of slightly coarser quartz grains at the contact, while at one place a plagioclase crystal seems to be pressed into the border zone (see plate 42).

The many feldspar-bearing rock fragments contain

Plate 42. Photomicrograph of thin section E.9544 (B6I). Contact between chert fragment with clear contact zone and microbreccia, note plagioclase crystal pressed into chert at centre of plate (X 13).

Plate 41. Photomicrograph of thin section F.9755 (B60). Contact between shale fragment (right) and microbreccia (left) (X 13).



clouded feldspar or tiny clear plagioclase laths (see plates 43 and 44). They are up to 5 mm. in diameter and may contain up to 25% pyroxene which is much altered to a redbrown mass. The texture of these rock fragments is holocrystalline with no ophitic or porphyritic textures observable and the average grain size is 0.4 - 0.5 mm.

Some fragments of microgranite were seen macroscopically, but these were not encountered in thin section.

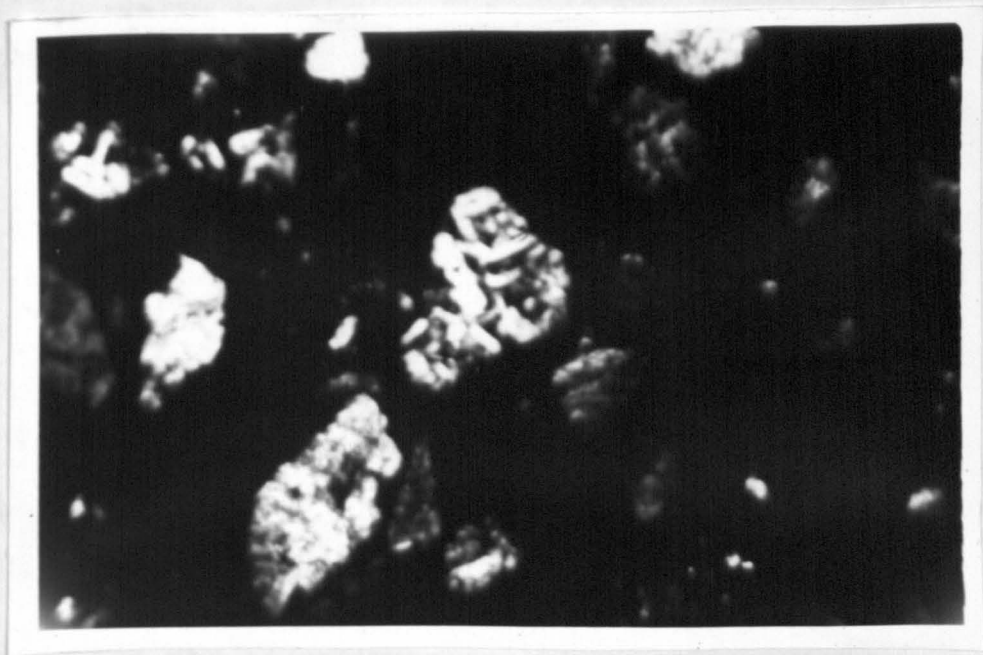
Matrix of the microbreccias. In order to determine the matrix of the microbreccias, several samples of material, rich in matrix were crushed, X-rayed and analysed. The X-ray patterns showed that the bulk of the samples consist of feldspar-dust, together with small amounts of quartz, magnesian calcite and dolomite.

The high potassium content of some of the microbreccias shows that the feldspar dust contains a considerable amount of potassium-feldspar, which cannot have been derived from the Nama sediments (see table 19).

Most of the rocks inside the vent possess a more or less inhomogeneous brecciated nature. However, an unusual homogeneous buff rock, which is very fine-grained and thinly bedded and resembles a porcellanite, occurs on the north side of the depression (see plate 26). It has a graded bedding and a conchoidal fracture. In thin

Plate 44. Photomicrograph of thin section F9545 (B65). Rounded fragments of plagioclase rock (3 mm. across) embedded in brown stained matrix of microbreccia (X 80).

Plate 43. Photomicrograph of thin section F9543 (B58). Fragments of clouded feldspar contained in the microbreccia (X 32).



section it shows cryptocrystalline particles and light-brown opaque dust. The graded bedding is caused by an increase in dust while the particles become smaller; after a sharp break follows again a zone with larger clear particles amongst which quartz can be recognized.

An X-ray pattern of the bulk of the rock, comparing the relative intensities of the main lines of the four constituents shows that it consists of feldspar and calcarian dolomite (Cc₆₅) in nearly equal amounts and smaller amounts of quartz and magnesian calcite (Cc₉₀), nearly equal in number but half the value of the first.

Compared with the Fish River sandstones the micro-breccias are richer in Ti, Al, Fe and alkalies and poorer in Si, while the trace element composition shows an enrichment in the ultrabasic suite (Co, Cr, Ni and V) as well as in the late-magmatic suite (Be, Li, Sr, Y and Zr) (see table 20).

TABLE 19. Analyses of Fish River sandstone and Brukkarøs
Microbreccias

	B66	B64	B65	B95	B62	B93	B89	B88
SiO ₂	85.5	66.5	51.0	63.5	65.5	64.0	77.0	66.0
TiO ₂	0.47	1.00	0.90	0.75	0.57	0.69	0.28	1.91
Al ₂ O ₃	6.8	7.2	11.5	11.5	10.8	11.8	9.0	12.0
Fe ₂ O ₃	0.77	6.10	8.34	5.80	4.43	4.77	1.15	1.76
FeO	1.57	1.77	1.04	2.13	3.21	2.97	1.57	3.21
MnO	0.06	0.10	0.19	0.11	0.15	0.09	0.10	0.06
MgO	trace	3.2	3.0	3.5	2.5	2.9	1.8	2.2
CaO	2.15	6.40	7.40	5.99	4.20	4.32	2.88	4.45
Na ₂ O	2.08	3.54	4.49	3.53	1.68	1.62	2.23	1.50
K ₂ O	0.68	1.35	2.46	2.50	4.30	5.34	1.90	7.35
H ₂ O ⁺	0.52	1.52	2.97	1.70	1.02	1.08	2.77	0.37
H ₂ O ⁻	0.47	0.34	0.32	0.08	1.41	1.16	0.16	0.35
P ₂ O ₅	n.d.	n.d.	n.d.	n.d.	n.d.	n.d.	n.d.	n.d.
CO ₂	-	-	7.15	-	-	-	-	-
	<u>101.07</u>	<u>99.02</u>	<u>100.76</u>	<u>101.09</u>	<u>99.77</u>	<u>100.74</u>	<u>100.84</u>	<u>101.16</u>

Analyst : Dr. G. Hornung

- B66 sandstone of Fish River series, near Mt. Brukkaros, S.W.A.
 B64 buff coloured microbreccia, Mt. Brukkaros, S.W.A.
 B65 red microbreccia, Mt. Brukkaros, S.W.A.
 B95 buff coloured very fine grained microbreccia,
 Mt. Brukkaros, S.W.S.
 B62 red microbreccia, Mt. Brukkaros, S.W.A.
 B93 red microbreccia, Mt. Brukkaros, S.W.A.
 B89 sandy shale, north of Mt. Brukkaros, S.W.A.
 B88 feldspathized shale, north slope of Mt. Brukkaros, S.W.A.

TABLE 20. Trace element composition of Fish River sandstone

	Ba	Be	Co	Cr	Ga	La	Li	Mn	Mo	Nb	Ni
B66	>1000	<3	<10	90	10	<100	<10	360	3	15	15
B65	170	5	15	120	15	<100	40	1500	5	<10	30
B64	350	15	20	700	10	<100	75	850	5	110	60

and Brukkaros microbreccias

	Pb	Rb	Sc	Sr	Ti	V	V	Zr
	15	50	20	55	>1000	50	25	200
	<10	55	<20	190	>1000	200	45	150
	10	50	25	140	>1000	400	100	300

Spectrographer : Miss J. Rooke.

B66 sandstone of Fish River series near Mt. Brukkaros,
S.W.A.

B65 red microbreccia, Mt. Brukkaros, S.W.A.

B64 buff coloured microbreccia, Mt. Brukkaros, S.W.A.

Heavy mineral concentrates from the microbreccias.

A few minerals of the type occurring in kimberlites, such as pyrope, chrome diopside and picro ilmenite were found in a concentrate, taken inside the central depression, 50 yards upstream from the first waterfall. It is possible that a kimberlite has used the Brukkaros vent as a channel for its own intrusion.

(iv) Discussion of formation

The most characteristic feature of the microbreccias of the central vent is that they contain no volcanic rock whatsoever. The crystal- and rock-fragments and the feldspathic matrix are all derived from sedimentary rocks, which have been brecciated and partly pulverized and transported into higher levels. The finely pulverized feldspathic matrix cannot have been derived from unaltered Nama sediments, as detrital or authigenic feldspathic beds are rare in these sediments. Feldspathization by ascending liquids or gases after the breccia was emplaced is equally unlikely, because the breccia contains a mixture of clear and clouded feldspar crystals in a matrix of varying degrees of feldspathization. It is most probable that the matrix has been derived from brecciation of a feldspathized rock at lower levels.

The near complete lack of granitic fragments, derived from the granitic basement indicates that the cause of the

brecciation must have been at comparatively shallow depth, somewhere on or above the boundary of the basement and the sediments, completely shattering the latter and thereby choking the vent so that no volcanic or granitic basement material could escape. The depth of the basement is known from a deep borehole near the village of Berseba and amounts to a little less than 3,200 feet.

The lack of any significant thermal metamorphism in the fragments or in the wall rock (except for bleached boundaries in shales) indicates that the temperature must have been low.

The fact that the fragments are still angular indicates that they have not been transported very far. Furthermore, the textures of the rock, especially texture B, are not incompatible with transport by a gas-solid suspension over short distances.

From the evidence, enumerated so far, the conclusion can be drawn that the microbreccias of the central vent have been produced by a violent explosion, which released a great amount of gases of low temperature, at shallow depth.

Explosions of this kind can be caused by (i) retrograde boiling and (ii) phreatic explosions.

(i) Retrograde boiling. Retrograde boiling results when a slowly cooling volatile-rich magma is subjected to sudden

releases of pressure. The formation of the many radial dykes and small vents through newly opened fractures probably resulted in sudden drops in pressure, which caused retrograde boiling and released great amounts of gases. However, McBirney (1959; 1963) showed that the energy necessary for the creation of a large explosion vent cannot have been produced by the volatile content of magmas only.

(ii) Phreatic explosions. A phreatic explosion generally results when the heat front of an ascending magma suddenly comes into contact with a large volume of water (seawater or groundwater). In the case of Mt. Brukkaros good water-carriers are provided by the well-jointed sandstones with intercalations of thin sandy shale beds. It is quite possible that sudden fractures in the upper basement brought a volatile-rich magma into contact with this water-soaked sediment, generating a large amount of watervapour.

A combination of the two processes has probably taken place. The Brukkaros central vent with its shallow centre of explosion, its very large diameter and no volcanic rocks, has most of the characteristic features of a phreatic explosion vent. After the initial phreatic explosion, smaller repeated outbursts caused by retrograde boiling probably modified the vent and deposited the various layers of microbreccia.

(c) Contact rocks

The maroon shales which form the wall rock around the central vent have been considerably affected. Signs of thermal metamorphism are lacking, but the wall rock is everywhere traversed and injected by veins of intrusive microbreccias (see plate 45), and numerous 2 to 3 inch wide quartzveins, which contain clear quartzcrystals up to 2 inch diameter. Vugs, lined with hyaline, are common.

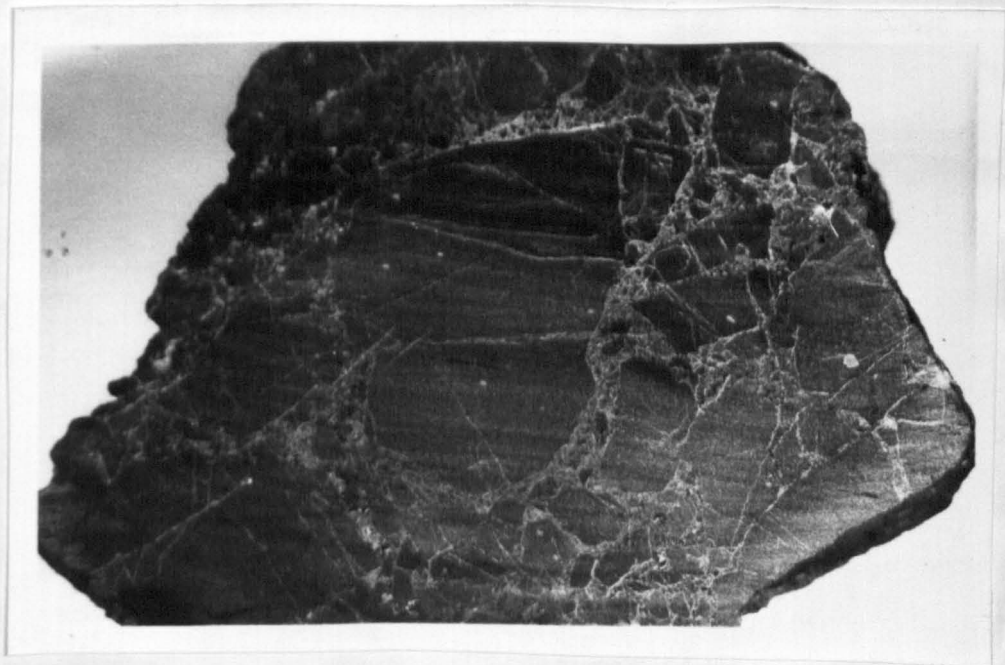
A large area of shales on the northwest side of the mountain has undergone a process of feldspathization. The shales are intricately fractured by small veins of potash feldspar and calcite and barite (see plate 46). As a result they have been hardened and are resisting erosion. Under the microscope the shales consist of very fine grained brown-stained clayey bands alternating with slightly coarser quartz-rich sandy bands. The introduced material forms light coloured veinlets with the potash feldspar and barite deposited in the wider parts of the veins and with calcite predominating the narrower parts.

(d) Breccias of the satellite vents(i) Description

In contrast to the finely fragmented microbreccias of the central vent, the satellite vents contain coarse angular fragments of sedimentary rock and coarse angular and rounded fragments of granitic gneisses (see plates

Plate 45. Tuffisite. Intrusive microbreccia has invaded the maroon shales at the contact (natural size).

Plate 46. Fractured shale with small veinlets of potash feldspar and calcite (natural size).



47 and 48).

These accidental inclusions, which consist entirely of non-volcanic material, are well over 32 mm. in diameter and can best be described as vent breccias (Pettijohn 1949).

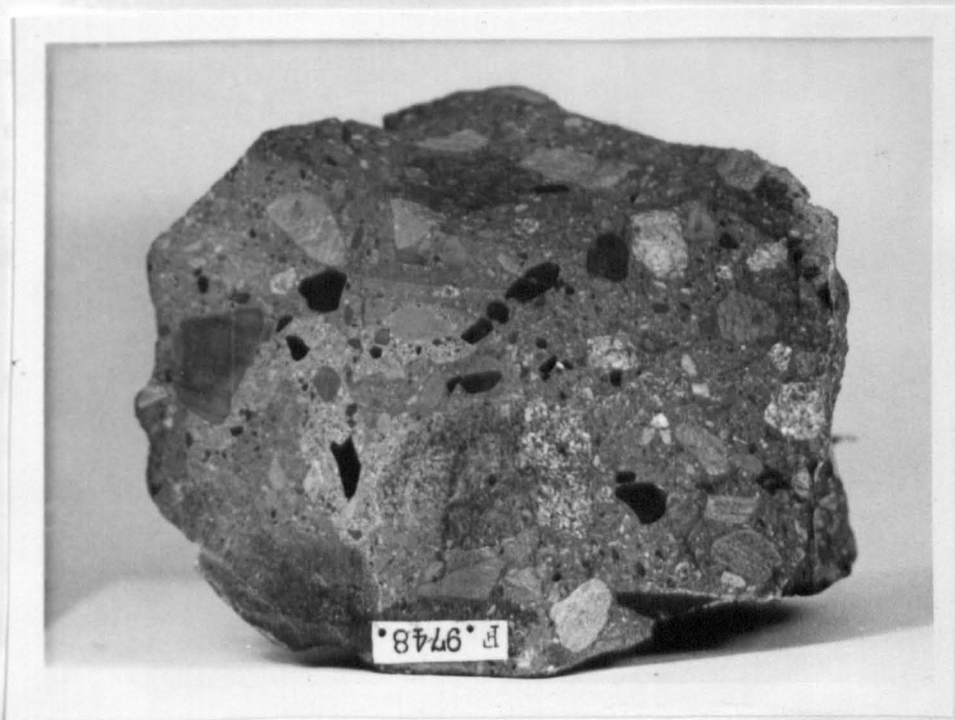
The fragmental sedimentary rocks are mainly derived from the Nama formation. They are mostly reddish sandstones, quartzites and shales from the Fish River series, but occasionally whitish quartzites and bluish green shales are found, which could have been derived from respectively the Kuibis series or the Schwarzrand series. However, limestone fragments from the Schwarzkalk have never been found. Fragments of blue or black slates are present and could have been derived from pre-Nama sediments, intercalated between the Nama formation and the basement or within the basement.

The angular or rounded gneissic fragments must have been derived from the granitic basement. They are mostly granite gneiss, gneissic muscovite granite, granodiorite gneiss. Biotite-hornblende-gneisses or amphibolite are rare.

The various fragments are embedded in a matrix of lamprophyric composition, which in most cases is completely altered to a buff coloured indurated mass of carbonates. Silicification is common and many of the rocks are traversed

Plate 47. Coarse vent breccia, vent G1 (X $\frac{1}{2}$)

Plate 48. Vent breccia, vent K1 (natural size)



by small quartz- and calcite veins.

(ii) Mineralogy

Rock fragments. In thin section the granite fragments are composed of muscovite granite with clear quartz and pink orthoclase, with a little plagioclase, muscovite and biotite.

The gneiss fragments are quartz-rich granite gneiss with microcline, a little plagioclase and biotite; they have a general cataclastic texture. The details of mineralogy are as follows :

Quartz is present in comparatively large grains over 10 mm. in diameter, it shows undulose extinction and strongly articulated boundaries, sometimes with myrmekitic intergrowths with microcline.

Microcline is strongly microperthitic. It has a large 2V (80°) and is more cataclastic than the quartz. Areas with small broken and recrystallized grains of microcline and quartz are wedged between large strained quartz-grains (mortar structure).

Plagioclase is less common. Clear small grains with albite twin lamellae show the nearly straight extinction of oligoclase.

Biotite is strained, has frayed margins, and is very strongly pleochroic from light brown to dark brown and contains dark streaks of ore minerals. The biotite is

stained red by alteration products and is probably an iron-rich biotite.

Mineral content. The matrix of the vent breccias is unfortunately in most cases completely altered. Less altered, bluish varieties show, however, a calcitic-dolomitic groundmass with minute crystals of magnetite and ilmenite, together with larger flakes of biotite and pseudomorphs of calcitic material after phenocrysts of olivine.

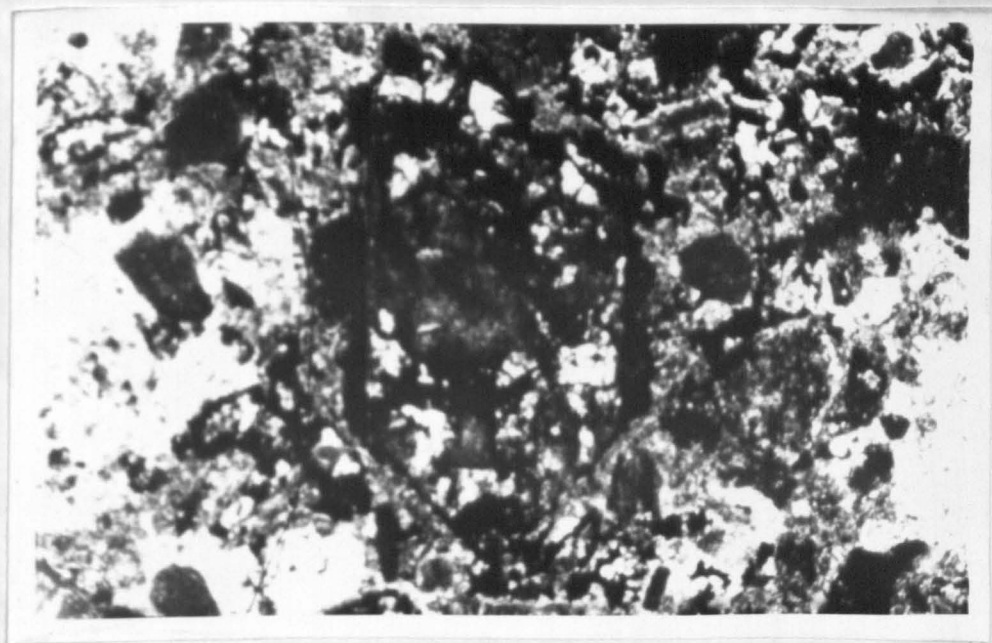
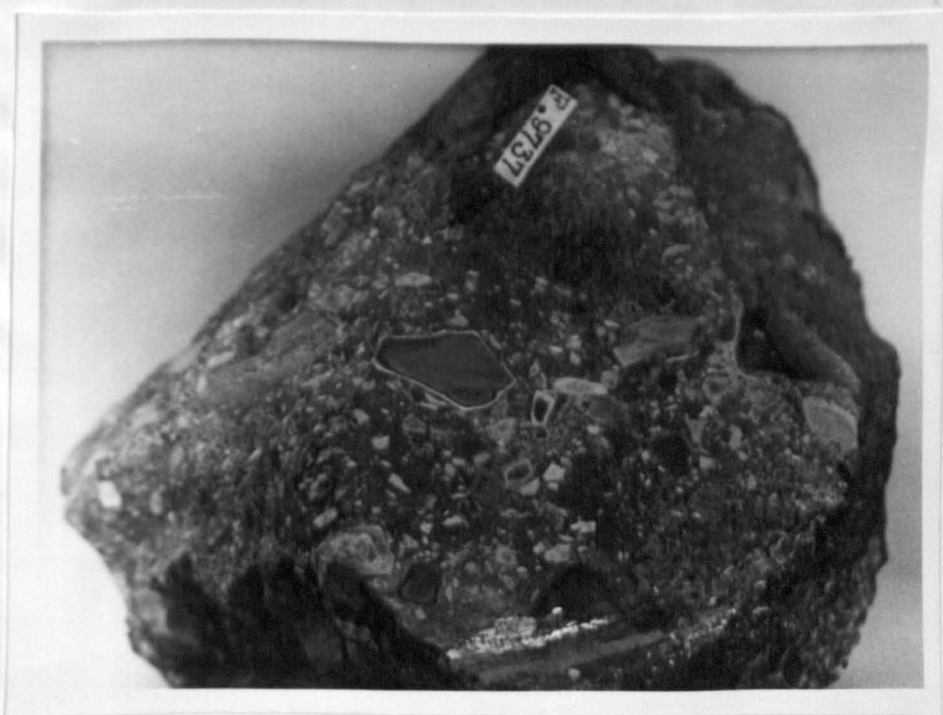
Olivine is almost completely altered to calcite and dolomite. In a few cases antigorite and light green chlorite still form part of the alteration products, but usually only a concentration of brown opaque stuff along cracks and crystal outlines gives an indication of the original shape of the crystal (see plate 50). Most of the crystal outlines show perfectly shaped euhedral olivines, but some of them could be pyroxene outlines.

Aegirine-augite is present in one of the least weathered specimens from vent A. It is a deep green pyroxene with a distinct pleochroism, and the following properties -

pleochroism	cleavage	X C	2V(-)
X = slightly bluish green	distinct	-1°	72°
Y = slightly yellowish- green	(110)		
Z = yellow green			

Plate 49. Vent breccia, vent D. Note sandstone fragment with bleached and baked boundary (natural size)

Plate 50. Photomicrograph of thin section F9737 (12). Outline of olivine phenocryst in matrix of vent breccia. (x32).



According to the determinative data of Tröger (1956) it is an aegirine-rich augite with ca. 70 mol% NaFe^{III}. Along rims and cracks the mineral is slightly altered to a brown opaque mass, probably limonite.

Biotite is always present. It has a very small 2V and a pleochroism which is strongly zonal with a lighter core and a darker rim. The core changes from grass green with dark streaks to light reddish green brown, while the rim changes from dark brown to light reddish brown. In many cases a concentration of black opaque minerals occurs along the darker rim. X-ray patterns show that it is phlogopite.

Magnetite is present in appreciable amount in samples of vents A and F.

Perovskite. Evidence for the presence of perovskite is inconclusive. Certain greyish black-rimmed equant crystals scattered through the groundmass of the vent breccias are very similar to crystals in the groundmass of a calcite-phlogopite rock, which have definitely been determined as perovskite. It is thought that the vent breccias may originally have contained perovskite, which has been bleached and altered to ilmenite along the rims.

Ilmenite could not be determined with certainty by optical means, but its presence was shown by X-ray patterns.

Groundmass. The composition of the calcitic-dolomitic groundmass was determined by X-ray diffraction. The results were as follows :

Dolomite forms the main constituents of the matrix.

It is a nearly pure dolomite (Cc 55). In the more weathered specimens dolomite (Cc 60) and a little quartz are the only constituents.

Quartz is present in nearly equal amounts to dolomite in some cases.

Calcite is occasionally present in small amounts.

Further constituents are : phlogopite, magnetite and ilmenite.

A thorough check was made to ascertain the original presence of melilite, which could account for the large amount of carbonate in the groundmass, but the texture of the groundmass is completely obscured by alteration products. Lath-like textures similar to the ones in the Mukorob rock cannot be observed, therefore no valid reference can be made about the presence or absence of original melilite.

Kimberlite minerals, such as pyrope, chrome diopside and micro-ilmenite were found in concentrates from small streams, draining the vents E, I and J, but they have not been found in situ (map 1).

(iii) Discussion of formation

The matrix of the vent breccias has some similarities to, but is not identical with, the groundmass of a kimberlite. The brecciated, inclusion rich texture is similar to that in kimberlites, the mineralogical composition is

similar, but in thin section the groundmass of a kimberlite consists mostly of light green serpentine, while in the vents the groundmass consists of grey calcite and red brown limonite. Also, secondary weathering alters a bluish kimberlite into a friable clayey yellow rock, while in this case a bluish lamprophyric rock is altered into a yellow brown calcitic rock of very tough character. Furthermore, the satellite vents do not contain any inclusions of nodular rocks, such as peridotites, garnet-pyroxenites, etc. which are typical for a kimberlite. They are, on the other hand nearly completely choked with coarse angular and subrounded fragments of host rock.

The rounded fragments of granitic material must have been transported from levels deeper than the sedimentary cover and are considered to be accidental inclusions in the matrix. Derivation of the rounded fragments from parts of the Dwyka tillite fallen into the vent is not probable. The tillite contains a large variety of rocks not found in the vent and the predominant gneiss and granite fragments in the vent are not similar to those of the tillite.

The rounding of the fragments is attributed to abrasion during transport in a gas solid suspension (Reynolds 1954). The lack of any significant thermal metamorphism in the fragments or wall rock indicates a low temperature in the mixture of

inclusions and olivine rich matrix.

No definite conclusion can be reached about the nature of the original matrix, but from the extensive alteration through the influence of CO_2 and H_2O and the presence of many olivine phenocryst-pseudomorphs, it can be deduced that the parent magma was ultrabasic and rich in calcium and volatiles.

The distribution of the satellite vents and the radial dykes around the central vent suggest that there is a close genetic connection between the three phenomena. It is believed that this volatile-rich ultrabasic magma was also responsible for the formation of the Brukkaros dome and for the phreatic eruptions which formed the microbreccias.

Table 21. Analyses of vent breccia and radial dykes
around Mt. Brukkaros

	B26	B47	B78	trace element composition of B78 in p.p.m.			
SiO ₂	42.5	26.0	2.93	Li	B	Ti	1000
TiO ₂	1.23	3.25	0.69	Rb	100	Zr	300
Al ₂ O ₃	6.5	4.0	0.68	Sr	220	Pb	30
Fe ₂ O ₃	4.53	8.11	9.69	Ba	3000	V	130
FeO	3.48	2.76	0.00	Be	3	Nb	270
MnO	0.13	0.13	0.33	Sc	20	Cr	75
MgO	9.7	14.0	0.79	Y	100	Mo	5
CaO	14.4	17.1	45.63	La	400	Co	20
Na ₂ O	3.06	0.47	0.22	Ga	2	Ni	55
K ₂ O	1.73	2.08	0.03				
H ₂ O ⁺	3.54	2.93	1.49				
H ₂ O ⁻	0.58	0.64	0.72				
P ₂ O ₅	n.d.	n.d.	2.53				
CO ₂	9.31	19.89	34.29				
	<u>100.69</u>	<u>101.36</u>	<u>100.02</u>	Spectrographer : Miss J. Rooke.			

- B26 vent breccia, vent A, near Mt. Brukkaros, S.W.A.
Analyst : G. Hornung.
- B47 micaceous dyke near vent L, Mt. Brukkaros, S.W.A.
Analyst : G. Hornung.
- B78 carbonate dyke, near vent F, Mt. Brukkaros, S.W.A.
Analyst : J. R. Baldwin.

(e) Radial dykes

The precise petrological determination of the dyke rocks is made very difficult by their extensive alteration to a tough indurated mass of brown-stained carbonates.

Thin sections show a turbid brownish groundmass, which in some cases encloses phenocrysts of olivine, completely altered to calcite and dolomite, and laths of biotite.

A dyke near vent L (see map 1) contains numerous phenocrysts with idiomorphic outlines after olivine and many laths of biotite with ragged and bent margins and bleached rims with many grains of exsolved magnetite.

Light brown equant grains with typical re-entrant angles due to complex twinning are also present and probably represent bleached perovskite.

A completely calcitized dyke near vent F (see map 1) shows nothing more than a brown-stained turbid carbonate mass, but the trace element composition suggests carbonatic affinities (see table 21).

A definite conclusion whether these dykes are carbonates, ankeritic alvikites or picrite-beforsites, or kimberlites cannot be drawn.

From a petrographic point of view, the Hatzium dome dyke is in this category. It occurs in the centre of the dome as a $2\frac{1}{2}$ feet wide dyke consisting of dark grey tough rock, which weathers to a greenish-grey friable mass. In thin section it is

seen to consist of numerous pseudomorphs of antigorite, limonite and a little calcite after olivine, embedded in a groundmass of antigorite and calcite with minute crystals of magnetite and bleached perovskite.

(f) Summary of results

1. Mt. Brukkaros is not an ancient stratovolcano, but a dome built up by the local sandstones and shales of the Fish River series.

2. The fine grained clastic rocks (microbreccias) represent the remnants of a cover of clastic rocks derived from the brecciation of the Nama sediments and deposited around a large explosion vent of a phreatic nature. They have been protected from erosion partly by silicification and partly by sinking in the vent, thereby creating a central depression in the top of the dome.

3. The contact of the microbreccias with the host rocks is a disconformity, representing a time gap of late-Nama to post-Cave Sandstone times.

4. The Brukkaros complex is younger than the Cave Sandstone beds and older than the nearby kimberlites.

5. The satellite vents and the radial dykes are derived from a volatile-rich ultrabasic magma.

6. The presence of aegirine in satellite vent A, the feldspathization of the shales of the "balcony" and the feldspar-rich groundmass of the microbreccias suggest that this magma has alkaline affinities and caused alkali-metasomatism.

4. Theories of formation of the Gross Brukkaros

(a) Previous theories

Rogers (1915b) compared Mt. Brukkaros to the Barringer Crater, in Arizona. He remarked on the close similarity to the Arizona crater from the description by G. K. Gilbert (1896) who favoured a volcanic explosion theory for the Arizona crater and rejected the meteorite impact theory. There are, however, important differences between the two "craters"; the main difference being that the host rocks at Mt. Brukkaros dip inwards, while at the Arizona crater they dip outwards. The difference in size between the two structures is :

Mt. Brukkaros	:	crater diameter 1.3 miles; bottom of crater 1000 feet below the rim;
Barringer	:	crater diameter 0.75 miles; bottom of crater 570 feet below the rim.

Spencer (1941) called attention to the presence of many meteorites which have been found in an area 40 to 50 miles northeast of Mt. Brukkaros. From a comparative study of many meteorites he concluded that they represented a meteorite swarm instead of fragments of one big meteorite. He did not think, however, that the presence of these meteorites was enough evidence for a meteorite impact theory of origin for Mt. Brukkaros.

From the description of Bucher (1963), the Wells Creek Basin structure and the Hicks Dome in Tennessee and Illinois have a remarkable resemblance to Mt. Brukkaros and the Hatzium Dome. The Wells Creek Basin structure and the Hicks Dome are 90 miles apart and in between them there are many mafic dykes "peridotites with alkaline affinities" and "sedimentary breccias within a mafic alkaline matrix" (Bucher 1963). North of Wells Creek Basin there are three small "craterlets", filled with clays and sand. Mt. Brukkaros and the Hatzium Dome are 70 miles apart and in between them there are many kimberlite vents and dykes, while the radial dykes and satellite vents have similar petrological affinities to those in Tennessee. The resemblance goes even as far as the existence of the two "craterlets" on the farm Gründorner Fläche, 40 miles north of Mt. Brukkaros.

Dietz (1963) and Wilson (1953) and many others consider the Wells Creek Basin an example of meteorite impact and Wilson postulates a swarm of meteorites to explain the formation of the large Wells Creek Basin and the three craterlets.

Bucher (1963) emphasizes that meteorite impact should be completely random. If a cryptoexplosion structure can be connected with terrestrial structural patterns, then, in his view, a meteorite impact theory has to be rejected.

Accordingly, he connects the Wells Creek Basin with Hicks Dome and with the area of explosion ^{vents} at Avon in Southern Missouri (Rust 1937) and rejects the meteorite impact theory on regional structural grounds.

In the case of Mt. Brukkaros simple meteoritic impact is not sufficient to explain the regional setting. Moreover, the presence of the two main indications for a meteorite impact, namely coesite and shatter cones, has not been established in the microbreccias or in the host rocks and it is therefore considered that there is more evidence that Mt. Brukkaros is a "geobleme" (Bucher 1963), that is, a structure caused by processes from within the earth.

(b) Present hypothesis

Following Cloos' axiom "Hebung-Spaltung-Vulkanismus" (Cloos 1941), it is not unreasonable to assume that the sequence of events started with a slowly ascending volatile-rich magma which caused the large dome and gave rise to the radial dykes and the satellite explosion vents. This volatile-rich magma caused feldspathization of the overlying sediments, which were pulverized when the dome blew off its top in a series of phreatic explosions. It is considered that these explosions were caused by the rising heatfront of the magma meeting the water-soaked Nama sediments and that the combined gas pressure of the

volatiles of the magma and the watervapour of the sediments surpassed the lithostatic pressure of the overlying sediments. A large explosion vent was created which was filled with fine-grained clastic rock of non-volcanic origin. These rocks were deposited by many repeated outbursts of a gas-solid suspension of pulverized host rocks in watervapour; they were at first laid down horizontally or subhorizontally and later sunk and slumped back into the vent or were downwarped together with the host rocks when the central column of clastic rocks subsided after the gas pressure from below had decreased. This created a central depression which has been enlarged by erosion. The latest stage is represented by ascending silica-rich liquids hardening the clastic rocks and filling small vugs and fissures.

It would not be correct to refer to Mt. Brukkaros as a cryptovolcano, as this term usually implies a negative landscape form. The term pseudovolcano - a positive landscape form resembling a volcano, but without indications of the eruption of volcanic rocks - seems more appropriate.

V THE RELATIONSHIPS OF THE
ERUPTIVE ROCKS IN THE GIBBON
PROVINCE

The eruptive rocks of the Gibeon province comprise the following groups : (i) tholeiitic basalts and dolerites; (ii) kimberlites; (iii) carbonatitic dykes; and (iv) rocks belonging to the Brukkaros complex (including the monticellite peridotite). It is considered that the last three groups are related to each other in age, petrology and chemistry, while their relationship to the tholeiitic basalts is still uncertain.

1. Age relationships.

The history of volcanic events in the Gibeon province began in Karroo times with the formation of dolerite feeding ducts and tholeiitic basalt flows, some with alkaline affinities, over a large area. Subsequent erosion removed most of the flows except for the remnants still present in the Kub-Hoachanas-Mariental triangle (see figure 1). Because of the similarity with the Stormberg volcanics of South Africa, these lavas are considered to be of Stormberg (Jurassic) age.

Since they contain included fragments of the Kub lavas, the kimberlites are post-Jurassic. Moreover, they are overlain by the Kalahari Beds (early Middle Tertiary) and, by analogy with the South African kimberlites, they are thought to be late-Cretaceous.

The field relationships between the carbonatitic dykes and the kimberlites is not clear. The calcitic dyke at

Hatzium cuts the kimberlite, while the Amalia dyke stops close to the vent; the Mukorob dyke and the other calcitic dykes at Ovas cannot be followed near to a kimberlite. From the evidence at other localities, such as the Premier Diamond Mine (Daly 1925) where the carbonatites cut the kimberlite, and from the evidence of the Hatzium vent, it is concluded that the carbonatitic dykes are younger than the kimberlites.

The age of the Brukkaros complex is post-Cave Sandstone, while fragments of microbreccia included in one kimberlite in the Gibeon province suggest that it predated kimberlite formation. However, a breccia vent in Gordonia (South Africa) contains fragments of kimberlite, and Truter (1949) considers that the breccia vent formation is in general of Eocene age, and therefore younger than the kimberlites. In this regard it must be remembered that kimberlitic minerals have also been found in the Brukkaros vent and in some of the satellite vents and it may be that the kimberlites were formed during a longer interval of time, and that the breccia vents are younger than some kimberlites and older than others.

2. Petrological and chemical relationships.

The carbonatitic dykes, the groundmass of the kimberlites and the groundmass of the satellite vents of Brukkaros have close similarities. Mineralogically, they are rich

in olivine, biotite and calcite. In addition, the nearly complete replacement of basalt fragments by natrolite in the Gibeon Townlands 2 kimberlite (see figure 4) suggests that there has been alkali-metasomatism. This is of particular interest in that : (i) feldspathization of shales and sandstones has taken place in the rocks of the Brukkaros complex; (ii) aegirine occurs in vent A (see map 1); and (iii) Dawson (1960) concluded that alkali-metasomatism affected certain inclusions in the Basutoland kimberlites.

On a von Wolff diagram the chemical compositions of the accidental inclusions in the Gibeon kimberlites fall into three groups : (i) basalt fragments and dolerite and granulite nodules; (ii) pyroxene-bearing nodules; and (iii) olivine-bearing nodules. If it is accepted that (iii), (ii) and (i) represent successively shallower zones of derivation of these nodules, then chemically the inclusions show a trend towards greater undersaturation and higher calcemic content with increased depth. A fourth chemical group is formed by the kimberlites, the satellite vents and dykes of Brukkaros and the carbonatitic dykes (see figures 9 and 13). On the von Wolff diagram these rocks fall in a zone connecting the kimberlite field with the calcite corner (figure 9). This is even more clearly demonstrated in the diagrams of figure 13; figure 13a shows the relationship between kimberlites and carbonatites

from several localities in southern Africa (Garson 1962), while figure 13b shows that a similar relationship exists amongst the rocks of the Gibeon province.

3. Genetic relationships.

The Gibeon province represents a focus of volcanic activity, resulting in near to 50 kimberlite vents and related rocks. The extreme undersaturation of kimberlites and their content of high-pressure minerals, such as pyrope and, in certain cases, diamond, suggest that they have originated from very deep levels. Moreover, their high content of garnet peridotite nodules and the fact that large bodies of garnet peridotite do not exist in the crust, implies that kimberlites originated in the mantle. Other accidental deep-seated inclusions, which are mainly pyroxene-bearing, were acquired during intrusion through deep levels of the crust.

In recent years many authors (v. Eckermann 1948, 1958; Saether 1957; Garson 1962; Dawson 1960, 1964 and others) have postulated a genetic relationship between kimberlites and carbonatites. In particular, Garson evolved a theory which assumes that kimberlites under certain conditions may develop a volatile-rich top fraction with a carbonatitic composition. Williams (1932) and Mikheyenko and Nenashev (1962) suggested that kimberlites are intruded in large fissures in the crust, and that

these change into a cluster of vents at shallower depth. The depth of this change is considered to be 5 to 7 km. (v. Eckermann 1958; James 1963). Combining these ideas it is thought that in cases where the kimberlite did not reach the surface in the form of vents, it developed a volatile-rich top fraction which either changed into a carbonatite at shallow depth (v. Eckermann 1958; Garson 1962) or reached the surface as small carbonate tuff cones; such cones have recently been described from northern Tanganyika where they are thought to represent the surface expression of differentiated kimberlites (Dawson 1964).

From the chemical and mineralogical evidence of the satellite vents and the radial dykes, it is concluded that the Brukkaros dome was probably formed by a "volatile-rich calcium-rich ultrabasic magma with alkaline affinities". It is considered that the Brukkaros vent was formed by phreatic eruptions when this volatile-rich magma or a differentiated portion of it met the water-soaked sediments of the Nama Formation. The monticellite peridotite is thought to represent a part of the differentiated kimberlite which was depleted of volatiles.

Explanation of symbols of figure 13:

13a : rocks from many different localities

A= average mica-peridotite

B= average micaceous kimberlite

C= average basaltic kimberlite

D and E= carbonate-rich kimberlite, Kiwurungu, Tanganyika

F and G= Igwisi lavas, Tanganyika

H= carbonate dyke, Premier mine, Transvaal

J= sövite, Tundulu, Nyassaland

13b : rocks from the Gibeon province

BlandB2= monticellite peridotite and calcite-phlogopite rocks
table 17

A1, F13, Ha12= kimberlites, table 3

Ht16, A3= kimberlites, table 15

B47, B78= calcitic dykes, table 15 .

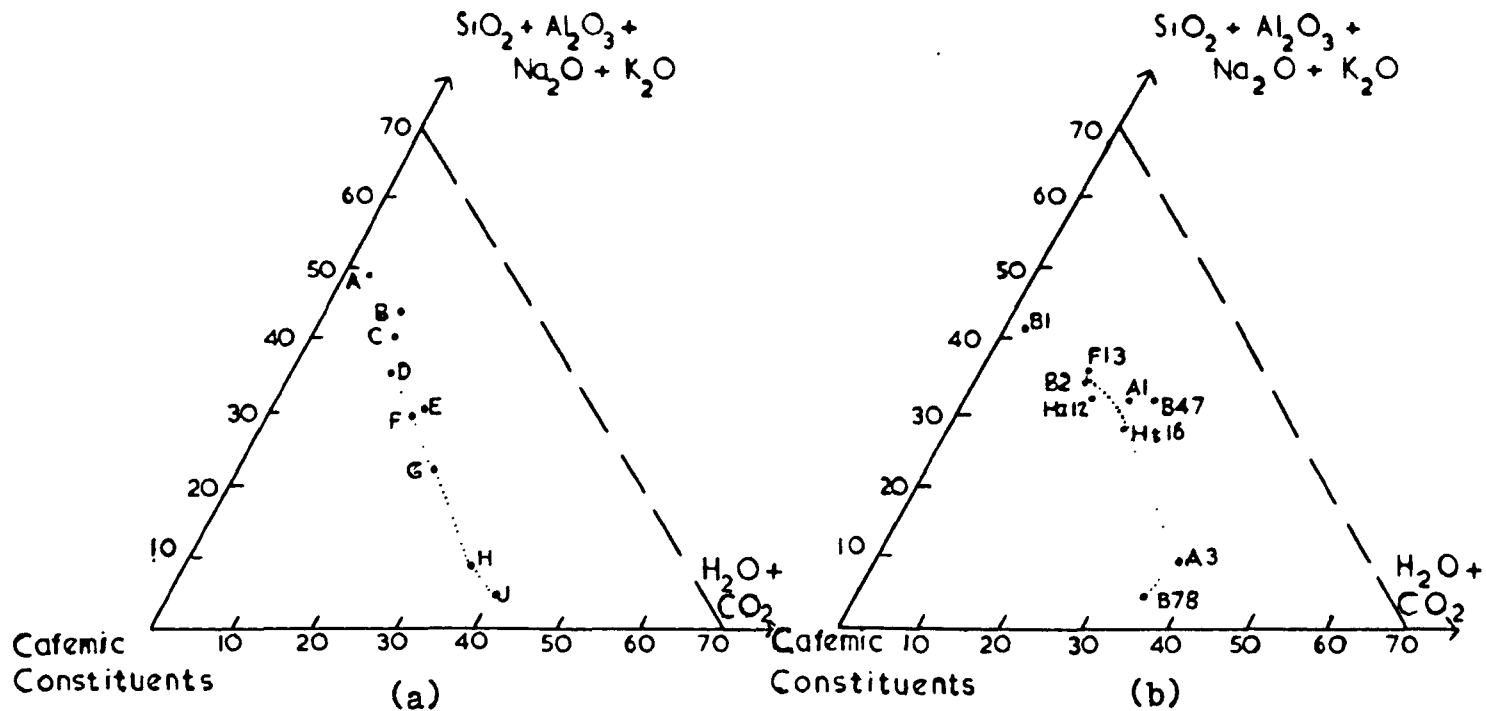


Fig. 13. Diagrams illustrating the petrogenetic relationships of the kimberlite-carbonatite series.

13a rocks from many different localities (after Garson 1962)

13b rocks from the Gibeon province

VI APPENDICES

APPENDIX ADescription of the main satellite vents around Mt. Brukkaros.

There are 8 large vents and 37 smaller ones. Several vents occur in clusters or in the same dyke swarm, these are designated by one capital letter and different figures.

Vent A

Location : 5 miles west of Mt. Brukkaros

Size : 50 x 50 yards

Intruded into : maroon shales

Contact with host rock : no visible disturbance

Contact metamorphism : not visible; none

Description of outcrop :

The outcrop forms a brown oval spot consisting of weathered brown rubble on the side of a low hill, flush with the surface. The rubble is composed of weathered buff coloured vent breccia with pebble-sized angular fragments of shale, sandstone, granite gneiss and dolerite. The matrix is blue reddish or buff and contains many flakes of biotite and a fair amount of magnetite.

Specimens : F.9741 Bluish-grey lamprophyre
(inclusion-rich)
B.28 bluish-grey lamprophyre
(magnetite-rich)
B.102 buff vent breccia.

Vents B.1 and B.2

Location : in a dyke 5 miles south of Mt. Brukkaros
at the intersection of two tangential
structures.

Intruded into : maroon shales

Contact with host rock : no visible disturbance

Contact metamorphism : not visible; none

Description of outcrop :

A N-S running buff coloured dyke splits into two branches which come together again including a big island of shales. Nearer to Vent B.1 the dyke contains many angular fragments of granite-gneiss (specimen B.17). The actual outcrop of B.1 looks like a scattered heap of rocks as is formed by a destroyed farm beacon and is about 10 yards in diameter. The breccia of vent B.2 is slightly coarser and contains besides angular fragments of gneiss (specimen F.10634) many more fragments of shale. The outcrop forms a slight hump of hard breccia and is about 30 yards in diameter.

Specimens	:	B.17	buff dyke breccia with angular granite inclusion.
		F.9738	fine grained vent breccia
		F.10634	granite gneiss inclusion.

Vent C.

Location : 2 miles south of Mt. Brukkaros

Size : 140 x 120 yards; forms a neck 100 feet high

Intruded into : maroon shales

Contact with host rock : hidden by scree

Contact metamorphism : not visible

Description of outcrop :

The hard vent breccia stands out as a large neck in the small floodplain, where the little stream draining the depression inside Mt. Brukkaros leaves the barranco. The vent breccia contains many angular fragments of shale, sandstone and quartzite of up to 1 to 2 ft. diameter. Some large boulders of granite gneiss are also present.

Specimen : B.69 buff vent breccia.

Vent D.

Location : 3 miles south of Mt. Brukkaros

Size : 100 x 60 yards, forms a neck 50 feet high.

Intruded into : maroon shales and flagstones

Contact with host rock : hidden by scree

Contact metamorphism : very slight, some change of the colour of red shales into blue-green.

Description of outcrop :

The hard breccia stands out as a neck in the plain between the Blue Hills and a long scree south of Mt. Brukkaros. The breccias of the last two mentioned vents C. and D. do not contain many fragments of gneiss. Fragments of shale, sandstone, chert and whitish quartzite are predominant, the first three are generally blue-grey or buff coloured, occasionally maroon, and have bleached boundaries. The matrix is yellow-brown, calcified or silicified.

Specimen : F.9737 vent breccia.

Vents E.1, E.2

Two very small vents, 10 yards by 20 yards in diameter

on the south slope of Mt. Brukkaros.

Vent F.

Location : in dyke swarm 2 miles west of Mt. Brukkaros

Size : nearly circular; 180 yards diameter

Intruded into : maroon shales

Contact with host rock : inward dipping shales (20° dip)

Contact metamorphism : none

Description of outcrop :

Six outcrops of hard breccia form low humps amidst shale and breccia debris. They are surrounded by a circle of inward dipping shales. Three 10" wide buff coloured dykes traverse the shales up to the boundary of the vent and continue their course at the opposite side of the vent. The dykes contain many angular fragments of granite gneiss nearer to the boundary with the vent (specimen B.22).

The centre of intrusion consists of a fine grained light yellow dolomite-breccia with minute fragments of chert and granite gneiss.

The other outcrops consist of coarse breccia with many angular fragments of reddish shale and sandstone, blue shale, gneiss, dolerite and amphibolite (few). A bluish-black weathered mica-lamprophyre is exposed on the north side of the vent (F.9740).

Specimens	:	F.9739	dolomite-breccia
		B.22	dyke-breccia with angular granite inclusion
		B.23	vent-breccia with many Nama sandstone fragments

F.9740 mica-lamprophyre

B.25 vent breccia.

Vents G.1, G.2, G.3, G.4, G.5

Location : on the west flank of Mt. Brukkaros

Size : G.1 50 x 30 yards; a neck 50 feet high

G.2 20 x 15 yards

G.3 15 x 10 yards

G.4 40 x 20 yards

G.5 10 yards diameter

Intruded into : shales and sandstones

Contact with host rock : no disturbance, partially
hidden by scree

Contact metamorphism : none

Description of outcrop :

The five vents are all surrounded or connected by dykes of buff coloured material. G.2, G.3 and G.5 form nothing more than a local widening of the dyke and are crowded with large angular fragments of shale and sandstone with very little matrix.

G.1 and G.4 contain, besides angular fragments, many boulders, cobbles and pebbles of muscovite granite, gneiss and quartzite.

The breccia of G.1 forms a little neck, 50 feet high, which can be noticed from afar as a little wart on the skyline of the west flank of Mt. Brukkaros.

Specimens : B.29 buff vent breccia with quartz veins

B.31 buff vent breccia with coarse rounded fragments.

Vent G.6

The same dyke swarm which connects the vents G.1, G.2, G.3, G.4 and G.5 contains also several fracture zones. They look like "dykes" of hardened brecciated sandstone, about 12 feet wide and stand 4 feet above the surface. The sandstone is brecciated and riddled with quartz veins and inclusions of buff dyke breccia. At one place the dyke widens to form the initial stage of a vent, G.6.

Specimens : F.9745 vent breccia in sandstone
 B.33 sandstone with quartz veins
 F.9746 sandstone from fracture zone.

Vents H.1, H.2, H.3, H.4 and H.5

Location : 2 miles north west of Mt. Brukkaros.

Intruded into : shales

Contact with host rock : no disturbance

Contact metamorphism : none

Description of outcrop :

H.1 : size 100 x 30 yards; a neck about 60 feet high buff breccia with mainly angular fragments of shale and chert; one very large block of over 30 feet diameter. The breccia is traversed by many quartz veins.

Specimen : B.36 buff breccia with inclusions of shale.

H.2 : size 20 x 18 yards; breccia with many fragments pebbles and cobbles.

Specimen : B.37

H.3 : size 30 x 15 yards; buff breccia with inclusions of dark brown weathering breccia.

Specimen : B.38

H.4 : size 15 x 8 yards; buff breccia with many bleached shale fragments.

Specimen : B.39 dyke breccia with zonal arrangements of inclusions.

H.5 : size 15 x 15 yards; buff breccia with mainly shale and sandstone fragments; barite veins.

Specimens : B.80 buff dyke breccia

B.99 barite.

Vent I.

Location : 3 miles north of Mt. Brukkaros

Size : 120 x 80 yards approximately

Intruded into : Nama shales

Contact with host rock : obscured by debris

Contact metamorphism : probable (see below).

Description of outcrop :

Two outcrops of grey vent breccia form low humps amidst a lot of blue shale and breccia debris. The largest outcrop (ca 60 yards diameter) contains vent breccia with inclusions of pebbles and cobbles of gneiss and large fragments of shale. One large inclusion (ca 10 feet diameter) of dolerite is present.

It is separated by a small fault from a smaller outcrop

(ca 30 yards diameter) which contains many fragments of bluish-grey slate, possibly derived from the wall rock by metamorphism of the red Nama shales.

Specimen : B.41 bluish-grey slate

B.42 grey vent breccia

Vent J.1

Location : 3 miles north of Mt. Brukkaros

Size : 300 x 100 yards; forms a large neck over
200 feet high.

Intruded into : shales

Contact with host rock : the contact with the maroon shale is formed by a 20 feet wide zone of extremely brecciated shale; partially hidden by scree.

Contact metamorphism : none

Description of outcrop :

A very steep hill formed by a coarse grey vent breccia with fragments predominantly of shale and sandstone. Also many rounded boulders and cobbles of granite gneiss and few fragments of biotite schist and amphibolite. A mica-lamprophyre is exposed on the west slope on the hill (specimen B.43).

Narrow sills of weathered yellow material are exposed on the north and south side of the vent.

A very small vent is exposed about 500 yards to the east (vent J.2).

Specimens : F.9747 micaceous lamprophyre
 B.44 buff coloured sill with zeolites.

Vents K.1, K.2, K.3 and K.4

Four small vents of buff and grey breccia.

Specimen : F.9748 grey breccia with inclusions of
 black slate.

Vents L.1, L.2, L.3, L.4 and L.5

L.1 : location : 2 miles north of Mt. Brukkaros.

Size : 200 x 150 yards; a large neck of 150 feet high

Intruded into : Nama shales

Contact with host rock : obscured by debris

Contact metamorphism : not visible

Description of outcrop :

A very steep hill built up of buff coloured vent
 breccia with many inclusions. Several dykes run from this
 hill towards the central vent of Mt. Brukkaros. Vents L.2
 L.3, L.4 and L.5 are small "blows" in these dykes.

Specimens : F.9749 micaceous dyke (lamprophyre)
 B.48 fine aeolian sandstone inclusion.

Vent M.

Location : 2 miles north east of Mt. Brukkaros

Size : 140 x 120 yards; a large neck of 100
 feet high

Intruded into : Nama shales and terrace deposits

Contact with host rock : obscured by debris

Contact metamorphism : not visible

Description of outcrop : A solitary hill in a large terrace of scree deposits. Buff coloured breccia with many angular fragments.

Vent N.

A small vent 3 miles north east of Mt. Brukkaros.

Vents O.1, O.2 and O.3

Three small vents in the fractured shales on the north slope of Mt. Brukkaros.

Vent P.

A small vent on the east slope of Mt. Brukkaros.

Vent Q.1 and Q.2.

Two small vents (blows) in a dyke on the eastern slope of Mt. Brukkaros.

Vent R.

A small vent on the south east slope.

Vents S.1, S.2, S.3 and S.4.

Two dykes connect four small vents. The largest vent is 30 x 40 yards and contains a grey vent breccia which feels rather heavy. Inclusions of angular fragments of shale and sandstone and some rounded fragments of gneiss are embedded in a greyish-brown matrix with many flakes of biotite. A small vent nearby contains fine grained yellow microbreccia.

Specimens : F.9760 grey vent breccia.

F.9761 fine grained yellow microbreccia.

Vent T.

A small vent in the dyke crossing the path going into the barranco on the southern slope. The inclusions in this vent show a zonal arrangement.

Specimen : B.98 vent breccia.

Altogether 45 vents.

APPENDIX BDrainage systems in Great Namaland

The earliest recognizable drainage system in Great Namaland is an east-going consequent drainage towards the Kalahari Basin. The rim of the Great Escarpment forms in general the watershed between the seaward west- and interior east-going drainage, but at two places obsequent west-going rivers, the Tsondap and the Tsauchaub have cut back through the Naukluft and Zaris Mountains to drain the area east of the escarpment (figure 2). In particular, the Tsondap forms a spectacular gorge through the Naukluft Mts. (Naukluft means narrow gorge), while 1000 feet higher on top of the limestone plateau traces of an east-going consequent drainage were observed (Korn & Martin 1937).

The easterly drainage of the old land surface of the Schwarzrand (Cretaceous, Mabbutt 1955) changes to a southeasterly drainage on the Kalahari Surface (early Middle Tertiary, Mabbutt 1955). This direction is clearly shown by the Auob and Nossob river systems (figure 2).

The youngest drainage system (post lower Pleistocene, Mabbutt 1955) is the Fish River system, which has a south to southwesterly direction.

Fish River system

The headwaters of the Fish River and all the western tributaries draining the higher and lower Schwarzrand still

show the east-going Kalahari drainage pattern. Near Mariental a major re-orientation to a south-going drainage occurs and from ^{here} the Fish River runs south along the Uri-nanib escarpment following the western outcrop of the Dwyka series, which lie in a N-S longitudinal basin in the Nama formation. About 70 miles downstream from Mariental, the Fish River changes again from a south to a southeast direction, at first still following the western edge of the Dwyka outcrops, but later traversing Dwyka rocks, until another re-orientation to a south-going drainage occurs at Ganikobis (see figure 2). Five miles downstream a waterfall is formed where the river leaves the Dwyka tillite and comes back into the Nama shales. Upstream from the waterfall the Fish River is gently meandering between low sandy banks, but from here downstream it is incised into the bedrock, at first to the amount of tens of feet but lower downstream for several thousands of feet in the Fish River Canyon.

It seems then reasonable to presume that there were two major river captures. After a headward migrating erosion of the now incised part of the Fish River in a SSW-NNE direction, which pushed the edge of the Kalahari Limestone Plain far to the east, it captured the Kanibis River system at Ganikobis. The Upper Kanibis River still shows the southeasterly direction of the interior drainage of the

South Kalahari Basin, like the still uncaptured system of the Auob-Nossob Rivers. A line of pans or vleis in a southeasterly direction, east of Ganikobis might be an indication of the lower course of the Kanibes River before its capture.

After renewed headward erosion in a northerly direction, capturing all the east-going drainage from the Schwarzrand, another major river capture, the Kam River system, occurred just north of Mariental. The main trunk river in the Fish River headwaters is still the Kam River, which has again a southeasterly direction. At the same point the southeasterly Schaap-Usib-River system has nearly been captured, but masses of Kalahari sand (the Duineveld) has obscured the 5 to 10 mile wide indistinct watershed.

APPENDIX CDerivation of Nama names

The earliest traders and hunters came into South West Africa from across the Orange River or via Walvis Bay. The first local people they came into contact with were Hottentots of the Nama group of tribes and consequently most topographical names are derived from the Nama language and the country north of the Orange River was called Great Nama- (or Namaqua)-land.

In several cases the same topographical features have 4 names, respectively in Nama, German, Afrikaans and English.

Gross Brukkaros

The name Gross Brukkaros (also called Gross Brukaros or Mount Brukaros) is a literal translation of the Nama word Geitsi/Gubib. The symbol /g stands for one of the peculiar click sounds, common to the Nama speech. This click sound is produced by pressing the tip of the tongue against the base of the front teeth and drawing it slowly back. (Vedder, 1938, p.57). The word /gu means Karos, that is a piece of skin wrapped around the body, (gubib is the masculine gender of the word /gu, (Krönlein 1889), i.e. a karos worn by men as a form of trousers, which means Broek in Afrikaans-Dutch. The oe-sound in Dutch becomes u in German, hence brukkaros; gei means big, large, or gross in German. Indeed, the circular mountain has some resemblance to an old, greasy karos, standing up-

right by itself.

Schwarzrand

The Schwarzrand plateau is also named Hanami (or Hanam) plateau or Na-nanib plateau. The Nama name Hanami means "flats on which tubers (edible roots) grow" (Vedder, 1953), the German name Zwiebel Hochebene (Bulb plateau) is a literal translation of this. Na-nanib has been translated as black scarp (Schwarzrand) and should only be used for the escarpment itself and not for the plateau. It is surprising that the early travellers translated na or ~~f~~awa as black, (the right translation is red), because the na-nanib escarpment is formed by red shales and sandstones of the Nama System and is definitely not black (black is nu). On some old maps the name Nananib is also given to a low escarpment of red sandstones between the Fish and the Lower Rivers, south of Gibeon.

Further derivations are :

uri - white; uri-nanib - white scarp, low escarpment bordering the Kalahari Limestone Plateau.

/huib - limestone; Huib Plateau - limestone plateau west of lower Fish River.

oub (also spelled ob, eb, oup, op, ap) - river; Kamop - Lion River, Kuiseb - Root River.

gaus - confluence; Tsubgaus - confluence of Tsub and Lower Rivers.

aus - spring; Hanaus - bulb spring.

REFERENCES

- ALDERMAN, A.R., 1936. Eclogites in the neighbourhood of Glenelg, Inverness-shire : Quart. Journ. Geol. Soc. London, 92. 488-550
- ALEXANDER, Capt. Sir. J.E., 1836. An expedition of discovery into the interior of Africa : 2 vols. London
- BACALUND, H.G., 1936. Zur genetischen Deutung der Eclogite: Geol. Rundschau, 27, pt. 1, 47 - 61.
- BARDET, M.G., 1964. Contrôle géotectonique de la répartition des venues diamantifères dans le monde : Chronique des Mines et Rech. Min., 32, nrs 228-229, 67-89.
- BEEZ, W., 1922. The Konkiep formation on the borders of the Namib desert, north of Aus: Geol. Soc. S. Africa, Trans., 25, 23-40.
1924. On a great trough-valley in the Namib: Geol. Soc. S. Africa. Trans., 27, 1-38.
1926. Ueber Glazialschichten an der Basis der Nama-und Konkiep-Formation in der Namib Suedwestafrikas: Neues Jahrb. f. Min etc., Beilage-Bd 56, Abt. P, 437-481
1929. Versuch einer stratigraphische Gliederung der praekambrischen Formationen in der Namib Suedwestafrikas: Neues Jahrb. f. Min. etc., Beilage-Bd. 61, Abt. B, 41-60.
1933. Discussion on Dr. W. Gevers' paper: The hot springs of Windhoek, South West Africa: Geol. Soc. S. Africa, Proc., 36.
1938. Klimaschwankungen und Krustenbewegungen in Afrika suedlich des Aequators von der Kreidezeit bis zum Diluvium: Sonderveroeffentlichung 3 der Geogr. Ges. zu Hannover.

- BOBRIEVITCH, A.P., SMIRNOV, G.T. and SOBOLEV, V.S., 1959.
Xenolith of diamond-bearing eclogite: Doklady Akad. Nauk., S.S.S.R., 126, 637-640.
- BOBNEY, T.G., 1899. The parent rock of the diamond in South Africa: Proc. Roy. Soc. London, 65, 223-236.
- BOVENKERK, M.P., BUNDY, F.P., HALL, H.T., STRONG, H.M. and WENTORF, R.H., 1959. Preparation of diamond: Nature, 184, 1094-1098.
- BOYD, F.R. and ENGLAND, J.L., 1959. Experimentation at high pressures and temperatures; pyrope: Carnegie Inst., Ann. rep. geophys. lab., paper 1320, 83-87
- BRINK, A.B.A., 1961. Report to accompany geotechnical map of proposed trunk route Mariental-Asab, South West Africa: Pretoria, unpublished.
- BUCHER, W.H., 1963. Cryptoexplosion structures caused from without or from within the earth (Astroblemes or geoblemes): Am. Jour. Sci., 261, 597-649
- CHAPMAN, J., 1868. Travels in the interior of South Africa. 2 vols. London.
- CLOOS, H., 1937. Suedwestafrika. Reiseeindruecke 1936: Geol. Rundschau, 28, H.3.
1941. Bau und Taetigkeit von Tuffschloten. Geol. Rundschau, 32, H.6-8.
- DALY, R.A., 1925. Carbonate dykes of the Premier Diamond Mine, Transvaal: Journ. Geol 38, 659-684
- DAVIDSON, C.F., 1943. The archean rocks of the Rodil District, South Harris, Outer Hebrides: Roy. Soc. Edin. Trans., 61 71-112.
- DAWSON, J.B., 1960. A comparative study of the geology and petrography of kimberlites of the Basutolana province: Ph.D. thesis, Leeds.

- DAWSON, J.B., 1962. Basutoland kimberlites: Bull. Geol. Soc. Am., 73, 545-560.
1964. Carbonate tuff cones in northern Tanganyika: Geol. Mag., 101, 2, 129-137.
- DIETZ, R.S., 1961. Vredefort Ring structure, meteorite impact scar?: Journ. Geol. 69, 499-516.
1963. Cryptoexplosion structures, a discussion: Am. Journ. Sci., 261, 650-664.
- DIXEY, F., 1955. Erosion surfaces in Africa; some considerations of age & origin: Geol. Soc. S.Africa, Trans., 58, 265-280.
- ECKERMANN, H. von 1948. The alkaline district of Alnö Island Sverig. Geol. Unders., ser. Ca. 36
1958. The alkaline and carbonatitic dykes of the Alnö formation on the mainland area northwest of Alnö Island. Kungl. Svenk. Vetensk. Akad.-Handl., Fjärde Series 7, No.2.
- ESKOLA, P., 1921. On the eclogites of Norway: Krist. Vidensk Selskab Skrifter 1, Math.-Nat. Wiss. Kl. 8, 1-118.
- EVERSOLE, W.G., 1962. In Giardini, A.A. and Tydings, J.E. 1962: Diamond synthesis: Am. Mineral., 47, 1393-1421
- FRANKEL, J.J., 1956. An inclusion-bearing olivine melilitite from Mukorob, South West Africa: Roy. Soc. S.Africa, Trans., 35, p.2, 115-123
- FRECHEN, J., 1948. Die Genese der Olivinausscheidungen vom Dreisser Weiher (Eifel) und Finkenberg (Siebengebirge): Neues Jahrb. f. Min. etc. 79, Abt.A. 317-406.
- FRIETSCH, R., 1957. Determination of the composition of garnets without chemical analyses: Geol. F8r. Forh., 79, 43-51.
- GARSON, M.S., 1962. The Tundulu carbonatite ring-complex in southern Nyassaland: Nyassal. Geol. Surv. Mem. no. 2.

- GEVERS, T.W., 1928. The volcanic vents of western Stormberg. Geol. Soc. S. Africa, Trans., 31, 43-62
1931. An ancient tillite in South West Africa: Geol. Soc. S. Africa, Trans., 34.
- GILBERT, G.K., 1896. The origin of hypotheses, illustrated by the discussion of a topographic problem: Science, new ser., 3, 1-13
- GOLDSMITH, J.R. and GRAF, D.L., 1958. Relation between lattice constants and composition of the Ca-Mg carbonates: Am. Mineral. 43. 84-101.
- GRANTHAM, D.R., and ALLEN, J.B., 1960. Kimberlite in Sierra Leone: Overseas Geol. and Min. Res., 8, 5-25.
- GÜRICH, G., 1930. Die bislang aeltesten Spuren von Organismen in Suedafrika. 15th Intern. Geol. Congr. pt. 2, 670-680.
1933. Die Kuibis-Fossilien der Nama-Formation von Suedwestafrika. Palaeont. Zeits., 15, 1.7-154.
- HARRIS, P.G., 1957. Zone refining and the origin of potassic basalts: Geochim. et Cosmochim. Acta, 12, 195-208.
- and ROWELL, J.A., 1960. Geochemical aspects of the Mohorovicic discontinuity. Journ. Geophys. Res., 65, 2443-2459
- HAUGHTON, S.H., 1960. An archaeocyathid from the Nama System. Roy. Soc. S. Africa. Trans., 36, pt. 1, 57-59.
- and MARTIN, H. 1956. The Nama System in South and South West Africa: 20th Congreso Geol. Intern., El Sistema Cambrico, 1, 323-339.
- HELBERGER, H., 1934. Kann der Diamant kosmogenetischer Ursprungs sein? Zeits. Prabt. Geol., 42, 124-125.

- HESS, H.H., 1949. Chemical composition and optical properties of common clinopyroxenes: Am. Mineral., 34, 621-666.
- HOLMES, A., 1936. Contributions to the petrology of kimberlites and its inclusions: Geol. Soc. S. Africa, Trans., 39, 379-428.
- HORNUNG, G. 1963. The analyses of basalts and granites by X-ray spectrography: 7th. Ann. Rep. (1961-1962), Res. Inst. Afr. Geol., Univ. Leeds, 59-63.
- HOWIE, R.A., and SUBRAMANIAM, A.P., 1957. The paragenesis of garnets in charnockite, enderbite and related granulites. Mineral. Mag., 238, 565-586
- JAMES, T.C., 1963. The carbonatites of Tanganyika; a phase of continental-type volcanism: Ph.D. Thesis, London.
- JOHNSON, R.L., 1963. The geology of the Dorowa and Shawa carbonatite complexes, Southern Rhodesia: Geol. Soc. S. Africa, Trans., 64, 101-145.
- KAISER, E., 1926. Die Diamantgeweste Suedwestafrikas: 2 vols., Berlin, Dietrich Reimer.
- KNETSCH, G., 1937. Uebersicht ueber die Geologie des suedlichen Luederitzlandes: Geol. Rundschau, 28, 208-
- KNORRING, O. von and KENNEDY, W.O., 1958. The mineral paragenesis and metamorphic status of garnet-hornblende-pyroxene-scapolite gneiss from Ghana: Mineral. Mag. 241, 846-859.
- KOCK, W.P. de and GEVERS, T.W., 1932. The Chuos tillite in Rehoboth and Windhoek districts. Geol. Soc. S. Africa, Trans. 35.
- KORN, H. and MARTIN, H., 1937. Das Naukluftgebirge in Suedwestafrika: Geol. Rundschau, 28, 22 -226.

- KORN, H. and MARTIN, H., 1951. The seismicity of South West Africa: Geol. Soc. S. Africa, Trans., 54, 87-88.
- KROENLEIN, J.G., 1889. Wortschatz der Khoi-khoi (Nama-leute): Berlin.
- KUNO, H., 1959. Origin of Cenozoic petrographic provinces of Japan and surrounding areas: Bull. Volc., Ser. 2, 20, 37-76.
1960. High alumina basalt, J. Petrol. 1, 121-145.
- KUSHIRO, I., 1960. Si-Al relation in clinopyroxenes from igneous rocks. Am. Jour. Sc., 258, 548-554.
- and YODER, H.S., 1964. Phase equilibrium relation between olivine join and pyroxene join in the system CaO-MgO-SiO₂ at high pressures: Am. Geophys. Union, Trans., 45, nr. 1, 124-125
- LEBEDEV, A.P., 1964. Kimberlites of northeastern U.S.S.R. and allied problems: Geol. Jour. 4, pt. 1, 87-105.
- LEWIS, H.C., 1888. The matrix of the diamond II: Geol. Mag., third dec., 5, 129-131
- LINGEN, J. van der, 1928. Garnets. S. African Journ. Sci, 25, 10-15.
- MAEBUTT, J.A., 1955. Erosion surfaces in Namaqualand and the ages of surface deposits in the south-western Kalahari: Geol. Soc. S. Africa, 58, 13-30
- MACDONALD, G.J.F., 1959. Chondrites and the chemical composition of the earth in Researches in Geochem. ed. Abelson, Wiley, New York, 476-494.
- MARTIN, H., 1950. Suedwestafrika. Bericht ueber einen Vortrag: Geol. Rundschau, 38, 6-14

- MARTIN, H., 1953. Notes on the Dwyka succession and on some pre-Dwyka valleys in South West Africa: Geol. Soc. S. Africa, Trans., 56, 37-41.
1956. in Haughton, S.H. and Martin, H., 1956. The Nama System in South & South West Africa: 20th Congreso Geol. Intern., El Sistema Cambrico, 1, 323-339.
- McBIRNEY, A.R., 1959. Factors governing the emplacement of volcanic necks: Am. Jour. Sci., 257, 431-448.
1963. Breccia pipe near Cameron, Arizona, Discussion: Geol. Soc. Am. Bull., 74, 227-232
- MENZER, G., 1928. Die Kristallstruktur der Granate: Zeits. Krist., 69, 300-396.
- MERSH, S., 1952. Further study of the Majgawan Diamond Mine, Panna State, Central India: Quart. J. Geol. Soc. India, 24, 125-132.
- MILASHEV, V.A., KRUTOYARSKI, M.A., RABKIN, M.T. and EHRlich, E.M., 1963 (Kimberlitic rocks and picritic porphyries from the north-eastern Siberian Platform) in Russian: Arctic Geol. Res. Inst., Trans., 126, 96-101.
- MIKHEYENKO, V.I. and NENASHEV, N.I., 1962. Absolute age of formation and relative age of intrusion of the kimberlites of Yakutia: Intern. Geol. Review 4, 916-924.
- NIXON, P.H., 1960 A mineralogical and geochemical study of kimberlites and the associated xenoliths: Ph.D. Thesis, Univ. Leeds.
- NIXON, P.H., KNORRING, O. von and ROOKE, J.M., 1963. Kimberlites and associated inclusions of Basutoland: Am. Mineral., 48, 1090-1132.

- NOCKOLDS, S.R., 1954. Average chemical composition of some igneous rocks: Bull. Geol. Soc. Am., 65, 1007-1032.
- O'HARA, J.M. and MERCY, E.L.P., 1963. Petrology and petrogenesis of some garnetiferous peridotites: Roy. Soc. Edinb., Trans., 65, No.12, 251-314
- OXBURGH, E.R., 1964. Petrological evidence for the presence of amphibole in the upper mantle and its petrogenetic and geophysical implications. Geol. Mag., 101, 1-19.
- PETTIJOHN, F.J., 1949. Sedimentary rocks. Harper Bros., New York.
- POLDERVAART, A. and HESS, H.H., 1951. Pyroxenes in the crystallization of basaltic magma. Journ. Geol., 59, 472-489.
- RANGE, P. 1909. Die geologische Formationen des Namalandes: Monatsber. d. deuts. Geol. Ges. nr. 2, 126-127.
- 1912a. Geologie des deutschen Namalandes: Sonderabdruck Beitz, Geol. Erf. deuts. Schutzgeb., H2, Berlin.
- 1912b. Topography and geology of the German South Kalahari: Geol. Soc. S. Africa, Trans., 15, 65-73.
- RANGE, P. and REINISH, 1917. Zeits. d. deuts. Geol. Ges. 69, 63-71.
- REAY, A. and HARRIS, P.G. 1964. Partial fusion of peridotite Bull. Volc., (in the press).
- REHBOCK, Th., 1898a. DSW Afrika, seine wirtschaftliche Erschliesung: Berlin.
- 1898b. DSW Afrika, 96 photographs, 1 map, Berlin.
- REYNOLDS, D., 1954. Fluidization as a geological process and its bearing on the problem of intrusive granites. Am. Jour. Sci. 252, 577-614.

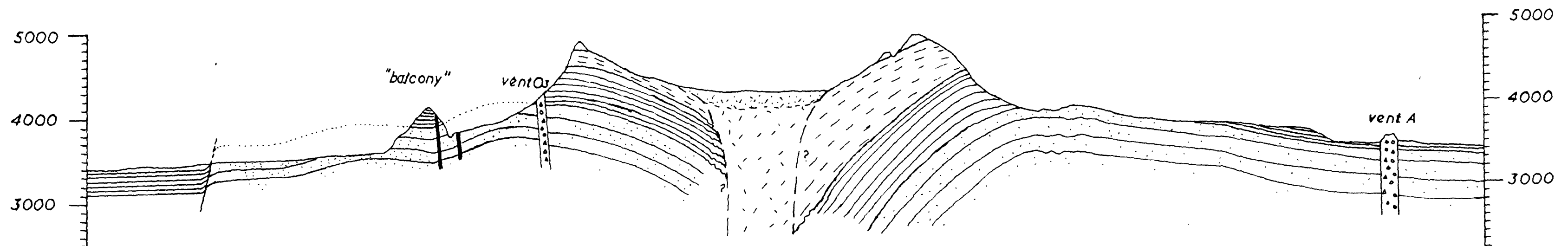
- RICHTER, R., 1955. Die aeltesten Fossilien Sued-Afrikas: Senckenb. Leth., 36. 245-289.
- RICHTER, D.H. and MURATA, K.J. 1961. Xenolithic nodules in the 1800-1801 Kaupulehu flow of Hualalai Volcano: Short Papers etc. U.S. Geol. Surv. Prof. Paper, 424-B, 215-217.
- RINGWOOD, 1959. Constitution of the mantle, a revision: Geochim. et Cosmochim. Acta, 16, 192-195.
- ROEX, H.D. le, 1941. A tillite in the Otavi Mountains, S.W.A; Geol. Soc. S. Africa, Trans. 44, 207-218
- ROGERS, A.W. 1910. The Kheis Series: Geol. Soc. S. Africa, Trans., 13, 100-
1912. The Nama system in the Cape Province: Geol. Soc. S. Africa, Trans., 15, 51-50.
- 1915a. The geology of part of Namaqualand: Geol. Soc. S. Africa, Trans., 18, 72-101.
- 1915b. Geitsi/Gubib, an old volcano: Roy. Soc. S. Africa, Trans., 5, 247-258
1920. Origin of the Great Escarpment: Geol. Soc. S. Africa, Proc. 25. p.25.
- ROSS, C.S., FOSTER, M.D. and MYERS, A.T., 1954. Origin of dumites and of olivine-rich inclusions in basaltic rocks. Am. Mineral., 39, 693-737.
- RUST, G.W., 1937. Preliminary notes on explosive volcanism in south eastern Missouri: Jour. Geol., 45.
- SAETHER, E., 1957. The alkaline rock province of the Fen area in southern Norway: Norsk. Vidensk. Selskab Skrifter, 1.

- SCHENK, A., 1886. Zur Geologie von Angra Pequena und Grosz-Namaland: Zeits. d. deuts. Geol. Ges.
1893. Gebirgsbau und Bodengestaltung von DSW Afrika. Verhandl. d. 13th deuts. Geogr. Tag zu Berlin, p.131.
- 1901a. Der Geitsi/Gubib, ein prophyrischer Stratovulkan DSW Afrikas: Zeits. d. deuts. Geol. Ges., 4, p.54
- 1901b. DSW Afrika im Vergleich zum uebrigen Suedafrika: Verhandl. d. 16th Geogr. Tag zu Breslau, p.157.
1910. in H. Meyer: Das deutsche Kolonialreich, Bd 2, 151-198. DSW Afrika. Leipzig und Wien.
- SCHEIBE, A., 1906. Der "blue ground" des DSW Afrikas im Vergleich mit dem des englischen Suedafrikas. Prog. de Koenigl. Berg. Akad. zu Berlin.
- SCHIEFERDECKER, A.A.G. ed. 1959. Geological nomenclature. Noorduyn en Zoon, Gorkum.
- SCHINZ, H. 1891. Deutsch Sued-West Afrika. Oldenburg und Leipzig (p.464).
- SCHULTZE, L., 1907. Aus Namaland und Kalahari. Jena. (p.159).
- SCHWELLNUS, C.M., 1941. The Nama tillite in the Klein Kharas Mountains, S.W.S: Geol. Soc. S. Africa, Trans., 44, 19-341
- SHAND, S.J., 1934. The heavy minerals of kimberlites: Geol. Soc. S. Africa, Trans., 37. 57-68.
- SMIRNOV, G.T., 1959. Mineralogy of Siberian kimberlites: Internat. Geol. Rev., 1, No.12, 21-39.
- SMITH. J.V. and SAHAMA, Th.G., 1954. Determination of the composition of natural nephelines by an X-ray method: Mineral. Mag. 226, 459.449.

- SMULIKOWSKI, K., 1960. Comments on eclogite facies in regional metamorphism: 21st Intern. Geol. Congr. pt.13, 372-382.
- SOHNGE, P.G. and VILLIERS, J. de, 1959. Geology of the Richtersveld and eastern Sperrgebiet Geol. Sur. S. Africa, Mem. 48.
- SPENCER, L.J., 1941. The Gibeon shower of meteoritic irons in South West Africa: Mineral.Mag. 26, nr 173, 19-35.
- STROMER VON REICHENBACH, 1896. Die Geologie des deutschen Schutz-gebiete in Afrika. DSW Afrika, pp.111-156. Muenchen und Leipzig.
- TALJAARD, M.S., 1936. South African melilite basalts and their relations: Geol. Soc. S. Africa, Trans., 39, 281-316.
- TEX, E. den and VOGEL, D.E., 1962. A "Granulitgebirge" at Cabo Ortegal (N.W. Spain): Geol. Rundschau, 52, 95-112.
- TOIT, A.L. du, 1916. Notes on the Karroo System in the southern Kalahari: Geol. Soc. S. Africa, Trans., 19, 1-15.
1954. Geology of South Africa. Oliver and Boyd, Edinburgh.
- TRÖGER, W.E. 1956. Optische Bestimmung der gesteinsbildenden Minerale, 1, Bestimmungstabellen. Stuttgart, Schweizerbart
1959. Die Granatgruppe. Neues Jahrb. f. Min. etc. 93, 1-44.
- TRUTER, F.C., 1949. A review of volcanism in the geological history of South Africa: Geol. Soc. S. Africa, Proc., 52. 29-89.
- TURNER, F.J. and VERHOOGEN, J. 1960. Igneous and metamorphic petrology: McGraw-Hill, 2nd edition.

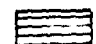
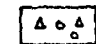
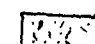
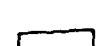
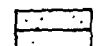

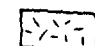
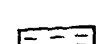
- TWENHOFEL, W.H., 1939. Principles of sedimentation. McGraw-Hill, New York.
- VEDDER, H. 1938. South West Africa in early times. Oxford Univ. Press.
- VERHOOGEN, J. 1958. Les pipes de kimberlite du Katanga: Annal. Serv. Mines Com. Spec. Katanga, tome 9.
- VILLIERS, J. de, 1945. The age of the Numees tillite, relative to the Nama System: Geol. Soc. S. Africa, Trans., 48. 48, 139-148.
- WAGNER, P.A., 1914. The diamond fields of southern Africa Johannesburg, The Transvaal Leader
1915. The Dwyka Series in South West Africa: Geol. Soc. S. Africa, Trans., 18, 102-117.
1928. The evidence of kimberlite pipes on the constitution of outer parts of the earth: S. Afr. Jour. Sci., 25, 127-148.
1929. in Handbuch der Regionalen Geologie: South Africa by Rogers, Hall, Wagner and Haughton: Heidelberg, 7 7a, 148-158
- WATERMEYER, J.C., 1899. Notes on a journey in German S.W. Africa: Phil. Soc. S. Africa. Trans., 11, p.28.
- WILLIAMS, A.F., 1932. The genesis of the diamond. Two vols., London, Ernest Benn Ltd.
- WILLSHIRE, H.G. and BINNS, R.A., 1961. Basic and ultrabasic xenoliths from volcanic rocks of New South Wales: J. Petrol., 2. 185-208.
- WILSON, C.W. Jr., 1953. Wilcox deposits in explosion craters, Stewart County, Tennessee, and their relation to origin and age of Wells Creek Basin structure: Geol. Soc. Am. Bull., 64, 755-768.

- WINCHELL, A.N., and WINCHELL, H., 1956. The elements of optical mineralogy, pt. 2, New York, Wiley and Sons.
- YODER, H.S. and SAHAMA, Th. G., 1957. Olivine X-ray determinative curve: Am. Mineral., 42, 475-491.
- YODER, H.S. and TILLEY, C.E., 1962. Origin of basalt magmas: J. Petrol., 3, 342-532.



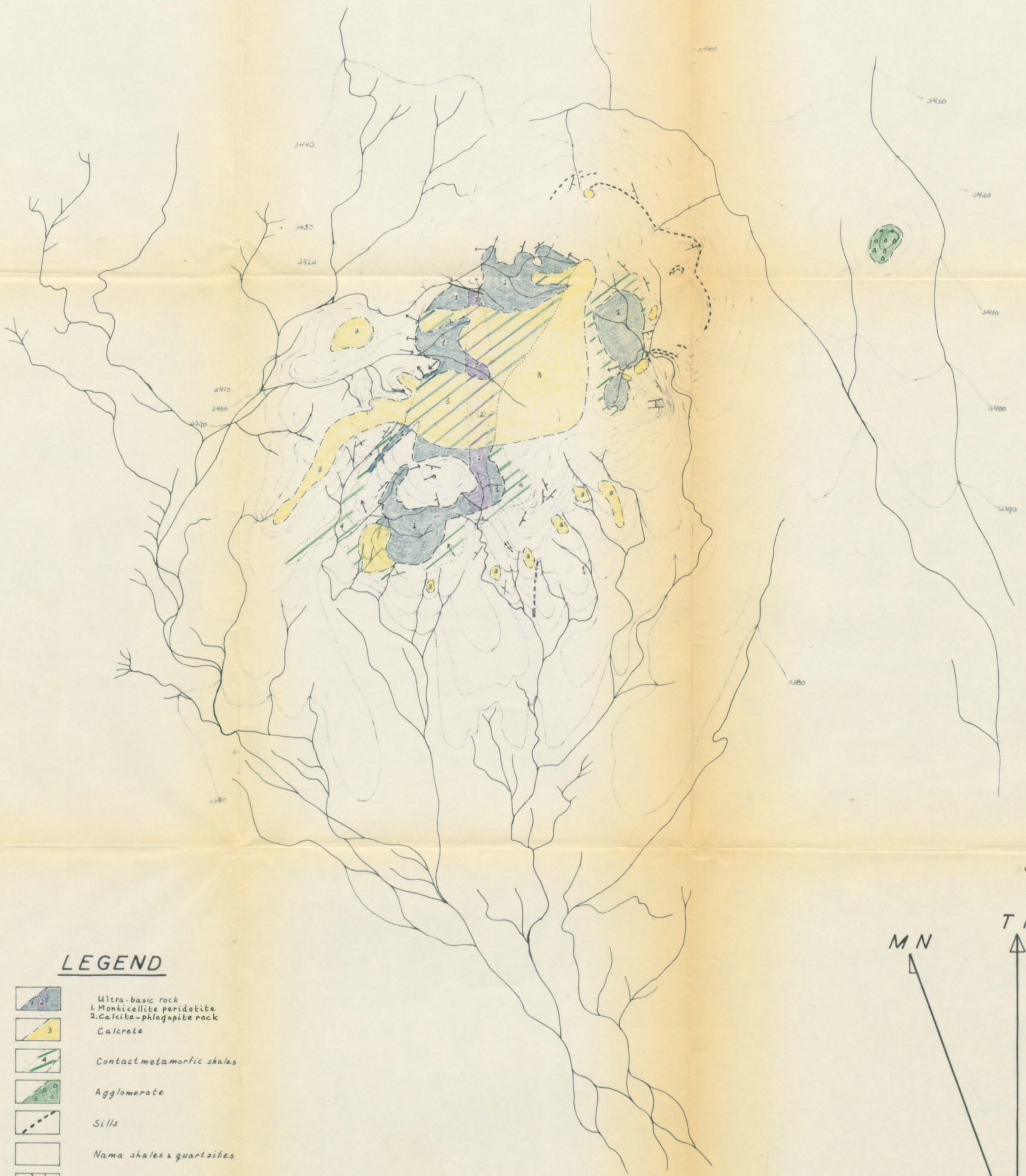
Cross Section through the GROSS BRUKKAROS

Horizontal Scale 1:25.000
Vertical Scale 1:12.000


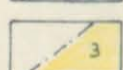



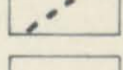
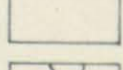
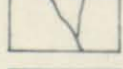
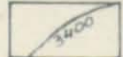
- | | | | |
|--|---|---|--|
|  shales |  satellite vents |  debris |  micro-breccia (silicified) |
|  sandstones |  radial dykes |  micro-breccia |  micro-breccia (bedded) |

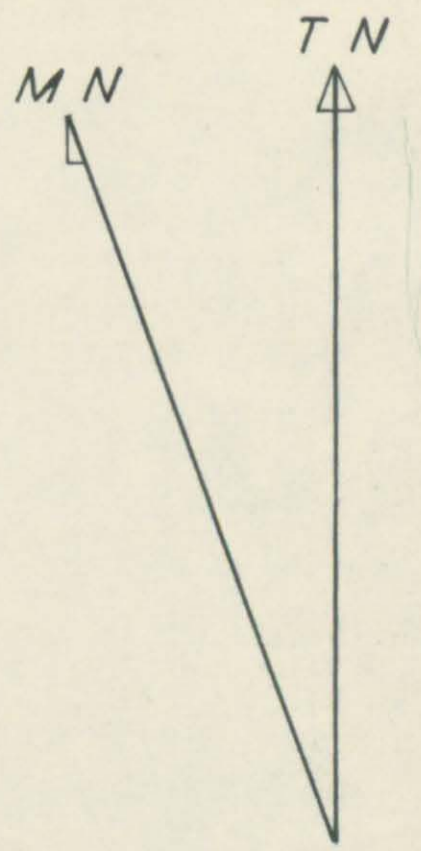
GEOLOGICAL SKETCH MAP OF THE BLUE HILLS VENT

BERSEBA NATIVE RESERVE



LEGEND

-  1. Ultra-basic rock
-  2. Monticellite peridotite
-  3. Calcicrete
-  4. Contact metamorphic shales
-  5. Agglomerate
-  6. Sills
-  Nama shales & quartzites
-  Streams
-  Contours



0 100 200 300 400 500 600

SCALE IN YARDS

Contour lines surveyed with aneroid barometer by R. Baxter-Brown & J. A. Mills
Geology by R. Baxter-Brown, J. A. Mills & A. J. A. Janse